MAGNETOM Flash

SCMR Edition 2021

siemens-healthineers.com/magnetom-world

Page 4
Editorial Comment
Gemma Figtree

Page 8
Role of CMR in Non-ischemic Cardiomyopathies
Jeanette Schulz-Menger, et al.

Page 19
The Diagnostic Challenges of Myocarditis
Syasya Hafisyatul Aiza Zainal Abidin

Page 38
Whole-heart High-resolution LGE in Clinical Routine
Hubert Cochet, et al.

Page 57
Clinical Implementation of 4D Flow MRI in a Large Cardiovascular Imaging Practice
Bradley D. Allen, et al.

Page 69
A Hybrid Cardio-Neuro MR Suite at the Geneva University Hospital in the Treatment of Cardiac Tachyarrhythmias
Paul Vallée, et al.

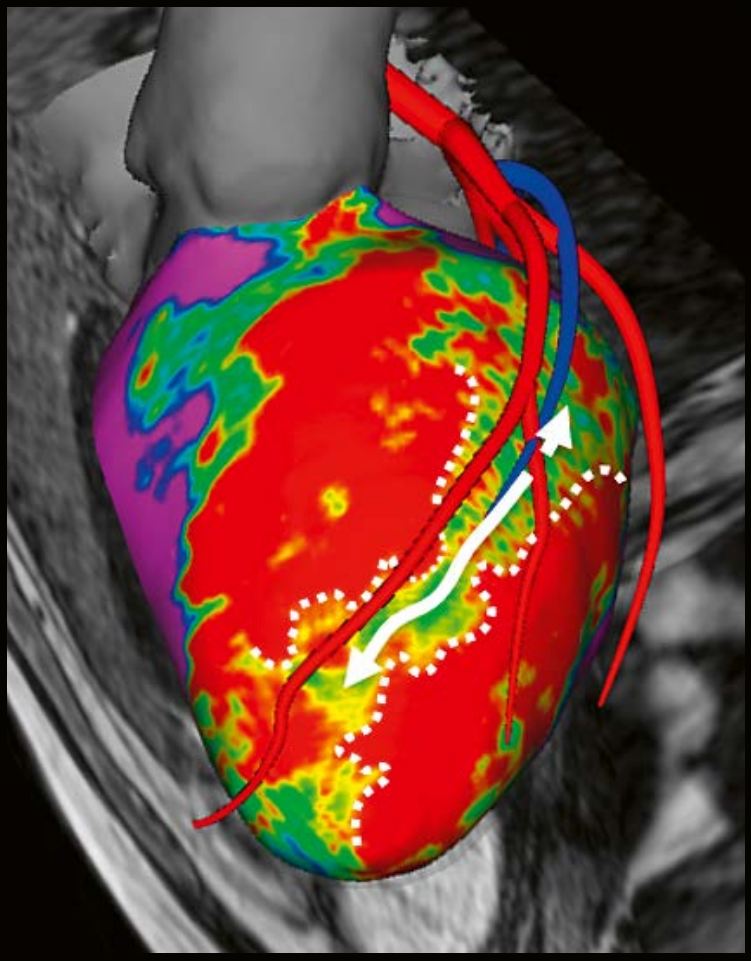

SIEMENS Healthineers

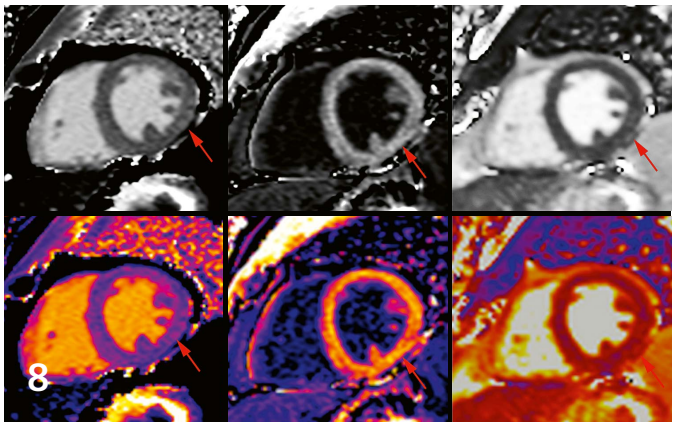

Myocardial inflammation caused by SARS-CoV-2

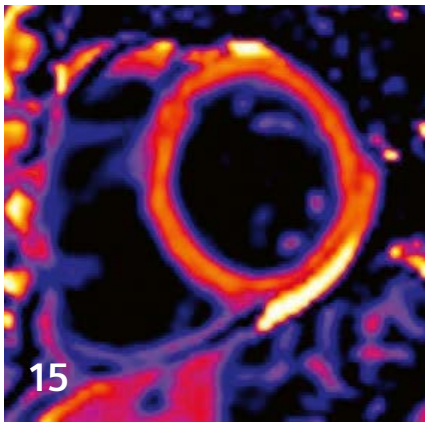

CMR in Autoimmune Rheumatic Diseases

Editorial Comment

4 **How CMR Contributes to the Emerging World of Precision Medicine and Patient Stratification in Cardiology and Heart Failure**
Gemma Figtree
University of Sydney, Australia

CRM Imaging in Cardiomyopathies

8 **Role of CMR in Non-ischemic Cardiomyopathies**
Jeanette Schulz Menger, et al.
Charité and HELIOS Hospital Berlin-Buch, Germany

15 **Case Report: CMR of Myocardial Inflammation Regression in Convalescence of Acute Myocarditis Caused by SARS-CoV-2**
Carlos Rochitte, et al.
Hospital do Coração, São Paulo, Brazil

19 **The Diagnostic Challenges of Myocarditis: Importance of Bioimaging Signatures with Parametric Mapping**
Syasya Hafisyatul Aiza Zainal Abidin
Department of Cardiology, Faculty of Medicine, Universiti Teknologi MARA (UiTM) Sg Buloh, Selangor, Malaysia

22 **Cardiovascular Magnetic Resonance in Autoimmune Rheumatic Diseases: Translating the Greek Experience to the International Arena**
Sophie I. Mavrogeni et al.
Onassis Cardiac Surgery Center, Athens, Greece

26 **Magnetic Resonance Spectroscopy as a Clinical Tool for the Prognosis and Diagnosis of Diabetic Heart Disease**
Eylem Levelt, et al.
University of Leeds, UK

30 **How to do Cardiac Single Voxel ^{1}H Spectroscopy**
Morten Asp Vonsild Lund, et al.
Copenhagen University Hospital, Denmark

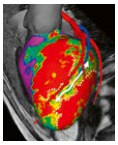

Cover image from Hubert Cochet, et al., *Whole-heart High-resolution Late Gadolinium Enhancement in Clinical Routine*, Hôpital Cardiologique du Haut-Lévêque, CHU de Bordeaux, Pessac, France

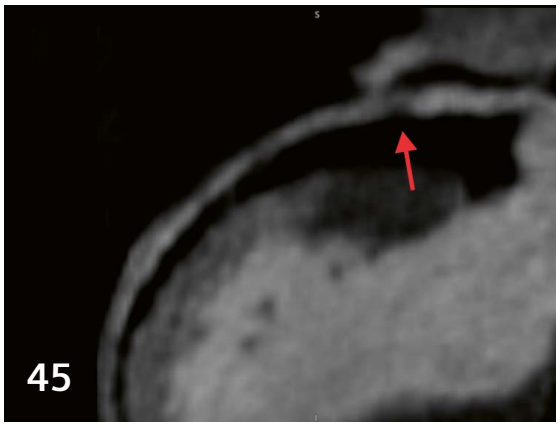

3D coronary MRA integrated in a fast free-breathing CMR exam

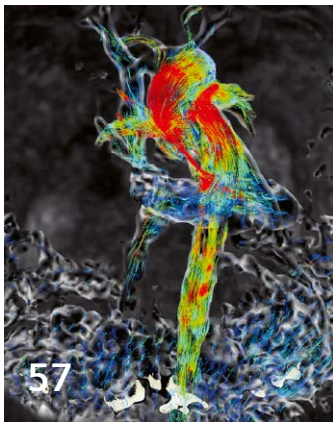

4D Flow MRI

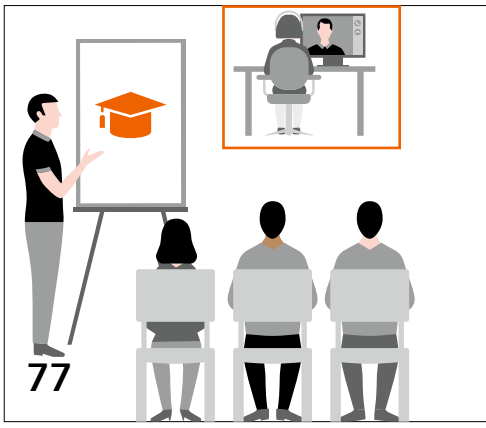

SmartSimulator remote training

Whole-heart Imaging

34 **3D Late Gadolinium Enhancement CMR**
Reza Nezafat, et al.
Cardiovascular Division, Beth Israel Deaconess Medical Center and Harvard Medical School, Boston, MA, USA

38 **Whole-heart High-resolution Late Gadolinium Enhancement in Clinical Routine**
Hubert Cochet, et al.
Hôpital Cardiologique du Haut-Lévêque, CHU de Bordeaux, Pessac, France

45 **3D Coronary MRA Integrated in a Fast and Comprehensive Free-breathing CMR Exam**
Juliano de Lara Fernandes, et al.
Jose Michel Kalaf Research Institute, Campinas, Brazil

4D Flow Imaging

57 **Clinical Implementation of 4D Flow MRI in a Large Cardiovascular Imaging Practice: Motivation, Strategies, and Initial Experience**
Ryan J. Avery, Bradley D. Allen, et al.
Northwestern University, Chicago, USA

64 **4D Flow MRI for the Evaluation of Aortic Endovascular Graft**
Caterina Beatrice Monti, et al.
Department of Biomedical Sciences for Health, Università degli Studi di Milano, Italy

Interventional CMR

69 **A Hybrid Cardio-Neuro MR Suite at the Geneva University Hospital in the Treatment of Cardiac Tachyarrhythmias**
Jean-Paul Vallée, et al.
Geneva University Hospital, Switzerland

How I do it

74 **Extending the Reach of MRI with Remote Operations**
Bac Nguyen, et al.
ARISTRA, Rasta, Norway

Meet Siemens Healthineers

77 **Introducing Olga Dreger and Michelle Steinkrug**
PEP-Connect, Siemens Healthineers, Erlangen, Germany

Gemma Figtree is a Professor in Medicine at the University of Sydney and an Interventional Cardiologist at Royal North Shore Hospital in Sydney. She co-leads the Cardiovascular Theme for Sydney Health Partners, a NHMRC Advanced Health Research and Translation Centre and is the Chair of the University of Sydney's multi-disciplinary Cardiovascular Initiative. Gemma completed her DPhil at Oxford University in 2002 supported by a Rhodes Scholarship making fundamental discoveries regarding estrogen's actions and factors regulating NO/redox balance in the cardiovascular system. She is committed to improving the care for heart attack patients – using her knowledge of molecular and cellular biology to develop methods of identifying those at highest risk of adverse outcome, and discovering novel therapies to prevent and treat events, inspired by her clinical work as an interventional cardiologist. She has dedicated herself throughout her career to unravelling key mechanisms underlying susceptibility and response to heart attack, with studies extending from the bench to large cohort studies and clinical trials. Discoveries in her Laboratory have been published in leading journals Circulation, JACC and European Heart Journal, with > 160 publications. Gemma is a principal investigator on grants >$12.5

How CMR Contributes to the Emerging World of Precision Medicine and Patient Stratification in Cardiology and Heart Failure

Dear readers and colleagues,

What a fabulous welcome to 2021, with a comprehensive review and series of global expert perspectives on state-of-the art CMR imaging in non-ischaemic cardiomyopathy in the SCMR edition of MAGNETOM Flash. Leading CMR investigators and clinicians have contributed to this edition from all corners of the world – Europe, Asia, North, and South America, providing insights into clinical applications, pragmatic challenges as well as technical developments and future directions.

Cardiomyopathy, with clinical presentations from heart failure to arrhythmia, is a massive burden across the globe, impacting patients and families through well-acknowledged mortality and morbidity, but also with major economic impact. It is a syndrome characterised by classic clinical history and physical findings. Mostly due to necessity related to our historic inability to differentiate the many underlying pathophysiological mechanisms with prior diagnostic technologies, patients have been bucketed together. The rather gross separation of heart failure patients into those with reduced versus preserved ejection fraction by echocardiography illustrates this well. In this edition, the enormous opportunity for CMR to transform the clinical stratification of heart failure patients in a way that more closely aligns with underlying biology is highlighted. This will have important benefits to patients immediately through the ability to identify early myopathic processes, help risk stratify and guide management, as well as diagnose potential secondary causes of heart failure amendable to targeted treatment approaches.

In addition, there are broader long-term and "big picture" benefits of improved phenotyping of cardiomyopathy, stratifying the enormous and heterogeneous syndrome into biologically relevant groups and allowing for more focused development of therapies relevant to specific mechanisms, with flow on effects such as improved ability to measure response to therapy in more powerful clinical trials.

Biomarkers, whether they are imaging or blood based molecular markers, are most powerful when they closely reflect underlying biology. Measures of inflammation and fibrosis within the myocardium, as well as patterns of distribution, now possible through technical advances with CMR, as highlighted in this edition of MAGNETOM Flash, have opened up a new eye for cardiologists, and combined with improved blood measures, offer the hope of improved "precision" medicine far beyond what we could "see" with echocardiography. They are obviously of direct relevance to cardiomyopathy and heart failure – reflecting specific mechanisms as well as being of value for risk stratification and measuring response to therapy. In order to get the most out of this valuable information, multi-disciplinary strategic leadership across the whole pipeline is required, helping us bring together fundamental molecular and cellular biology with clinical and imaging phenotype. Stratification of patient groups in this manner is our best chance of translating potential new therapies targeted to specific subgroups of non-ischaemic cardiomyopathy. With CMR as a tool, we can learn from the massive steps that the oncology field has been able to take once molecular characterisation was possible to stratify tumours

mill. She was awarded a National Health and Medical Research Council (NHMRC) Excellence Award for Top Ranked Practitioner Fellow (Australia), commencing in 2018. In 2019 she received the prestigious NSW Ministerial Award for Cardiovascular Research Excellence. Gemma is committed to the advancement of her field and serves as a member of the Editorial Board of leading international cardiovascular journals Circulation and Cardiovascular Research, as well as being a founding editorial board member for Redox Biology, and an Associate Editor for Heart, Lung and Circulation. Her research and clinical perspective and leadership are recognised by her membership of the Scientific Board of Cardiac Society of Australia and New Zealand (responsible for International Relations), and her appointment to the Expert Advisory Panel for NHMRC Structural Review of Grants Program (2016–17), and as well as the Clinical Committee of the Heart Foundation. She is committed to the promotion and advocacy of cardiovascular research, working as President of the Australian Cardiovascular Alliance with a national team to secure $220 Million Federal funding for the Mission for Cardiovascular Health, as well as a member of the NSW CVD Advisory Committee. She now chairs the Mission (CV) Expert Advisory Panel. She is a graduate of the Australian Institute of Company Directors and serves/has served as a non-executive Director on multiple community Boards.

previously lumped together, and now treated with a diverse range of biological agents targeted to specific mechanisms.

Magnetic resonance spectroscopy perhaps offers the most physiologically relevant insight to cellular function in the myocardium and has offered enormous hope for over a decade. Levelt and colleagues from the UK [1] provide a state-of-the-art update on its use as a clinical tool for the prognosis and diagnosis of diabetic heart disease, where the common problem of diabetes mellitus can cause similar clinical syndrome through multiple mechanisms, with potential impact on prognosis and management. These include impaired cardiac high energy phosphate metabolism, coronary microvascular dysfunction, and ectopic lipid deposition. Increased oxidative stress and dysregulated cellular metabolism drives alterations to Na+ and Ca2+ handling, impacting contractility, relaxation and susceptibility to arrhythmias [2]. Magnetic resonance spectroscopy methods, particularly those based on interrogating ^{1}H and ^{31}P metabolites, have now been shown to add an additional layer of information to clinical imaging data. The challenges of upscaling this potentially powerful clinical investigation tool are discussed. The most significant deterrents include the need for dedicated hardware, expert input during acquisition compared to standard imaging, dedicated time for the pre-scan adjustments, and exceptional sensitivity to cardiac and respiratory motion. Technical advancements that make spectroscopy more reproducible in a wide array of clinical settings may help in the next decade.

The importance of bioimaging signatures with parametric mapping in addressing the diagnostic challenges of myocarditis is expertly laid out by Dr. Abidin [3] from Malaysia, including with very pragmatic and representative cases. As she summarizes, although late gadolinium imaging is a sensitive technique to detect focal myocardial damage, it lacks the ability to differentiate the state of the disease activity, especially in myocarditis. Furthermore, "the incorporation of bioimaging signatures with parametric maps and LGE imaging, using our standardized exam card, allows for shorter examination time and provides a productive and highly reproducible technique for diagnosing myocarditis" [3]. Examples are also given by Dr. Mavrogeni from Greece, on integrating advances in CMR inflammatory measures into the diagnosis, risk stratification and management of patients with autoimmune rheumatic disease involving the heart [4].

Measures of inflammation and fibrosis within the myocardium, as well as patterns of distribution, now possible through technical advances with CMR, have opened up a new eye for cardiologists and, combined with improved blood measures, offer the hope of improved "precision" medicine.

The purpose and approaches of whole-heart high-resolution late gadolinium enhancement are summarized by Dr. Cochet and colleagues from France [5]. Initially developed to assess fibrosis in the very thin walled left atrium [6], the technique is recognised to achieve much higher spatial resolution, but with the disadvantage of longer scan time. A pragmatic approach is taken in the application of the technique to the assessment of the left ventricle, highlighting that HR-LGE is not required in every

patient. However, patients with a number of key conditions have been shown to benefit, particularly when traditional CMR imaging is normal or inconclusive. These include patients with myocardial infarction with non-obstructive coronary arteries (MINOCA- where HR-LGE resulted in a change in the final diagnosis in 26% of the patients), ventricular arrhythmia, and it has been increasingly used in planning and assessment of patients with pulmonary vein isolation for atrial fibrillation. Dr. Nezafat et al. also shares the experience of clinicians at Beth Israel Deconess Medical Center where they have applying free-breathing 3D LGE for high resolution LGE imaging for over a decade [7].

Pragmatic experiences and approaches to applying 4D Flow MRI in clinical practice are well described by Dr. Avery and colleagues from the USA, and Dr. Monti from Italy. Whilst initial practical implementation has been to assess complex congenital heart disease, and large vessel abnormalities, including the aortic endovascular graft described by Dr. Monti [8] due to its ability to assess blood flow velocity and wall shear stress, there is also the real hope that 4D Flow can play a role in improving the speed and reproducibility of routine haemodynamic measures [9], and ultimately, although with need for considerable technical advances, provide measures of cardiac energetics previously only available through complex invasive pressure volume relation measures to easily applicable to the clinical setting [10].

Artificial Intelligence and machine learning approaches are emerging as excellent approaches to better cluster patient populations and derive more tightly circumscribed patient cohorts. Such unbiassed segmentation of patient populations has the advantage of reaching beyond our existing knowledge, potentially identifying new risk markers, and groups who may be linked by common mechanisms. CMR data, with its improved quantitation of physiologically and pathophysiological relevant myocardial function, along with more traditional clinical measures make for a perfect substrate for new discovery and approaches to longstanding and common cardiovascular problems as recently discussed by Bhuva and colleagues in Circulation: Cardiovascular Imaging [11], and is very relevant to consideration of this SCMR edition of MAGNETOM Flash.

A major challenge for the cardiovascular field in developing and translating new therapies has been the high bar set, with primary endpoints focussed on mortality. Whilst being careful not to lower the ultimate bar, validated surrogate measures that reflect underlying disease activity have the potential to play an important role in working towards a staged regulatory process, reducing the cost and improving the power of early phase trials and ensuring efficiency. This may have some impact in reversing the current trend away from cardiovascular clinical trials related to high costs and perceived high risk.

With rapid improvements in CMR and other tools that improve our clinical phenotype and understanding of contributing factors to an individual's heart failure syndrome, we need to continue to invest in rigorous assessment and implementation for new diagnostic pathways, with a particular focus on the benefit to the patient. *Does new information translate to improved care and outcome?* For this, global leadership, aligning new developments with efficient and innovative clinical trial platforms, and guideline experts are required to ensure we have a strong evidence-base to guide clinical implementation. Dr. Schulz-Menger and colleagues from Germany have provided a considered commentary regarding the evolution of guidelines that play a critical role in the implementation of CMR as a diagnostic tool for non-ischaemic cardiomyopathies [12], driving clinical quality and minimising clinical variation. As they astutely state "it has become more and more evident, that the quantification of cardiac function and myocardial structure is crucial for a diagnostic decision. This major step will also challenge the community as a significant effort is needed to ensure quality assurance including standardization" [12]. Whilst there may be some argument against widespread use of CMR from the "payers" in the system, the economic savings that can be made by early accurate diagnosis of underlying pathophysiology as well as risk stratifying features also needs to be clearly identified and placed in the equation.

Whilst it is invigorating to observe the progress in technology and clinical application of CMR as it pertains to heart failure and non-ischemic cardiomyopathy, we need to continue to wrestle with the immense challenge of implementing equitable access to evidence-based clinical pathways and diagnostic tools. For CMR this includes collaborative approaches to improve access to hardware, sequences, technical and clinical expertise in clinical settings around the globe, as well as efforts to accelerate acquisition and sharpen reproducibility in non-expert hands. This is highlighted by the powerful final sentence in the review by Dr. Abidin "Now the task is to make parametric mapping with CMR technically available across the globe" [3]. Improvements in remote support, as presented by Bac Nyguyen [13] from Norway, is one critical ingredient in this ambition.

In conclusion, this SCMR edition of MAGNETOM Flash provides its broad readership with an excellent overview regarding the emerging role of CMR with more stratified approaches to common clinical cardiology challenges. Better stratification by underlying mechanistic markers – both imaging and blood based – will be the central ingredients to making the next advances in prevention, early detection and treatment of many cardiovascular conditions. CMR and the non-invasive window that it provides into myocardial pathology, without the need for myocardial biopsy, will

undoubtedly be a central player in both better diagnosis management of individual patients as well as advances in the field through coordinated stratification and targeting of novel therapies in more efficient and powerful trials. Ongoing partnerships between academia and industry, as well as clinical guideline and policy experts are required to ensure we maximise the huge potential going forward.

Gemma Figtree

References

1 Levelt et al., Magnetic Resonance Spectroscopy as a Clinical Tool for the Prognosis and Diagnosis of Diabetic Heart Disease. On page 26 of this issue.
2 Figtree et al., Oxidative regulation of the Na(+)-K(+) pump in the cardiovascular system. Free Radic Biol Med. 2012 Dec 15;53(12):2263-8. doi: 10.1016/j.freeradbiomed.2012.10.539.
3 Hafisyatul Aiza Zainal Abidin, The Diagnostic Challenges of Myocarditis: Importance of Bioimaging Signatures with Parametric Mapping. On page 19 of this issue.
4 Mavrogeni et al., Cardiovascular Magnetic Resonance in Autoimmune Rheumatic Diseases: Translating the Greek Experience to the International Arena. On page 22 of this issue.
5 Cochet et al., Whole-heart High-resolution Late Gadolinium Enhancement in Clinical Routine. On page 38 of this issue.
6 Marrouche et al., Association of atrial tissue fibrosis identified by delayed enhancement MRI and atrial fibrillation catheter ablation: the DECAAF study. JAMA. 2014;311(5):498–506. doi: 10.1001/jama.2014.3. Erratum in: JAMA. 2014;312(17):1805.
7 Nezafat et al., 3D Late Gadolinium Enhancement CMR. On page 34 of this issue.
8 Monti et al., 4D Flow MRI for the Evaluation of Aortic Endovascular Graft. On page 64 of this issue.
9 Avery et al., Clinical Implementation of 4D Flow MRI in a Large Cardiovascular Imaging Practice: Motivation, Strategies, and Initial Experience. On page 57 of this issue.
10 Fernandes et al., Right ventricular energetics and power in pulmonary regurgitation vs. stenosis using four dimensional phase contrast magnetic resonance. Int J Cardiol. 2018;263:165-170. doi: 10.1016/j.ijcard.2018.03.136.
11 Bhuva et al., A Multicenter, Scan-Rescan, Human and Machine Learning CMR Study to Test Generalizability and Precision in Imaging Biomarker Analysis. Circ Cardiovasc Imaging. 2019;12(10):e009214. doi: 10.1161/CIRCIMAGING.119.009214.
12 Schulz-Menger et al., Role of CMR in Non-ischemic Cardiomyopathies. On page 8 of this issue.
13 Nguyen et al., Extending the Reach of MRI with Remote Operations. On page 74 of this issue.

We appreciate your comments.
Please contact us at magnetomworld.team@siemens-healthineers.com

Editorial Board

Review Board

Role of CMR in Non-ischemic Cardiomyopathies

Jan Gröschel; Maximilian Fenski; Edyta Blaszczyk; Jeanette Schulz-Menger

Charité – Universitätsmedizin Berlin, corporate member of Freie Universität Berlin, Humboldt-Universität zu Berlin, and Berlin Institute of Health, Working Group on Cardiovascular Magnetic Resonance, Experimental and Clinical Research Center, a joint cooperation between the Charité Medical Faculty and the Max-Delbrück Center for Molecular Medicine and HELIOS Hospital Berlin-Buch, Department of Cardiology and Nephrology, Medical University Berlin, Charité Campus Buch, Berlin, Germany

Abstract

Cardiovascular magnetic resonance (CMR) plays a growing role in therapeutic decision-making as it allows to differentiate etiologies and provides prognostic information. Compared with other imaging modalities, CMR has the unique ability to identify myocardial injury, not only in ischemic, but also in non-ischemic heart disease (NIHD). It enables the identification of reversible, irreversible, acute and, chronic damage. The detection of inflammation in myocarditis and of myocardial involvement in systemic disorders, and the differentiation of left ventricular hypertrophy (LVH), including storage diseases, were two of the door-openers into different clinical guidelines. This was already recognized in 2016, with CMR specifically recommended in more than 50% of the guidelines of the European Society of Cardiology (ESC), and in 50% of AHA/ACC guidelines [1, 2]. The recognition of CMR in guidelines

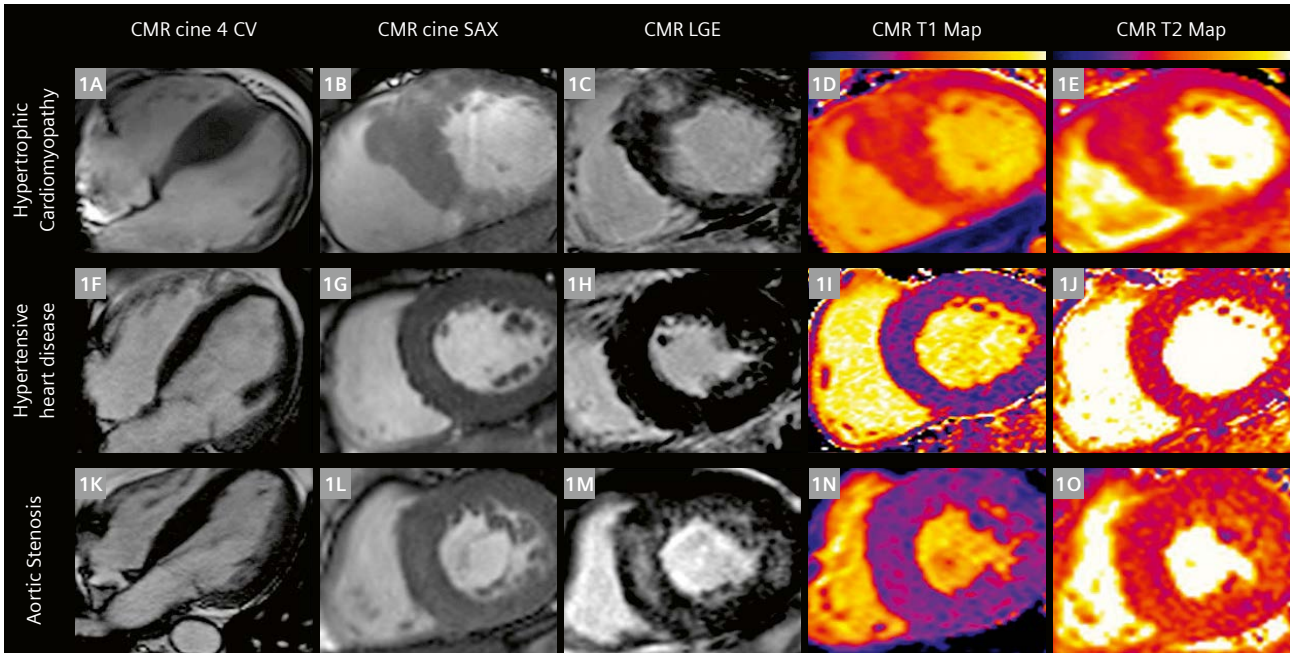

1 Patient diagnosed with hypertrophic cardiomyopathy **(1A–E)**. 4-chamber view and short axis cine images showing basal septal hypertrophy **(1A–B)**. Intramyocardial LGE basal septal within hypertrophic segments **(1c)**. Corresponding native T1 and T2 Maps **(1D–E)**.
Images from a patient with hypertensive heart disease **(1F–J)**. 4-chamber view and short axis cine images showing concentric hypertrophy **(1F–G)**. Normal LGE **(1H)**. Corresponding native T1 and T2 Maps **(1I–J)**.
A case with a patient suffering from severe aortic stenosis with a bicuspid aortic valve **(1K–O)**. 4-chamber view and short axis cine images showing concentric hypertrophy **(1K–L)**. Focal (septal) and diffuse fibrosis in a basal slice **(1M)**. Corresponding native T1 and T2 Maps **(1N–O)**.

is still growing, leading to an increased understanding of the impact of CMR for patients outside the expert community. Fortunately, in recent years the application of CMR in NIHD has also been integrated into the clinical workup of patients with acute coronary syndrome and non-ST-segment-elevation infarction, as the symptoms might be caused by myocarditis, takotsubo cardiomyopathy, or myocardial infarction with no obstructive coronary atherosclerosis (MINOCA) [3]. Interestingly, athletes at different levels should be guided based on CMR, as published last year in the ESC Guidelines on sports cardiology [4]. For example, athletes with a history of myocarditis should only return to competitive sports after a persistent myocardial injury has been excluded by CMR.

During the last years, it has become increasingly evident that the quantification of the cardiac function and myocardial structure is crucial for a diagnostic decision. This major step will also challenge the community, as a significant effort is needed to ensure quality assurance and standardization. Most of the diagnoses in NIHD are based on quantitative measures.

In the following sections, we will highlight some aspects of this topic.

Differentiation of left ventricular hypertrophy

Left ventricular hypertrophy (LVH) is usually diagnosed by echocardiography or CMR based on detecting a left ventricular wall thickness at end-diastole of at least 13–15 mm [5, 6] and/or an increased left ventricular mass index [7]. Both methods can additionally provide the mass-volume index and the relative wall thickness, which can help to differentiate between concentric and eccentric hypertrophy, and to stratify the risk of cardiovascular events [8, 9]. The true challenge lies in breaking down the broad differential diagnosis of LVH, which is either caused by a pathophysiological stimulus like pressure or volume overload, or by pathological causes ranging from genetic to infiltrative disorders [10].

In all cases of unknown LVH, hypertrophic cardiomyopathy (HCM) should be ruled out [5], as it is one of the major contributors to sudden cardiac death (SCD). The strength of CMR in this entity is the detection of areas of fibrosis using late gadolinium enhancement (LGE) (Fig. 1C) as a modifier in the risk stratification and to delineate it from physiological causes of LVH. Even in cases without LGE, increased native T1 and/or ECV values can detect diffuse fibrosis and aid in the differential diagnosis [11]. Furthermore, CMR can provide quantitative planimetric evaluation of the left ventricular outflow tract. This robust marker can be used to accurately differentiate obstructive from non-obstructive disease and to monitor the effect of septal reduction therapies [10]. It is important to remember that other disorders can hide behind an HCM phenotype.

One chameleon capable of mimicking HCM is hypertensive heart disease (HHD) due to long-term arterial hypertension. Assessment of LV cine images might show concentric hypertrophy [12] and LGE in a nonspecific intramyocardial pattern [13] (Fig. 1F–J). Follow-up exams with CMR can monitor left ventricular wall thickness in response to anti-remodeling therapy in HHD [14]. Our recent study, currently in review, compared cine acquisitions accelerated by compressed sensing to standard bSSFP acquisitions. We could prove that without compromising diagnostic capability, equivalent function and mass assessment of LV and RV is possible with a time reduction of more than 50%, making frequent CMR exams even more feasible. Aortic stenosis, which causes LVH in a similar manner, could lead to diffuse fibrosis of the myocardium. Quantitative markers such as T1 and ECV could help in the future to decide about the timing of therapy and to predict outcomes and prognoses. [15] (Fig. 1K–O).

Another important entity to consider in the workup of LVH and HCM is the so-called athlete's heart, a condition linked to an increased exercise burden. T1, T2, and ECV values are of help as they appear to be in the normal range in most cases with exercise-induced LVH [16].

LVH can also be caused by storage diseases. This differentiation is one of the strongest applications of CMR as the diagnosis will change the therapy. Different entities will be discussed in the chapter about restrictive cardiomyopathies (RCM).

Figure 1 summarizes different causes of left ventricular hypertrophy and their appearance in CMR.

Restrictive cardiomyopathies

A rare but nevertheless important group of NIHD are restrictive cardiomyopathies (RCM) caused by systemic and infiltrative disorders. CMR plays a crucial role in amyloidosis. LGE shows diffuse myocardial involvement with characteristic hypointense blood and hyperintense myocardium with coexisting pericardial and pleural effusions. This pattern is often diagnosed in AL-amyloidosis, whereas parametric mapping also allows the identification of other subgroups. Typically, significantly elevated T1 and/or ECV values are found throughout the myocardium (Fig. 2A–E). The native T1 and ECV values are useful markers for monitoring the progression of the disease [17, 18].

On the opposite end of the spectrum is Fabry disease where low native T1 values, caused by lipid accumulation, often raise suspicion. In addition, CMR can often detect a characteristic inferolateral fibrosis by LGE (Fig. 2F–J). Furthermore, CMR can aid in the decision when to start enzyme replacement and monitoring its effects [19].

CMR can provide evidence for cardiac involvement in sarcoidosis by means of cardiac morphology assessment, LGE, or T2-based imaging [10]. Unfortunately, the disease is a great imitator and can appear as HCM-, RCM- or dilated cardiomyopathy (DCM)-phenotypes. Even normal heart chambers on cine imaging can be found. LGE has a negative impact on the prognosis and often presents as a striking hyperintense subepicardial pattern [20] (Fig. 2K–O) [21].

Figure 2 exemplarily shows the wide array of tissue properties that CMR can provide during one scan.

Dilated cardiomyopathies

DCM refers to a spectrum of heterogeneous myocardial disorders and is defined by the presence of ventricular dilation and systolic dysfunction in the absence of any condition (hypertension, valvular, congenital, or ischemic heart disease) sufficient to cause global systolic impairment [22]. The role of CMR in the diagnostic and prognostic evaluation as well as in guiding treatment strategies in DCM patients has significantly increased in recent years. A CMR scan as part of the diagnostic workup should deploy a protocol that assesses the heart anatomy, left and right ventricular function, possible edema, myocardial tissue characterization, and scar formation. Cine imaging in long- and short-axis is recommended for right and left cardiac volume, function, and mass assessment due to its high accuracy and reproducibility [23]. A T2-based marker (T2W or T2-mapping) for edema, an essential component of acute or active inflammation, should be included, as well as T1-imaging (preferably T1-mapping and ECV-imaging, if available) for tissue characterization. Therefore, by deploying the updated Lake Louise criteria, CMR offers good specificity and sensitivity in detecting acute myocarditis, a frequent cause of ventricular dilatation [24] (Fig. 3F–J). Furthermore, cardiac involvement in systemic inflammatory diseases, which can cause subclini-

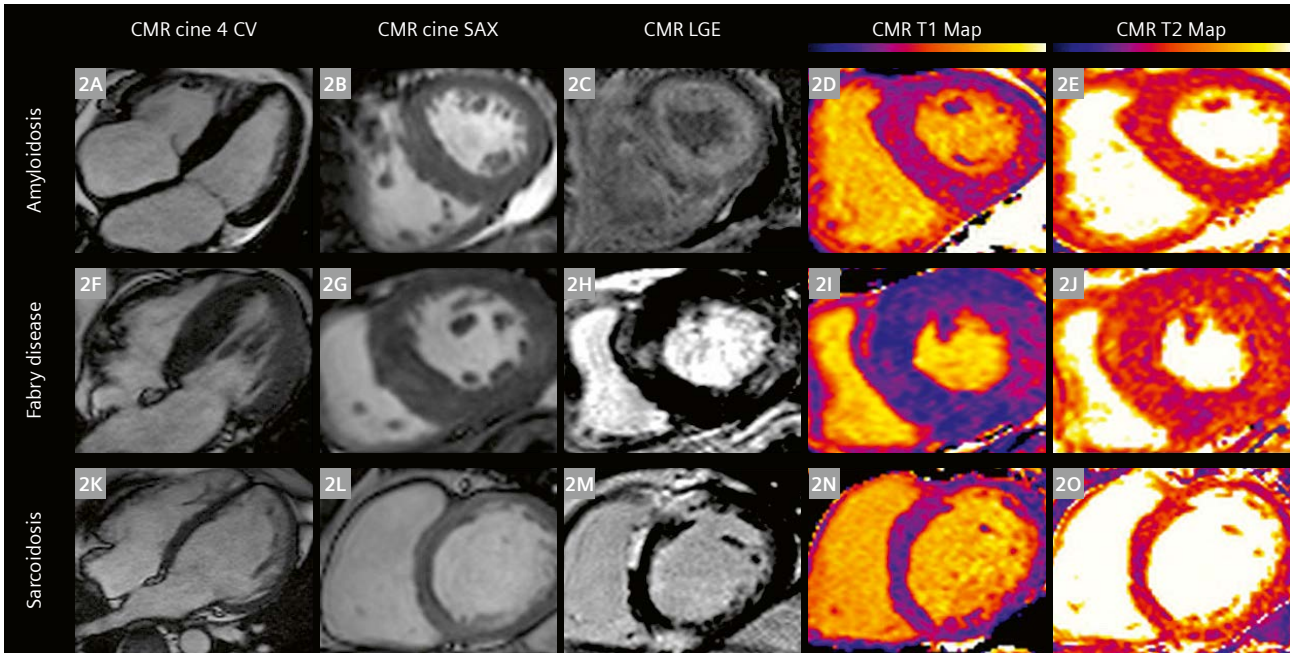

2 Images from a patient with cardiac amyloidosis **(2A–E)**. 4-chamber view and short axis cine images showing global hypertrophy accentuated septally **(2A–B)**. Characteristic LGE with hypointense blood pool and hyperintense myocardium **(2C)**. Corresponding native T1 and T2 Maps **(2D–E)**.
Images from a patient with Fabry disease **(2F–J)**. 4-chamber view and short axis cine images showing global left ventricular hypertrophy and increased papillary muscles **(2F–G)**. Characteristic focal LGE basal inferolateral and septal intramyocardial **(2H)**. Native T1 Map showing corresponding focally increased T1 values Please note the overall lower T1 values (violet colour) **(2I)**. Corresponding T2 Maps **(2J)**.
Images from a patient with confirmed sarcoidosis **(2K–O)**. 4-chamber view and short axis cine images showing a dilated left ventricle **(2K–L)**. Subepicardial, sharply demarcated LGE basal inferior and anteroseptal. Note the striking hyperintensity of the scars **(2M)**. Corresponding native T1 and T2 Maps **(2N–O)**.

cal myocarditis, can be detected and CMR parameters correlate with disease activity [25]. LGE-imaging is crucial for the diagnostic workup in DCM patients. It can differentiate between ischemic and non-ischemic causes of LV dilatation and systolic dysfunction [26]. In one quarter of patients with DCM, a typical intramural basal anteroseptal LGE is found, also known as "mid-wall sign" (Fig. 3C). LGE imaging in DCM patients can predict sudden cardiac death (SCD) and might identify patients who will benefit from an implantable cardioverter-defibrillator implantation, despite a left ventricular ejection fraction (LV-EF) >35% [27–29]. It should be kept in mind that many infiltrative cardiomyopathies that can present as RCMs can also mimic and present as DCMs. Once again, native T1-mapping and ECV-imaging provides myocardial tissue characterization and combined with specific LGE-patterns shows an excellent diagnostic accuracy in these entities as mentioned above [10] (Fig. 2).

Apart from sarcoidosis, other systemic disorders can also lead to DCM, but might also present with a preserved LVEF. Systemic diseases are characterized by the involvement of multiple organs with an autoimmune background. From a cardiological point of view, these disorders can present with inflammation of the peri- and myocardial tissues as well as early onset arterial disease [25]. The role of CMR is the assessment of potential myocardial involvement by detecting inflammation or fibrosis by the methods mentioned above [24]. Cardiac involvement in systemic lupus erythematosus (SLE) can be detected by CMR applying LGE and parametric sequences, even in subclinical stages [30, 31]. SLE as well as other entities may not only appear as a NIHD, but the coronaries could be affected as well. Especially vasculitic disorders are known to affect all vessels including the coronaries and the small intramyocardial vasculature [32].

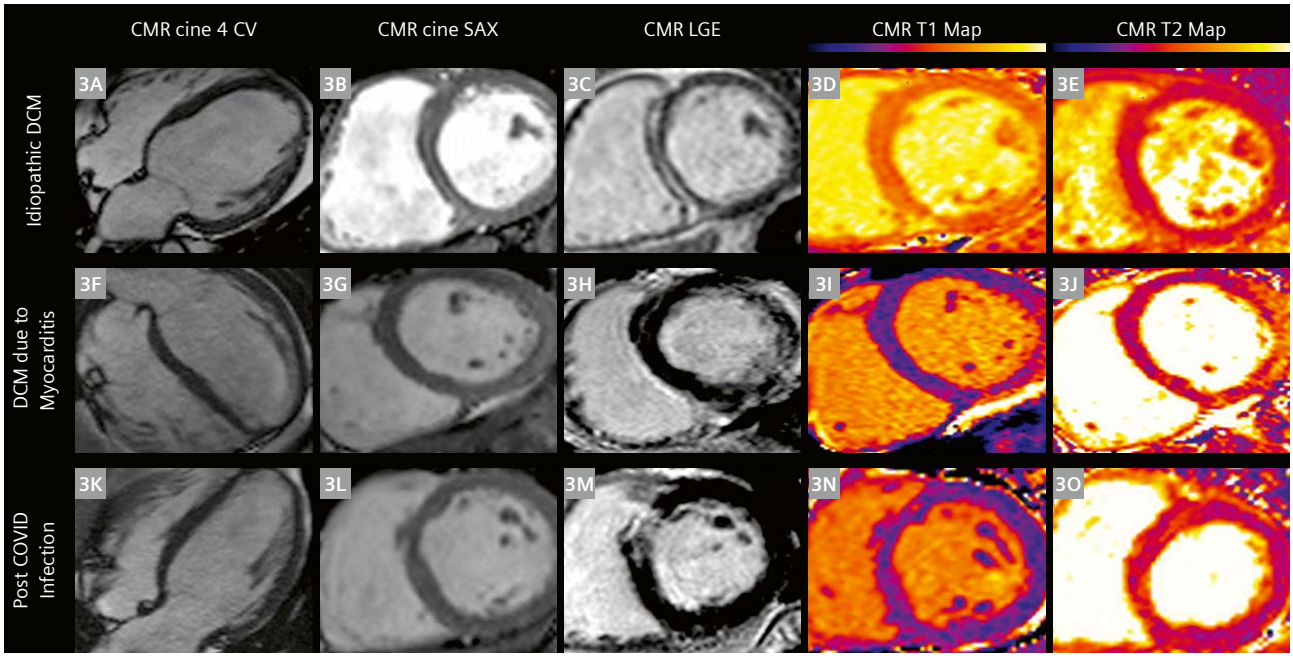

3 Images from a patient with an idiopathic dilated cardiomyopathy and excluded ischemic heart disease **(3A–E)**. 4-chamber view and short axis cine images showing a dilated left ventricle **(3A–B)**. LGE with mid-wall sign **(3C)**. Corresponding native T1 map with increased T1 values in the septal wall and T2 Map with normal values **(3D–E)**.
A case of dilated cardiomyopathy due to myocarditis **(3F–J)**. 4-chamber view and short axis cine images showing a dilated left ventricle **(3F–G)**. Focal subepicardial fibrosis/necrosis basal anterior and anterolateral **(3H)**. Corresponding native T1 and T2 Maps with increased values in segments with positive LGE **(3I–J)**.
A patient with dyspnoe and fatigue after a COVID-19 infection **(3K–O)**. 4-chamber view and short axis cine images **(3K–L)**. Small, focal subepicardial fibrosis basal inferior and septal. Possible of thromboembolic origin **(3M)**. Native T1 Map with increased values anteroseptal and corresponding T2 map with normal T2 values Map **(3N–O)**.

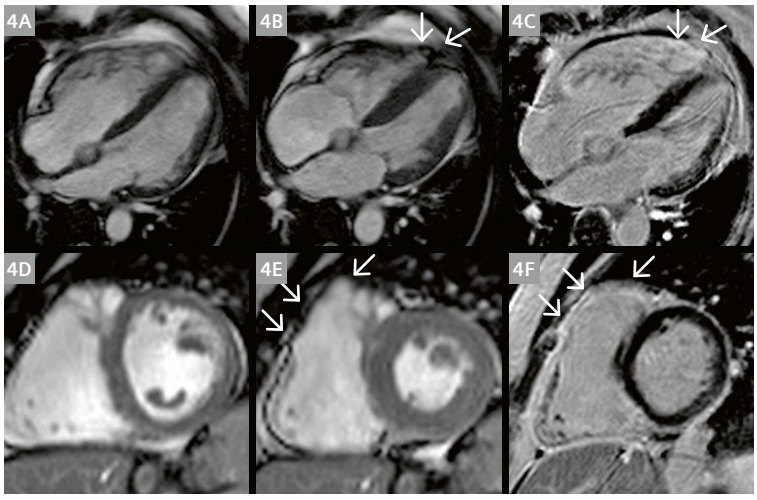

4 Cine imaging in a 39-year-old patient with AC and ventricular tachycardias and 2x syncope. Long axis **(4A–B)** and short axis **(4D–E)** end-diastolic (left) and end-systolic (middle) image. RV dilatation (EDV: 205 ml) and dysfunction (RVEF 38%). Focal RV dyskinetic wall motion **(arrows, 4B, 4E)**. Late gadolinium enhancement long axis **(4C)** and short axis **(4F)**. Focal enhancement in RV free wall, corresponding to the dysfunctional areas **(arrows, 4F)**.

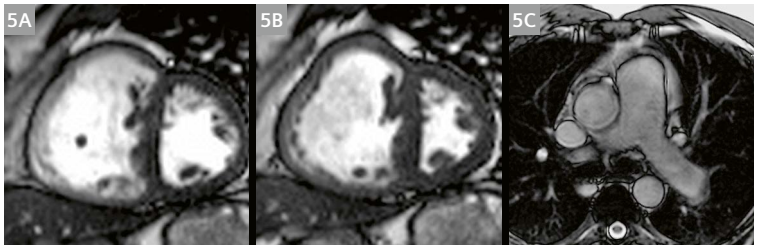

5 Cine imaging in a 40-year-old patient with pulmonary hypertension. Short axis end-diastolic **(5A)** and end-systolic **(5B)**. The interventricular septum bows leftwards (D-sign). RV dilatation (EDV: 293 ml) and dysfunction (RVEF 32%). RV hypertrophy and dilated central pulmonary artery **(5C)**.

Right ventricular diseases

The assessment and evaluation of the right ventricle is playing an increasing role in cardiovascular imaging. Several CMR studies could show that right ventricular systolic function might have an impact on the prognosis in a wide variety of disorders, including DCM [33], systemic sclerosis [34], sarcoidosis [35], and other forms of NIHD [36]. This evidence underlines the importance of continuing to investigate the role and the disorders of the right ventricle.

Arrhythmogenic right ventricular cardiomyopathy (ARVC) is a rare inherited heart muscle disease that may be a cause of SCD, particularly in young people. Due to known biventricular and left ventriclular involvement, the term "arrhythmogenic cardiomyopathy" (AC) has been suggested as a redefinition of this disease [37, 38].

To improve diagnosis and management of the disease, the minor and major Task Force criteria for AC were modified in 2010 by combining multiple aspects such as family history, ECG, arrhythmic, structural and functional, and histopathological findings [39]. Molecular genetics are playing an increasing role in the diagnosis of AC; however, it still remains very challenging.

CMR has become the gold-standard for assessing ventricular volumetric indexed measurements, systolic function, and regional wall motion abnormalities such as akinesia, dyskinesia, aneurysm, and bulging. The characterization of fibrofatty myocardial tissue composition is another method that is gaining clinical importance, but it still needs clinical validation [40]. The presence of intramyocardial fatty infiltration itself was not included due to difficulties in interpretation and low specificity [41]. Cine images are usually performed in four long axes: 4-chamber view (CV), 2CV, 3CV, and RV, as well as in a short-axis stack with whole RV coverage. However, in our experience, transversal cine images are best for evaluating the RV free wall and subtricuspid region [42]. LGE improves the diagnostic accuracy of CMR due to identification of fibrofatty changes (up to 70%) that correspond to the dysfunctional areas of cine imaging (Fig. 4) and to histopathological changes [43]. Additionally, use of LGE is of interest to evaluate concomitant LV involvement. Distinguishing fat from fibrosis by LGE sequences is challenging, but the improvement of fat-water (F/W) techniques has drastically optimized image quality and diagnostic accuracy. Interestingly, LV fatty infiltration was shown to be a prevalent finding in ARVC and can also lead to RV wall hypertrophy [44]. For this reason alone, F/W imaging should be a part of AC protocols.

Accurate interpretation of CMR in AC patients (Fig. 4) requires a great deal of expertise. The differential diagnosis should include congenital heart diseases, idiopathic right ventricular outflow tract tachycardia, pulmonary arterial hypertension (Fig. 5), Brugada syndrome, athlete's heart [45], genetic neuromuscular disorders, and myocarditis.

Summary

NHID may have different etiologies of which only some could be covered in this overview. NIHD is often the cause of heart failure (HF), with reduced or preserved cardiac function. HF affects a high percentage of patients and its impact is increasing in an ageing society. The etiology of HF is relevant for therapeutic decision-making. This highlights the impact of CMR, as opposed to other cardiac imaging modalities, because it can differentiate between underlying diseases and, in case of NIHD, it may act like a virtual biopsy. The current technology and knowledge allow us to drive these decisions already today, but the continuous developments on all aspects of the imaging process will enable us to further increase diagnostic accuracy.

Adapting a statement from one of the former SCMR boards in 2016, one could summarize:

Utilizing CMR instead of other imaging techniques provides more definitive, relevant, and actionable answers as a CMR exam provides comprehensive information and has superior and often unique diagnostic and prognostic power, without exposing patients to radiation. Therefore, CMR is a key enabler for precision medicine.

References

1 von Knobelsdorff-Brenkenhoff F, Pilz G, Schulz-Menger J. Representation of cardiovascular magnetic resonance in the AHA/ACC guidelines. J Cardiovasc Magn Reson. 2017;19(1):70.

2 von Knobelsdorff-Brenkenhoff F, Schulz-Menger J. Role of cardiovascular magnetic resonance in the guidelines of the European Society of Cardiology. J Cardiovasc Magn Reson. 2016;18:6.

3 Collet JP, Thiele H, Barbato E, Barthelemy O, Bauersachs J, Bhatt DL, et al. 2020 ESC Guidelines for the management of acute coronary syndromes in patients presenting without persistent ST-segment elevation. Eur Heart J. 2020; ehaa575.

4 Pelliccia A, Sharma S, Gati S, Back M, Borjesson M, Caselli S, et al. 2020 ESC Guidelines on sports cardiology and exercise in patients with cardiovascular disease. Eur Heart J. 2021;42(1):17-96.

5 Writing Committee M, Ommen SR, Mital S, Burke MA, Day SM, Deswal A, et al. 2020 AHA/ACC Guideline for the Diagnosis and Treatment of Patients With Hypertrophic Cardiomyopathy: Executive Summary: A Report of the American College of Cardiology/American Heart Association Joint Committee on Clinical Practice Guidelines. Circulation. 2020;142(25):e533-e57.

6 Authors/Task Force m, Elliott PM, Anastasakis A, Borger MA, Borggrefe M, Cecchi F, et al. 2014 ESC Guidelines on diagnosis and management of hypertrophic cardiomyopathy: the Task Force for the Diagnosis and Management of Hypertrophic Cardiomyopathy of the European Society of Cardiology (ESC). Eur Heart J. 2014;35(39):2733-79.

7 Lang RM, Badano LP, Mor-Avi V, Afilalo J, Armstrong A, Ernande L, et al. Recommendations for cardiac chamber quantification by echocardiography in adults: an update from the American Society of Echocardiography and the European Association of Cardiovascular Imaging. Eur Heart J Cardiovasc Imaging. 2015;16(3):233-70.

8 Corden B, de Marvao A, Dawes TJ, Shi W, Rueckert D, Cook SA, et al. Relationship between body composition and left ventricular geometry using three dimensional cardiovascular magnetic resonance. J Cardiovasc Magn Reson. 2016;18(1):32.

9 Tsao CW, Gona PN, Salton CJ, Chuang ML, Levy D, Manning WJ, et al. Left Ventricular Structure and Risk of Cardiovascular Events: A Framingham Heart Study Cardiac Magnetic Resonance Study. J Am Heart Assoc. 2015;4(9):e002188.

10 Leiner T, Bogaert J, Friedrich MG, Mohiaddin R, Muthurangu V, Myerson S, et al. SCMR Position Paper (2020) on clinical indications for cardiovascular magnetic resonance. J Cardiovasc Magn Reson. 2020;22(1):76.

11 Arcari L, Hinojar R, Engel J, Freiwald T, Platschek S, Zainal H, et al. Native T1 and T2 provide distinctive signatures in hypertrophic cardiac conditions - Comparison of uremic, hypertensive and hypertrophic cardiomyopathy. Int J Cardiol. 2020;306:102-108.

12 Rodrigues JC, Rohan S, Ghosh Dastidar A, Harries I, Lawton CB, Ratcliffe LE, et al. Hypertensive heart disease versus hypertrophic cardiomyopathy: multi-parametric cardiovascular magnetic resonance discriminators when end-diastolic wall thickness ≥ 15 mm. Eur Radiol. 2017;27(3):1125-35.

13 Rudolph A, Abdel-Aty H, Bohl S, Boye P, Zagrosek A, Dietz R, et al. Noninvasive detection of fibrosis applying contrast-enhanced cardiac magnetic resonance in different forms of left ventricular hypertrophy relation to remodeling. J Am Coll Cardiol. 2009;53(3):284-91.

14 Williams B, Mancia G, Spiering W, Agabiti Rosei E, Azizi M, Burnier M, et al. 2018 ESC/ESH Guidelines for the management of arterial hypertension. Eur Heart J. 2018;39(33):3021-104.

15 Everett RJ, Treibel TA, Fukui M, Lee H, Rigolli M, Singh A, et al. Extracellular Myocardial Volume in Patients With Aortic Stenosis. J Am Coll Cardiol. 2020;75(3):304-16.

16 Mordi I, Carrick D, Bezerra H, Tzemos N. T1 and T2 mapping for early diagnosis of dilated non-ischaemic cardiomyopathy in middle-aged patients and differentiation from normal physiological adaptation. Eur Heart J Cardiovasc Imaging. 2016;17(7):797-803.

17 Maurer MS, Bokhari S, Damy T, Dorbala S, Drachman BM, Fontana M, et al. Expert Consensus Recommendations for the Suspicion and Diagnosis of Transthyretin Cardiac Amyloidosis. Circ Heart Fail. 2019;12(9):e006075.

18 Martinez-Naharro A, Kotecha T, Norrington K, Boldrini M, Rezk T, Quarta C, et al. Native T1 and Extracellular Volume in Transthyretin Amyloidosis. JACC Cardiovasc Imaging. 2019;12(5):810-819.

19 Nordin S, Kozor R, Vijapurapu R, Augusto JB, Knott KD, Captur G, et al. Myocardial Storage, Inflammation, and Cardiac Phenotype in Fabry Disease After One Year of Enzyme Replacement Therapy. Circ Cardiovasc Imaging. 2019;12(12):e009430.

20 Schulz-Menger J, Wassmuth R, Abdel-Aty H, Siegel I, Franke A, Dietz R, et al. Patterns of myocardial inflammation and scarring in sarcoidosis as assessed by cardiovascular magnetic resonance. Heart. 2006;92(3):399-400.

21 Flamee L, Symons R, Degtiarova G, Dresselaers T, Gheysens O, Wuyts W, et al. Prognostic value of cardiovascular magnetic resonance in patients with biopsy-proven systemic sarcoidosis. Eur Radiol. 2020;30(7):3702-3710.

22 Pinto YM, Elliott PM, Arbustini E, Adler Y, Anastasakis A, Bohm M, et al. Proposal for a revised definition of dilated cardiomyopathy, hypokinetic non-dilated cardiomyopathy, and its implications for clinical practice: a position statement of the ESC working group on myocardial and pericardial diseases. Eur Heart J. 2016;37(23):1850-1858.

23 Grothues F, Smith GC, Moon JC, Bellenger NG, Collins P, Klein HU, et al. Comparison of interstudy reproducibility of cardiovascular magnetic resonance with two-dimensional echocardiography in normal subjects and in patients with heart failure or left ventricular hypertrophy. Am J Cardiol. 2002;90(1):29-34.

24 Ferreira VM, Schulz-Menger J, Holmvang G, Kramer CM, Carbone I, Sechtem U, et al. Cardiovascular Magnetic Resonance in Nonischemic Myocardial Inflammation: Expert Recommendations. J Am Coll Cardiol. 2018;72(24):3158-3176.

25 Caforio ALP, Adler Y, Agostini C, Allanore Y, Anastasakis A, Arad M, et al. Diagnosis and management of myocardial involvement in systemic immune-mediated diseases: a position statement of the European Society of Cardiology Working Group on Myocardial and Pericardial Disease. Eur Heart J. 2017;38(35):2649-62.

26 McCrohon JA, Moon JC, Prasad SK, McKenna WJ, Lorenz CH, Coats AJ, et al. Differentiation of heart failure related to dilated cardiomyopathy and coronary artery disease using gadolinium-enhanced cardiovascular magnetic resonance. Circulation. 2003;108(1):54-9.

27 Assomull RG, Prasad SK, Lyne J, Smith G, Burman ED, Khan M, et al. Cardiovascular magnetic resonance, fibrosis, and prognosis in dilated cardiomyopathy. J Am Coll Cardiol. 2006;48(10):1977-85.

28 Di Marco A, Anguera I, Schmitt M, Klem I, Neilan TG, White JA, et al. Late Gadolinium Enhancement and the Risk for Ventricular Arrhythmias or Sudden Death in Dilated Cardiomyopathy: Systematic Review and Meta-Analysis. JACC Heart Fail. 2017;5(1):28-38.

29 Halliday BP, Gulati A, Ali A, Guha K, Newsome S, Arzanauskaite M, et al. Association Between Midwall Late Gadolinium Enhancement and Sudden Cardiac Death in Patients With Dilated Cardiomyopathy and Mild and Moderate Left Ventricular Systolic Dysfunction. Circulation. 2017;135(22):2106-2115.

30 Guo Q, Wu LM, Wang Z, Shen JY, Su X, Wang CQ, et al. Early Detection of Silent Myocardial Impairment in Drug-Naive Patients With New-Onset Systemic Lupus Erythematosus: A Three-Center Prospective Study. Arthritis Rheumatol. 2018;70(12):2014-2024.

31 Mavrogeni S, Bratis K, Markussis V, Spargias C, Papadopoulou E, Papamentzelopoulos S, et al. The diagnostic role of cardiac magnetic resonance imaging in detecting myocardial inflammation in systemic lupus erythematosus. Differentiation from viral myocarditis. Lupus. 2013;22(1):34-43.

32 Raman SV, Aneja A, Jarjour WN. CMR in inflammatory vasculitis. J Cardiovasc Magn Reson. 2012;14(1):82.

33 Gulati A, Ismail TF, Jabbour A, Alpendurada F, Guha K, Ismail NA, et al. The prevalence and prognostic significance of right ventricular systolic dysfunction in nonischemic dilated cardiomyopathy. Circulation. 2013;128(15):1623-33.

34 Hachulla AL, Launay D, Gaxotte V, de Groote P, Lamblin N, Devos P, et al. Cardiac magnetic resonance imaging in systemic sclerosis: a cross-sectional observational study of 52 patients. Ann Rheum Dis. 2009;68(12):1878-84.

35 Velangi PS, Chen KA, Kazmirczak F, Okasha O, von Wald L, Roukoz H, et al. Right Ventricular Abnormalities on Cardiovascular Magnetic Resonance Imaging in Patients With Sarcoidosis. JACC Cardiovasc Imaging. 2020;13(6):1395-1405.

36 Pueschner A, Chattranukulchai P, Heitner JF, Shah DJ, Hayes B, Rehwald W, et al. The Prevalence, Correlates, and Impact on Cardiac Mortality of Right Ventricular Dysfunction in Nonischemic Cardiomyopathy. JACC Cardiovasc Imaging. 2017;10(10 Pt B):1225-1236.

37 Sen-Chowdhry S, Syrris P, Prasad SK, Hughes SE, Merrifield R, Ward D, et al. Left-dominant arrhythmogenic cardiomyopathy: an under-recognized clinical entity. J Am Coll Cardiol. 2008;52(25):2175-87.

38 Corrado D, van Tintelen PJ, McKenna WJ, Hauer RNW, Anastastakis A, Asimaki A, et al. Arrhythmogenic right ventricular cardiomyopathy: evaluation of the current diagnostic criteria and differential diagnosis. Eur Heart J. 2020;41(14):1414-1429.

39 Marcus FI, McKenna WJ, Sherrill D, Basso C, Bauce B, Bluemke DA, et al. Diagnosis of arrhythmogenic right ventricular cardiomyopathy/dysplasia: proposed modification of the task force criteria. Circulation. 2010;121(13):1533-41.

40 Perazzolo Marra M, Rizzo S, Bauce B, De Lazzari M, Pilichou K, Corrado D, et al. Arrhythmogenic right ventricular cardiomyopathy. Contribution of cardiac magnetic resonance imaging to the diagnosis. Herz. 2015;40(4):600-6.

41 Tandri H, Castillo E, Ferrari VA, Nasir K, Dalal D, Bomma C, et al. Magnetic resonance imaging of arrhythmogenic right ventricular dysplasia: sensitivity, specificity, and observer variability of fat detection versus functional analysis of the right ventricle. J Am Coll Cardiol. 2006;48(11):2277-84.

42 Schulz-Menger J, Bluemke DA, Bremerich J, Flamm SD, Fogel MA, Friedrich MG, et al. Standardized image interpretation and post-processing in cardiovascular magnetic resonance – 2020 update: Society for Cardiovascular Magnetic Resonance (SCMR): Board of Trustees Task Force on Standardized Post-Processing. J Cardiovasc Magn Reson. 2020;22(1):19.

43 Tandri H, Saranathan M, Rodriguez ER, Martinez C, Bomma C, Nasir K, et al. Noninvasive detection of myocardial fibrosis in arrhythmogenic right ventricular cardiomyopathy using delayed-enhancement magnetic resonance imaging. J Am Coll Cardiol. 2005;45(1):98-103.

44 Te Riele AS, James CA, Philips B, Rastegar N, Bhonsale A, Groeneweg JA, et al. Mutation-positive arrhythmogenic right ventricular dysplasia/cardiomyopathy: the triangle of dysplasia displaced. J Cardiovasc Electrophysiol. 2013;24(12):1311-20.

45 D'Ascenzi F, Pisicchio C, Caselli S, Di Paolo FM, Spataro A, Pelliccia A. RV Remodeling in Olympic Athletes. JACC Cardiovasc Imaging. 2017;10(4):385-93.

Contact

Professor Jeanette Schulz-Menger, M.D.
University Medicine Berlin
Charité Campus Buch, ECRC
HELIOS Clinics Berlin-Buch
Department of Cardiology and Nephrology
Lindenberger Weg 80
13125 Berlin
Germany
Tel.: +49 30 040153536
jeanette.schulz-menger@charite.de

Jeanette Schulz-Menger

Jan Gröschel

Maximilian Fenski

Edyta Blaszczyk

Case Report: CMR of Myocardial Inflammation Regression in Convalescence of Acute Myocarditis Caused by SARS-CoV-2

Felipe Toth Renda Dias; Fernanda Albano; Lara Leite; Camila Silveira; Bruno A. de Azevedo; Manuel Nicolas Cano; Silvia Judith Fortunato de Cano; Carlos E. Prazereres[1]; Juliana M. Bello; Adriano Carneiro; Valeria M. Moreira; Tiago A. Magalhães; Carlos Eduardo Rochitte

[1]Hospital do Coração de São Paulo, HCOR, Cardiovascular CMR and CCT sector, São Paulo, Brazil

Abstract

A patient with recent COVID-19 infection and chest pain was diagnosed with acute myocarditis caused by SARS-CoV-2. Cardiovascular magnetic resonance (CMR) imaging performed on presentation and two months later demonstrated myocardial inflammation regression, defined by disappearance of myocardial edema on T2-weighted images, and significant decline in the extent of late gadolinium enhancement (LGE) between CMR exams. Despite the favorable imaging and clinical evolution of the acute myocarditis, T1 and T2 myocardial values and extracellular volume measurements remained slightly elevated in segments previously affected by edema and LGE compared to unaffected segments.

Case report

A 58-year-old male patient with dyslipidemia receiving rosuvastatin and with a positive RT-PCR for COVID-19 from April 28, 2020, arrived at the emergency department of a tertiary hospital in São Paulo, Brazil, on May 12, 2020. He presented with intermittent chest pain radiating out to the left arm and lasting four hours with progressive worsening. On admission, a hypothesis of acute coronary syndrome was made. ECG showed sinus rhythm without ST segment elevation, and troponin I was elevated with 8.3 ng/mL (reference value: below 0.034 ng/mL). He was medicated with 200 mg aspirin and 600 mg clopidogrel, and referred for invasive coronary cardiac catheterization. An uneventful procedure was performed showing a 40% stenotic ostial lesion in the first diagonal branch, without signs of unstable coronary plaque. Acute coronary syndrome was therefore ruled out. Due to the patient's previous COVID-19 infection, a new RT-PCR was performed on the day he was admitted, and returned a positive result. He was placed on the intensive care unit, and a progressive increase in troponin (up to 12.5 ng/mL) was observed. This led to a new working diagnostic hypothesis of acute myocarditis secondary to COVID-19. COVID-19 serological tests showed elevated IgG and IgM levels (41.86 AU/ml and 1.81 AU/ml, respectively), confirming a current infection by SARS-CoV-2. Other acute viral infections were ruled out by specific serological tests: negative tests for Coxsackie B antibodies, adenovirus, HIV, toxoplasmosis, cytomegalovirus, Epstein-Barr virus (last three tests: IgM negative and IgG positive, indicating previous infection). He was then referred for a cardiovascular magnetic resonance (CMR)

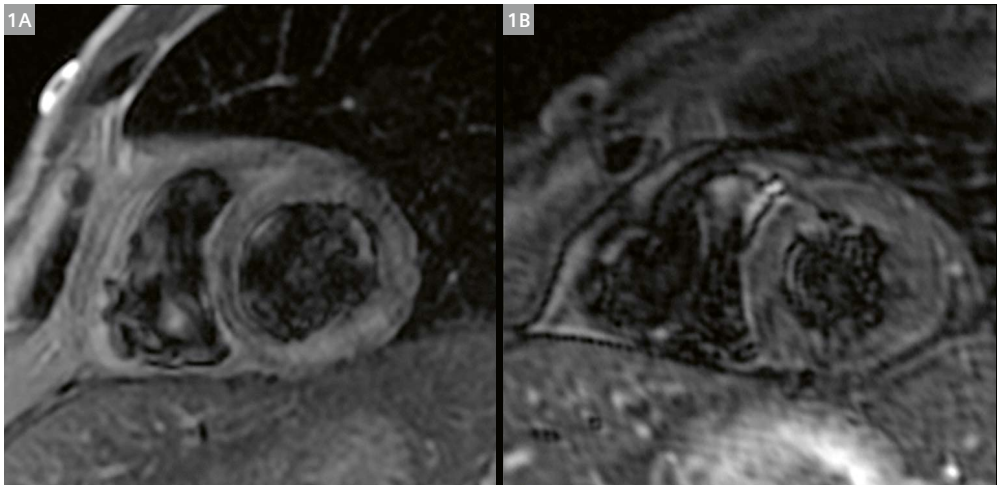

1 Myocardial Edema Regression: left ventricle short-axis T2-weighted images during acute phase of myocarditis **(1A)** with evident increase in signal intensity in inferior and inferolateral segments; resolution of the increased myocardial signal intensity in the same segments on images from a CMR exam two months later **(1B)**.

exam. The left ventricle showed preserved dimensions and ejection fraction (LVEF of 64%). Myocardial edema in the basal and middle anteroseptal and inferolateral segments were noted (Fig. 1A). Late gadolinium enhancement at mid-wall and subepicardial layers in basal and middle anteroseptal and inferolateral segments was also observed, compatible with non-ischemic myocardial injury (Fig. 2A) and confirming the acute myocarditis diagnosis. Losartan was then introduced to the therapeutic regimen. The patient showed a decline in troponin levels (2.94 and 0.7 ng/mL) and clinical improvement, and was discharged on May 19, 2020, for outpatient follow-up. On July 13, 2020, nine weeks after his hospitalization, the patient returned, asymptomatic, to undergo a follow-up CMR. Preserved cardiac chamber dimensions and LVEF, and resolution of myocardial edema were seen (Fig. 1B). Myocardial LGE was still present (Fig. 2B), though its extent was significantly decreased compared to baseline CMR (9 vs. 4 LV segments with LGE, and 15.4 g or 11.1% of LV mass vs. 5.3 g or 3.7% of LV mass, Fig. 2B). In the follow-up CMR, myocardial maps were also acquired, and native T1 and T2 values and extracellular volume (ECV)

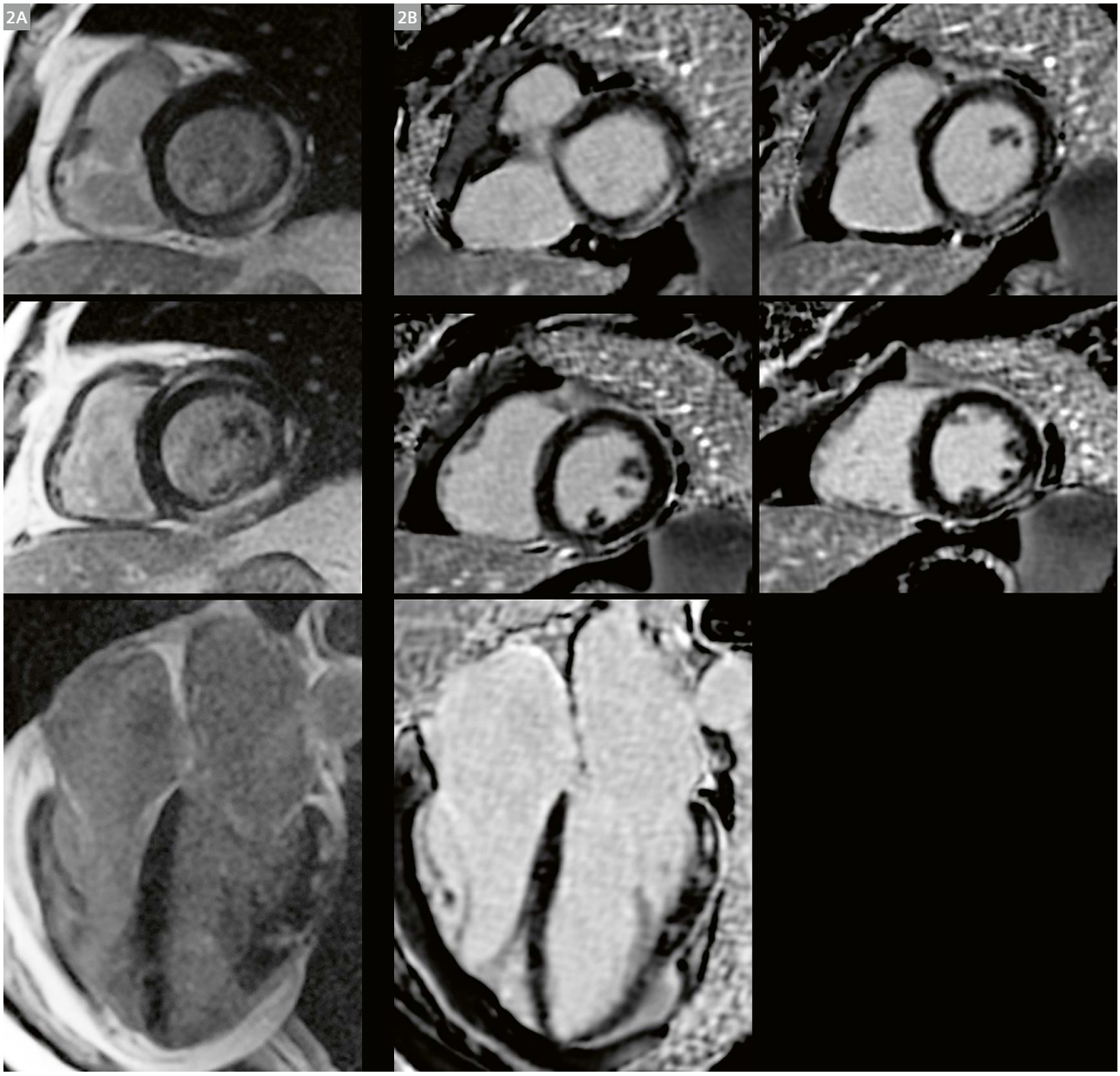

2 **Myocardial Late Gadolinium Enhancement (LGE) Regression:** long-axis (bottom row) and short-axis LGE images during acute phase of myocarditis **(2A)** and at two-month follow-up CMR exam **(2B)**; significant reduction of the extent of LGE seen in the short-axis and long-axis views.

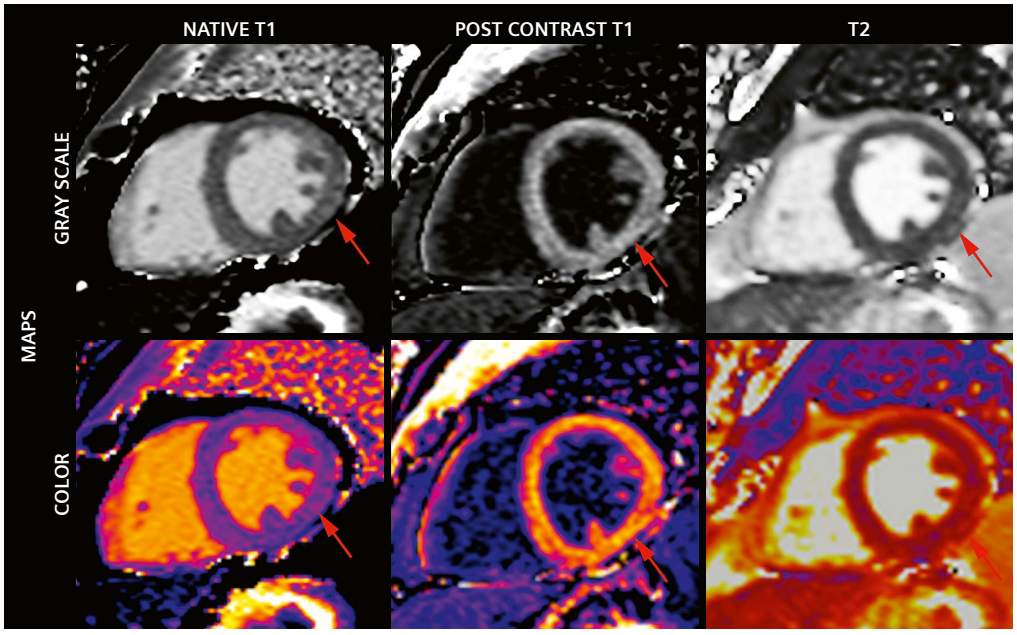

3 **Myocardial Maps:** native T1, post-contrast T1 and T2; grayscale (top row) and color (bottom row) maps; red arrows indicate inferolateral segments with mildly elevated myocardial T1 and T2 values compared to inferoseptal values (see text).

were still elevated in the lateral wall compared to segments without LGE (native T1 myocardial values: 1014 ms vs. 982 ms; T2 values: 50 ms vs. 42 ms; and ECV 27% vs. 23%, respectively, Fig. 3). Despite the lack of myocardial T1 and T2 values on the baseline CMR, resolution of myocardial edema in T2w images and the reduction of LGE extent over the two-month period between the two CMR exams, along with the clinical improvement, indicate in this case a favorable evolution of myocardial inflammation after COVID-19 myocarditis. Nonetheless, elevated T1, T2, and ECV myocardial values in segments previously affected by LGE and edema compared to unaffected segments suggest that myocardial abnormalities may persist for a longer period with still-unknown clinical relevance in the specific context of COVID-19.

Conclusion

To our knowledge, this is the first case of convalescent COVID-19 with demonstration of myocardial inflammation regression in a short-term CMR follow-up for acute myocarditis caused by COVID-19. The case report also shows how Compressed Sensing CINE and free-breathing late gadolinium enhancement (LGE) allowed good diagnostic imaging even in a patient who was severely short of breath. However, despite the favorable evolution of the myocardial inflammation, the follow-up CMR also indicated that myocardial abnormalities may continue beyond two months. Further research on the clinical relevance of this in a COVID-19 setting is needed.

References

1 Huang L, Zhao P, Tang D, Zhu T, Han R, Zhan C, et al. Cardiac Involvement in Patients Recovered from COVID-2019 Identified Using Magnetic Resonance Imaging. JACC Cardiovasc Imaging. 2020;S1936-878X(20)30403-4. doi: 10.1016/j.jcmg.2020.05.004. Epub ahead of print.

2 Puntmann VO, Carerj ML, Wieters I, Fahim M, Arendt C, Hoffmann J, et al. Outcomes of Cardiovascular Magnetic Resonance Imaging in Patients Recently Recovered from Coronavirus Disease 2019 (COVID-19). JAMA Cardiol. 2020;e203557. doi: 10.1001/jamacardio.2020.3557. Epub ahead of print.

3 Rudski L, Januzzi JL, Rigolin VH, Bohula EA, Blankstein R, Patel AR, et al. Multimodality Imaging in Evaluation of Cardiovascular Complications in Patients with COVID-19: JACC Scientific Expert Panel. J Am Coll Cardiol. 2020;76(11):1345-1357. doi: 10.1016/j.jacc.2020.06.080. Epub 2020 Jul 22.

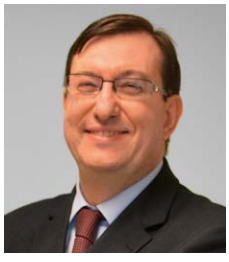

Contact

Carlos Eduardo Rochitte
Cardiovascular CMR and CCT Coordinator
Hospital do Coração, HCOR,
Cardiovascular CMR and CCT sector
Rua Desembargador Eliseu Guilherme, 147
Paraíso – São Paulo – SP – Brazil
Zip – 04004-030
rochitte@gmail.com

90-day trial licenses

Try them on your system

Recent publications [1–4] have shown that myocardial injury is not uncommon among COVID-19 patients. Cardiovascular MRI can be useful in both detecting and monitoring cardiac injury (e.g. myocarditis) as a possible complication of COVID-19.

To help clinicians perform comprehensive CMR exams, we offer free, 90-day trial licenses for our advanced cardiac applications (e.g. MyoMaps, PSIR HeartFreeze, Compressed Sensing Cardiac Cine).

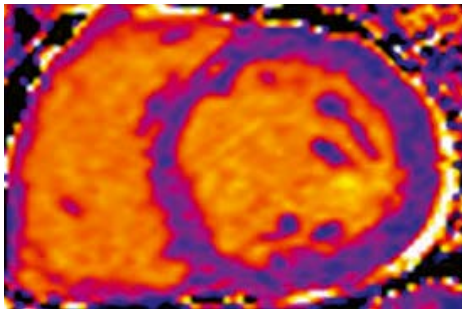

Image courtesy of: WG CMR Charité/ Helios Clinics Berlin-Buch

For further details, product overviews, image galleries, and general requirements visit us at:
www.siemens-healthineers.com/magnetic-resonance-imaging/options-and-upgrades

[1] *Shi S, Qin M, Shen B, et al. Association of Cardiac Injury with Mortality in Hospitalized Patients with COVID-19 in Wuhan, China. JAMA Cardiol. 2020 Jul 1;5(7):802-810. doi: 10.1001/jamacardio.2020.0950.*

[2] *Guo T, Fan Y, Chen M, et al. Cardiovascular Implications of Fatal Outcomes of Patients With Coronavirus Disease 2019 (COVID-19). JAMA Cardiol. 2020 Jul 1;5(7):811-818. doi: 10.1001/jamacardio.2020.1017. Erratum in: JAMA Cardiol. 2020 Jul 1;5(7):848.*

[3] *Inciardi RM, Lupi L, Zaccone G, et al. Cardiac Involvement in a Patient with Coronavirus Disease 2019 (COVID-19). JAMA Cardiol. 2020 Jul 1;5(7):819-824. doi: 10.1001/jamacardio.2020.1096.*

[4] *Puntmann VO, Carerj ML, Wieters I, et al. Outcomes of Cardiovascular Magnetic Resonance Imaging in Patients Recently Recovered from Coronavirus Disease 2019 (COVID-19). JAMA Cardiol. 2020 Nov 1;5(11):1265-1273. doi: 10.1001/jamacardio.2020.3557. Erratum in: JAMA Cardiol. 2020 Nov 1;5(11):1308.*

SIEMENS Healthineers

The Diagnostic Challenges of Myocarditis: Importance of Bioimaging Signatures with Parametric Mapping

Dr. Hafisyatul Aiza Zainal Abidin

Consultant Cardiologist, Department of Cardiology, Faculty of Medicine, Universiti Teknologi MARA (UiTM) Sg Buloh, Selangor, Malaysia

Introduction

Diagnosing myocarditis still poses a conundrum in cardiology practice, due to the disease's complexity and dynamic evolution [1, 2]. Presentation of myocarditis is non-specific; ranging from infarct-like chest pain, to heart failure, and even to sudden cardiac death [1]. Symptoms can last for days up to months, yet the duration and the progress of symptoms does not necessarily reflect the phases of myocarditis.

Endomyocardial biopsy was introduced in 1987 and became the gold standard for the diagnosis of myocarditis. It was the only way to access the histological changes of active inflammation in the myocardium (the presence of lymphocytes or macrophages, or evidence of myocyte necrosis) and to detect the presence of viral infection. Immunohistochemistry analysis has further improved the diagnostic sensitivity of this approach, and is particularly useful in subacute or chronic myocarditis [3].

Unfortunately, endomyocardial biopsy comes with several clinical and technical challenges. It requires skilled operators, adequate quality of myocardial sample, and an accredited pathologist to interpret the results. There is also a lack of standardization across pathology labs, and the procedure carries some clinical risk [3, 4].

Technical advances in cardiovascular magnetic resonance (CMR) enable both qualitative and quantitative assessment of myocardial inflammation non-invasively. CMR also offers the advantage of a diagnostic approach without ionizing radiation, and provides online image availability, unlike nuclear techniques.

The following cases illustrate the effective diagnosis and assessment of myocarditis with non-invasive CMR imaging.

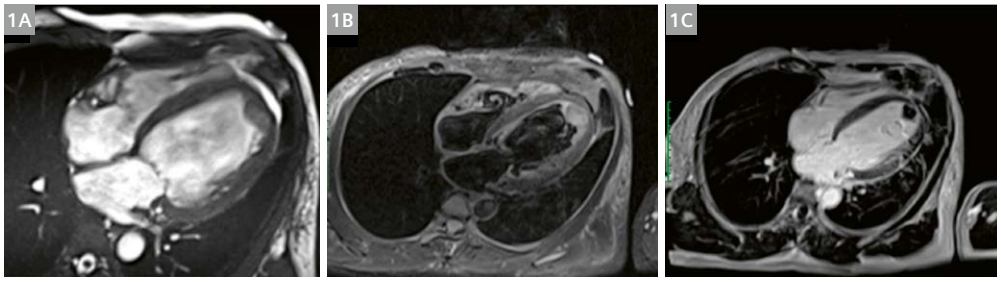

1 On admission. **(1A)** shows cine image of dilated left ventricle (LV), **(1B)** shows T2 STIR image with no evidence of hyperintensity signal, **(1C)** shows LGE image with no hyperenhancement.

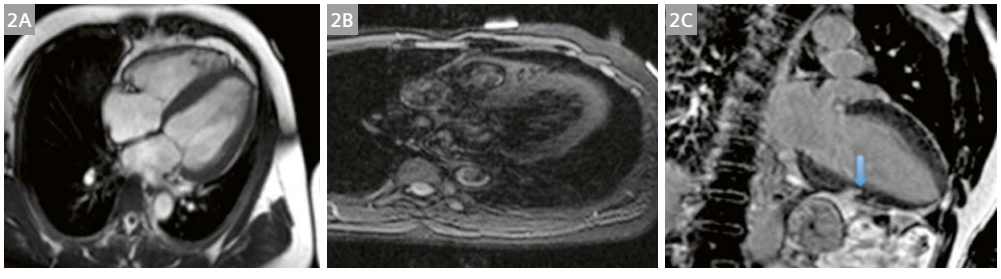

2 At 3 months. **(2A)** shows cine image of normalization of LV size, **(2B)** shows T2 STIR with no hyperintensity signal, **(2C)** shows LGE image with focal epicardial enhancement.

Case 1

A 45-year-old male was referred for evaluation with a one-week history of dyspnea. He was clinically in heart failure on presentation. His troponin T was normal. Coronary angiography revealed normal coronary arteries. He tested positive for human immunodeficiency virus (HIV). The patient was sent for a CMR exam to assess the etiology of his heart failure.

Figures 1A-C show imaging performed at admission. The LV chamber was dilated with global hypokinesia. Systolic function was depressed. There was no evidence of edema on the T2 STIR image (Fig. 1B), or presence of replacement scar on late gadolinium enhancement (LGE) imaging, except the presence of apical LV clot. The patient was treated with guideline directed medical therapy for heart failure, plus anticoagulants.

Follow-up CMR imaging, performed after three months, is shown in Figures 2A-C. LV volume had normalized, with marked improvement of systolic function to 45%. The LV clot had resolved. However, there was non-ischemic focal epicardial LGE (Fig. 2C blue arrow), seen at the mid inferior wall, suggestive of myocarditis.

Case 2

A 68-year-old male, with known atypical chest pain for one month, was sent for CMR to assess his underlying risk for coronary ischemia and possible non-coronary chest pain etiology. He was known to have had HIV for five years, and to have been very compliant to his highly active anti-retroviral therapy (HAART) medications. He also had a history of previously treated syphilis seven years before.

Figures 3C-D show the presence of non-ischemic LGE at the basal to mid inferolateral and inferior wall. On a 3T scanner (MAGNETOM Skyra, Siemens Healthcare, Erlangen, Germany) native T1 and native T2 values (Figs. 3A, B) are both markedly elevated. Viral load remained suppressed, but reevaluation of syphilis serology showed reactivation of syphilis, which was treated again. A follow-up scan three months after syphilis treatment showed a similar replacement fibrosis burden. However, active inflammation had now resolved, with normalization of native T2 value (36 ms) and improvement in native T1 (1150 ms).

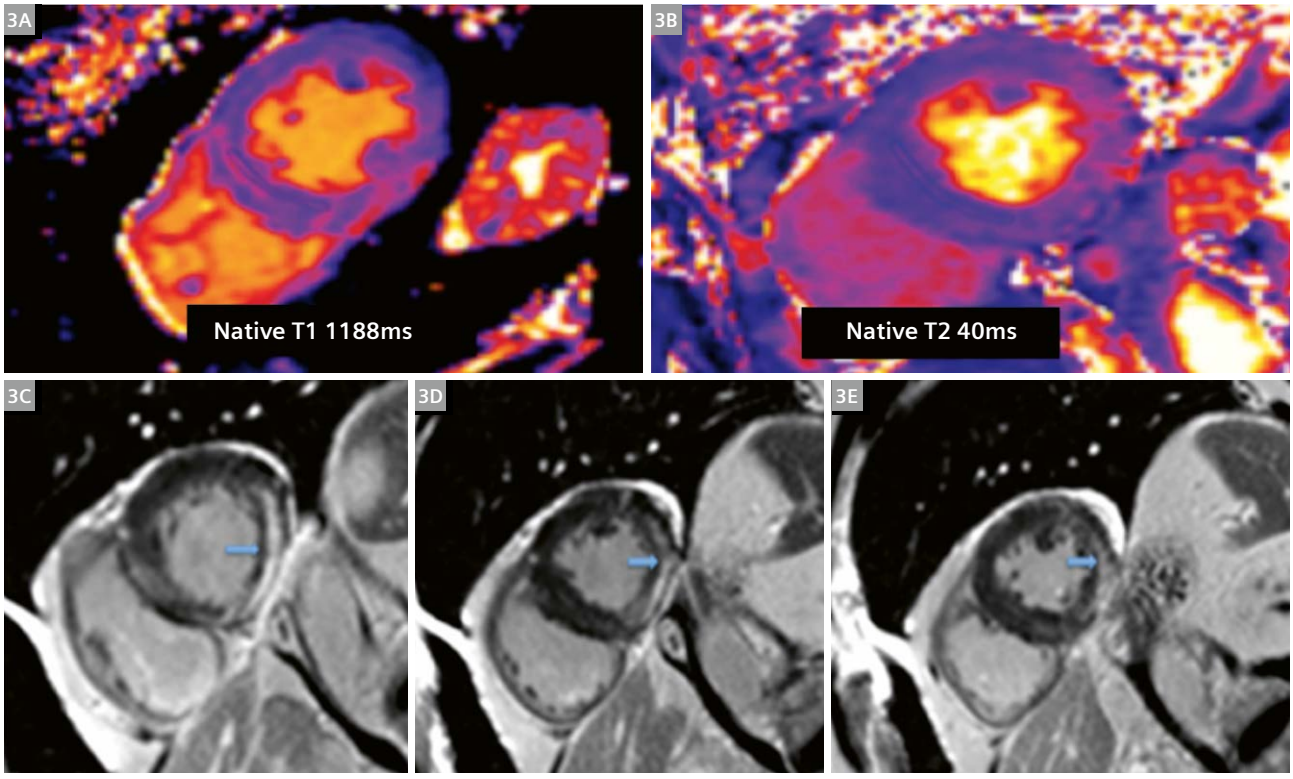

3 **(3A)** shows a native T1 value 1188 ms (normal < 1010 ms), **(3B)** shows elevated native T2 (normal < 37 ms), **(3C–E)** show LGE images with intramyocardial and epicardial enhancement at the inferolateral and inferior wall, as marked by the blue arrows.

Discussion

Case 1 illustrates a case of HIV myocarditis in which a retrospective diagnosis was made after detection of myocardial scar during follow-up imaging. The etiology of the patient's non-ischemic heart failure could not be determined during the initial scan, because CMR detects only the presence or absence of signal changes that are the result of underlying tissue inflammation.

Case 2 illustrates a case of syphilis in which the diagnosis of active myocarditis was made with elevated values of native T1 at 1188 ms and native T2 at 40 ms. Recovery progress was monitored at four months with improvement of bioimaging marker of native T1 (1150 ms) and native T2 (36 ms) despite a similar burden of non-ischemic scar as the initial scan.

These cases show that native T1 and native T2 techniques can objectively reveal interstitial fibrosis and tissue edema occurring as reactions to initial triggers (either viral or non-viral). Compared with biopsy, this approach allows better and earlier recognition of myocardial changes before the replacement fibrosis takes place.

Although LGE imaging is a sensitive technique to detect focal myocardial damage, it lacks the ability to differentiate the state of disease activity, especially in myocarditis. Qualitative assessment of the inflamed myocardium with T2-weighted and LGE imaging allows visualization of disease activity at the time of the scan, but can only track disease progress with follow-up scans.

The revolution of parametric mapping with CMR has narrowed the knowledge gap in myocarditis. The old paradigm, which categorized the condition as either acute or chronic myocarditis, has not allowed us to move forward in studying effective treatment for myocarditis as well as effective methods to monitor disease evolution. With these new insights from MyoMaps, we should view myocarditis with a new temporal perspective – as active myocarditis, recovering myocarditis, and healed myocarditis (which may have reoccurrences).

Despite differences in sequences employed to obtain mapping, the incorporation of bioimaging signatures with parametric maps and LGE imaging, using our standardized exam card, allows for shorter examination time and at the same time provides a productive and highly reproducible technique for diagnosing myocarditis. Now the task is to make parametric mapping with CMR technically available across the globe, especially in the Southeast Asia region, where I reside.

References

1 Cooper LT. Myocarditis. N Engl J Med. 2009;360(15):1526-38. Available from: https://doi.org/10.1056/NEJMra0800028
2 Heymans S, Eriksson U, Lehtonen J, Cooper LT. The Quest for New Approaches in Myocarditis and Inflammatory Cardiomyopathy. J Am Coll Cardiol. 2016;68(21):2348-64.
3 Caforio ALP, Pankuweit S, Arbustini E, Basso C, Gimeno-Blanes J, Felix SB, et al. Current state of knowledge on aetiology, diagnosis, management, and therapy of myocarditis: A position statement of the European Society of Cardiology Working Group on Myocardial and Pericardial Diseases. Eur Heart J. 2013;34(33):2636-48.
4 Puntmann VO, Zeiher AM, Nagel E. T1 and T2 mapping in myocarditis: seeing beyond the horizon of Lake Louise criteria and histopathology. Expert Rev Cardiovasc Ther. 2018;16(5):319-30. Available from: https://doi.org/10.1080/14779072.2018.1455499

Contact

Dr. Hafisyatul Aiza Zainal Abidin
Consultant Cardiologist
Department of Cardiology
Faculty of Medicine
Universiti Teknologi MARA (UiTM) Sg Buloh
Selangor
Malaysia
hafi_sya@yahoo.com

Cardiovascular Magnetic Resonance in Autoimmune Rheumatic Diseases: Translating the Greek Experience to the International Arena

George Markousis-Mavrogenis[1]; Anna Livaniou[2]; Fotini Lazarioti[2]; Sophie I. Mavrogeni[1,3]

[1]Onassis Cardiac Surgery Center, Athens, Greece
[2]Olympic Diagnostic Center, Piraeus, Greece
[3]National and Kapodistrian University of Athens, Greece

Introduction

Autoimmune rheumatic diseases (ARDs) are a diverse group of diseases that result from the dysregulation of immune tolerance and the subsequent generation of inappropriate immune responses to self-antigens [1]. ARDs can be localized to individual organ systems or may manifest with generalized multi-system involvement and/or multi-organ dysfunction [1]. Recent years have seen a considerable increase in our understanding of the molecular processes underlying the pathophysiology of ARDs and clinical management has changed dramatically with the advent of novel monoclonal antibodies and small molecule inhibitors that can effect targeted immunomodulation in these patients [2]. Yet despite improvements in overall prognosis and quality of life, ARD patients are still more likely to die than the general population [3–10].

This increased mortality has partially been attributed to a higher incidence of cardiovascular disease (CVD) in ARD patients. Traditionally, most practice guidelines suggest that the additional CVD risk observed in these patients is a consequence of systemic inflammation compounded by uncontrolled comorbidities such as hypertension, diabetes mellitus/metabolic syndrome, dyslipidemia etc. [5]. The guidelines therefore advise appropriate control of these comorbidities as the optimal method for combating CVD in ARD patients [11]. However, it has also become apparent that autoimmune cardiomyopathy is not an uncommon disease manifestation in ARD patients, and in some cases is accompanied by autoimmune vasculitis, microvascular dysfunction or other vascular pathology, valvular disease, pericarditis, or non-bacterial endocarditis [9]. Interestingly, many of these types of autoimmune CVD can be completely asymptomatic. Even when they start causing symptoms, such as reduced functional capacity or fatigue, these might simply be attributed to constitutional symp-

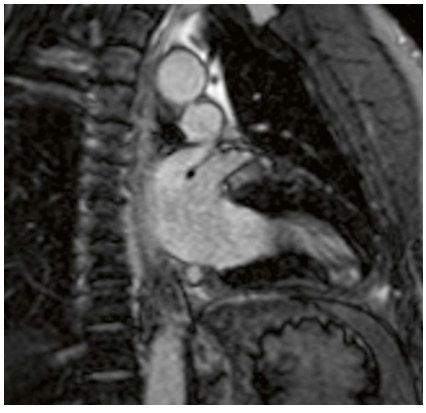

1 Transmural apical late gadolinium enhancement (LGE) due to myocardial infarction in a patient with rheumatoid arthritis.

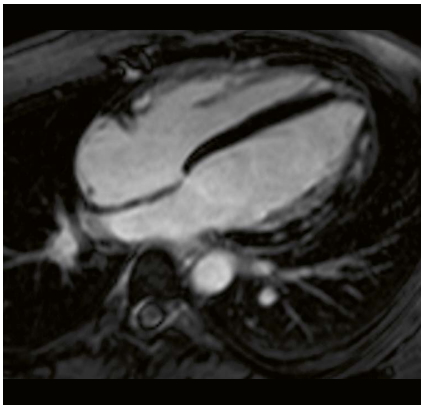

2 Subepicardial LGE in the lateral wall of the left ventricle in a patient with lupus myocarditis.

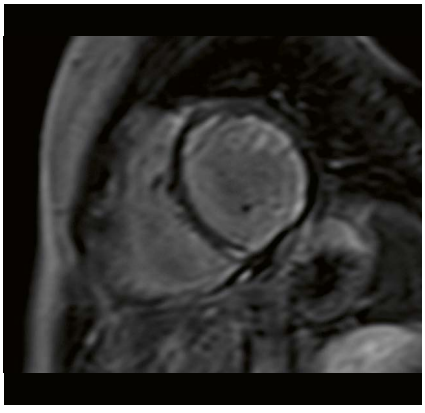

3 Diffuse subendocardial LGE due to small-vessel vasculitis in a patient with systemic sclerosis.

toms caused by the administered treatments and/or the patient's overall inflammatory state [7]. When overt signs of cardiac or vascular dysfunction do manifest, it may often be too late to prevent permanent cardiac damage and/or deterioration to heart failure [9]. It is therefore imperative to maintain a high index of suspicion in the clinical setting and to ensure early identification of these manifestations, as initiation of additional immunomodulatory treatment might be necessary to bring them under control [12].

Nevertheless, a high index of suspicion alone cannot ensure early identification of all cases of autoimmune CVD in ARD patients, since such cases are often asymptomatic. Furthermore, an echocardiographic examination, which is often used as a first-line test for evaluating the cardiovascular system, has considerable limitations, such as limited spatial resolution and dependence on a sufficient acoustic window for optimal image acquisition [12]. Lastly, the left ventricular ejection fraction (LVEF) is often used by healthcare professionals as a rough measure of systolic function. However, LVEF is preserved in the majority of ARD patients with autoimmune CVD, and cannot be used reliably as a rule-out indicator [12]. A more sensitive diagnostic tool is therefore required to fill this gap.

Cardiovascular magnetic resonance (CMR) is a non-invasive imaging modality that utilizes non-ionizing, radio-wavelength photons to generate high-quality images of human tissues [12]. CMR offers considerable advantages over other non-invasive imaging modalities when it comes to evaluating the cardiovascular system. It allows the determination of biventricular function with a high degree of accuracy and does not require an acoustic window. CMR can easily identify valvular and vascular abnormalities, enable the evaluation of myocardial perfusion without an exercise-based stress test, and, most importantly, characterize myocardial tissues with regard to edema and fibrosis [12]. The pathophysiological phenomena that should be identified – if present – in ARD patients include macro- or micro vasculopathy [9], myocardial inflammation [11–16], and myocardial fibrosis due to inflammation and/or myocardial infarction [13–16]. Based on the findings of the CMR examination, the acuity of any autoimmune inflammatory processes in the cardiovascular system can be estimated [13–16]. CMR additionally enables the identification of myocardial ischemia and/or subendocardial/transmural replacement or diffuse fibrosis, due to either macro- or micro-vascular coronary artery disease [12–17]. Furthermore, CMR can clarify the etiology of silent or overt heart failure, or cardiac rhythm disturbances [18–21]. Imaging patterns of myocardial replacement fibrosis are presented in Figures 1–3. Recently, the application of T1 and T2 mapping allowed the quantification of myocardial edema and diffuse fibrosis, which are the main pathophysiological phenomena that occur in the cardiovascular system of ARD patients [22–26] (Figs. 4A, B).

The role of CMR in motivating immunomodulatory treatment

Initiation/modification in ARD patients

CMR can detect cardiovascular involvement at any stage of the ARD, and often long before the ARD is fully expressed [19]. Unfortunately, echocardiography, which is the most common modality used in cardiology, is unable to detect these early lesions. Consequently, ARD patients with early lesions are not diagnosed and do not receive appropriate treatment, which explains the increased mortality in this population. The incidence of myocardial involvement varies in different ARDs; it is very high in systemic sclerosis, systemic lupus erythematosus, inflammatory myopathies, and vasculitis. However, multicenter studies comparing echocardiography or endomyocardial biopsy with CMR are still lacking.

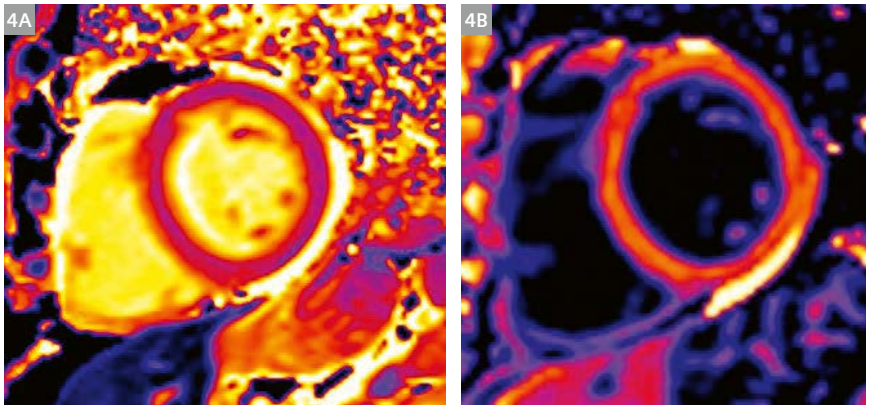

4 **(4A)** Short-axis native T1 mapping from a patient with systemic sclerosis; **(4B)** short-axis post-contrast T1 mapping from the same patient.

To our knowledge, there are also few studies coming from individual centers that support CMR's role in the evaluation of immunomodulatory and cardioprotective treatment in ARD patients. A previous study by our group showed that CMR can successfully evaluate the effect of both cardiac and immunomodulatory medication on the CV system. Furthermore, occult cardiac lesions seen on CMR – including myocardial edema, myocarditis, diffuse subendocardial fibrosis, and myocardial infarction – were not unusual in treatment-naïve ARD patients and can be reversed with appropriate treatment [19]. Additionally, stress CMR has successfully detected silent myocardial Raynaud's phenomenon in ARD patients with known peripheral Raynaud's phenomenon, and this resulted in early initiation of relevant cardiac treatment [13]. Moreover, CMR is capable of identifying ARD patients at high risk of cardiac rhythm disturbances that may lead to sudden cardiac death. CMR can therefore inform therapeutic decision-making for both cardiac and immunomodulatory treatment and specific CMR indices may also help to identify patients who might benefit most from implantation of a cardioverter defibrillator [20, 21]. With regard to this, it is worth noting that current criteria require an LVEF of < 35% to warrant implantation of a cardioverter defibrillator [27]. This is particularly problematic in ARD patients because, as mentioned above, they may have cardiovascular lesions with an otherwise preserved LVEF. Although the role of cardioprotective treatment is established for early morphological or functional cardiac changes [20, 21], clear guidelines for immunomodulatory treatment do not yet exist. However, the identification of myocardial inflammation using CMR is considered sufficient to warrant the initiation of immunomodulatory treatment, even if other clinical parameters are non-diagnostic [28].

When to consider a CMR examination for ARD patients

A baseline study that includes clinical, electrocardiographic, and echocardiographic evaluation should be performed when a diagnosis of any ARD is made. Based on our experience, a CMR examination may be considered in the following cases [12]:

- There is a mismatch between clinical findings and imaging/laboratory findings.
- The patient has developed new-onset heart failure.
- Cardiac rhythm disturbances of any type have been detected.
- The clinical picture requires modification of treatment with immunomodulatory agents.
- There is an increase in cardiac troponins, brain-type natriuretic peptide, N-terminal pro-brain-natriuretic peptide, or D-dimers, even if symptoms are only subtle.
- The patient mentions any kind of typical or atypical cardiac symptoms, and the routine cardiac evaluation is normal.

Recently, our team proposed a combined brain/heart MRI evaluation for the detection of silent brain lesions that are usually detected in ARD patients with CVD [29]. We believe that this combined approach will open a new avenue in the evaluation of ARDs and will facilitate early brain/heart treatment. However, there is currently insufficient information to recommend a combined brain/heart approach for all ARD patients. Identifying which patients to prioritize should be the focus of future studies.

Translating the Greek experience to the international arena

Greece is one of the first countries where the idea of cardio-rheumatology was conceived and developed, with CMR figuring prominently as a diagnostic tool [30]. This was the result of a collaboration between two professors of rheumatology (P. P. Sfikakis and G. D. Kitas) and a cardiologist and professor of CMR with extensive experience at the interface between cardiology and rheumatology (S. I. Mavrogeni, co-author of this paper). Since this collaboration began, cardio-rheumatology has attracted a great deal of interest and has found broad acceptance among the international rheumatology and cardiology community [31]. In recognition of this, the Society for Cardiovascular Magnetic Resonance (SCMR) created a targeted working group for cardio-rheumatology chaired by S. I. Mavrogeni. It was tasked with promoting collaborations for multicenter studies, with the goal of using CMR to evaluate the cardiovascular system in ARD patients. Currently, two such multicenter studies are underway in patients with systemic sclerosis and systemic lupus erythematosus. These are expected to increase our knowledge of the pathophysiology and management of CVD in these patients, and show us how to better identify high-risk patients that could benefit from therapeutic interventions. Although the journey of cardio-rheumatology is only just beginning, it is important that CMR has been the common denominator that has brought these different specialties together and provided them with a shared goal: to optimally identify ARD patients with CVD and initiate appropriate treatment.

Acknowledgments

We acknowledge the support of Dimitrios Kapatsoris and Fotini Zacharopoulou (Siemens Healthineers Hellas), and Ķostas Adamopoulos and D. Milionis (directors of the Olympic Diagnostic Center, Athens, Greece) in the development of our CMR research.

References

1 Pohl D, Benseler S . Systemic inflammatory and autoimmune disorders. Handb Clin Neurol. 2013;112:1243–52.
2 Aviña-Zubieta JA, Choi HK, Sadatsafavi M, Etminan M, Esdaile JM, Lacaille D. Risk of cardiovascular mortality in patients with rheumatoid arthritis: a meta-analysis of observational studies. Arthritis Rheum 2008;59(12):1690–7.
3 Sherer Y, Shoenfeld Y. Mechanisms of disease: atherosclerosis in autoimmune diseases. Nat Clin Pract Rheumatol. 2006;2(2):99–106.
4 Kitas GD, Gabriel SE. Cardiovascular disease in rheumatoid arthritis: state of the art and future perspectives. Ann. Rheum. Dis. 2011;70(1):8–14.
5 Hollan I, Meroni PL, Ahearn JM, Cohen Tervaert JW, Curran S, Goodyear CS, et al. Cardiovascular disease in autoimmune rheumatic diseases. Autoimmun Rev. 2013;12(10):1004–15.
6 Björnådal L, Yin L, Granath F, Klareskog L, Ekbom A. Cardiovascular disease a hazard despite improved prognosis in patients with systemic lupus erythematosus: results from a Swedish population based study 1964-95. J Rheumatol. 2004;31(4):713–9.
7 Symmons DP, Gabriel SE. Epidemiology of CVD in rheumatic disease, with a focus on RA and SLE. Nat Rev Rheumatol. 2011;7(7):399–408.
8 Gasparyan AY. Cardiovascular risk and inflammation: pathophysiological mechanisms, drug design, and targets. Curr Pharm Des. 2012;18(11):1447–9.
9 Dimitroulas T, Giannakoulas G, Karvounis H, Garyfallos A, Settas L, Kitas GD. Micro- and macrovascular treatment targets in scleroderma heart disease. Curr Pharm Des. 2014; 20(4):536–44.
10 Al-Dhaher FF, Pope JE, Ouimet JM. Determinants of morbidity and mortality of systemic sclerosis in Canada. Semin Arthritis Rheum. 2010;39(4):269–77.
11 Hansildaar R, Vedder D, Baniaamam M, Tausche AK, Gerritsen M, Nurmohamed MT. Cardiovascular risk in inflammatory arthritis: rheumatoid arthritis and gout. Lancet Rheumatol. 2020;doi: 10.1016/S2665-9913(20)30221-6 [Epub ahead of print].
12 Mavrogeni SI, Kitas GD, Dimitroulas T, Sfikakis PP, Seo P, Gabriel S, et al. Cardiovascular magnetic resonance in rheumatology: Current status and recommendations for use. Int J Cardiol. 2016;217:135–48.
13 Mavrogeni S, Sfikakis PP, Gialafos E, Bratis K, Karabela G, Stavropoulos E, et al. Cardiac tissue characterization and the diagnostic value of cardiovascular magnetic resonance in systemic connective tissue diseases. Arthritis Care Res (Hoboken). 2014;66(1):104–12.
14 Mavrogeni S, Spargias K, Markussis V, Kolovou G, Demerouti E, Papadopoulou E, et al. Myocardial inflammation in autoimmune diseases: investigation by cardiovascular magnetic resonance and endomyocardial biopsy. Inflamm Allergy Drug Targets. 2009;8(5):390–7.
15 Mavrogeni S, Manoussakis MN. Myocarditis and subclavian stenosis in Takayasu arteritis. Int J Cardiol. 2011;148(2):223–4.
16 Mavrogeni S, Sfikakis PP, Gialafos E, Karabela G, Stavropoulos E, Sfendouraki E, et al. Diffuse, subendocardial vasculitis. A new entity identified by cardiovascular magnetic resonance and its clinical implications. Int J Cardiol. 2013;168(3):2971–2.
17 Raman SV, Aneja A, Jarjour WN. CMR in inflammatory vasculitis. J Cardiovasc Magn Reson. 2012;14(1):82.
18 Mavrogeni S, Sfikakis PP, Gialafos E, Bratis K, Karabela G, Stavropoulos E, et al. Cardiac tissue characterization and the diagnostic value of cardiovascular magnetic resonance in systemic connective tissue diseases. Arthritis Care Res (Hoboken). 2014;66(1):104–12.
19 Mavrogeni S, Markousis-Mavrogenis G, Koutsogeorgopoulou L, Dimitroulas T, Bratis K, Kitas GD, et al. Cardiovascular magnetic resonance imaging pattern at the time of diagnosis of treatment naïve patients with connective tissue diseases. Int J Cardiol. 2017; 236:151–156.
20 Mavrogeni SI, Sfikakis PP, Dimitroulas T, Koutsogeorgopoulou L, Markousis-Mavrogenis G, et al. Prospects of using cardiovascular magnetic resonance in the identification of arrhythmogenic substrate in autoimmune rheumatic diseases. Rheumatol Int. 2018;38(9):1615–1621.
21 Mavrogeni S, Gargani L, Pepe A, Monti L, Markousis-Mavrogenis G, De Santis M, et al. Cardiac magnetic resonance predicts ventricular arrhythmias in scleroderma: the Scleroderma Arrhythmia Clinical Utility Study (SAnCtUS). Rheumatology (Oxford). 2020;59(8):1938–1948.
22 Ntusi NAB, Francis JM, Gumedze F, Karvounis H, Matthews PM, Wordsworth PB, et al. Cardiovascular magnetic resonance characterization of myocardial and vascular function in rheumatoid arthritis patients. Hellenic J Cardiol. 2019;60(1):28–35.
23 Ntusi NAB, Francis JM, Sever E, Liu A, Piechnik SK, Ferreira VM, et al. Anti-TNF modulation reduces myocardial inflammation and improves cardiovascular function in systemic rheumatic diseases. Int J Cardiol. 2018;270:253–259.
24 Greulich S, Mayr A, Kitterer D, Latus J, Henes J, Steubing H, et al. T1 and T2 mapping for evaluation of myocardial involvement in patients with ANCA-associated vasculitides. J Cardiovasc Magn Reson. 2017;19(1):6.
25 Hinojar R, Foote L, Sangle S, Marber M, Mayr M, Carr-White G, et al. Native T1 and T2 mapping by CMR in lupus myocarditis: disease recognition and response to treatment. Int J Cardiol. 2016;222:717–726.
26 Winau L, Hinojar Baydes R, Braner A, Drott U, Burkhardt H, Sangle S, et al. High-sensitive troponin is associated with subclinical imaging biosignature of inflammatory cardiovascular involvement in systemic lupus erythematosus. Ann Rheum Dis. 2018;77(11):1590–1598.
27 Myerburg RJ, Reddy V, Castellanos A. Indications for implantable cardioverter-defibrillators based on evidence and judgment. J Am Coll Cardiol. 2009;54(9):747–63.
28 Pieroni M, De Santis M, Zizzo G, Bosello S, Smaldone C, Campioni M, et al. Recognizing and treating myocarditis in recent-onset systemic sclerosis heart disease: potential utility of immunosuppressive therapy in cardiac damage progression. Semin Arthritis Rheum. 2014;43(4):526–35.
29 Markousis-Mavrogenis G, Mitsikostas DD, Koutsogeorgopoulou L, Dimitroulas T, Katsifis G, Argyriou P, et al. Combined brain-heart magnetic resonance imaging in autoimmune rheumatic disease patients with cardiac symptoms: hypothesis generating insights from a cross-sectional study. J Clin Med. 2020;9(2):447.
30 Mavrogeni S, Papadopoulos G, Douskou M, Kaklis S, Seimenis I, Baras P, et al. Magnetic resonance angiography is equivalent to X-ray coronary angiography for the evaluation of coronary arteries in Kawasaki disease. J Am Coll Cardiol. 2004;43(4):649–652.
31 Ruparelia N, Chai JT, Fisher EA, Choudhury RP. Inflammatory processes in cardiovascular disease: a route to targeted therapies. Nat Rev Cardiol. 2017; 14(3):133–144.

Contact

Professor Sophie Mavrogeni, M.D., Ph.D.
Onassis Cardiac Surgery Center
50 Esperou Street
17561 P. Faliro
Athens, Greece
Phone: +30 210 98 82 797
sophie.mavrogeni@gmail.com

Magnetic Resonance Spectroscopy as a Clinical Tool for the Prognosis and Diagnosis of Diabetic Heart Disease

Eylem Levelt, M.D., Ph.D.[1]; Karen Kettless, B.Sc. Hons.[2]; Maria-Alexandra Olaru, Ph.D.[1]

[1]University of Leeds, School of Medicine, Leeds, UK
[2]Siemens Healthineers, Ballerup, Denmark

Introduction

Type 2 diabetes mellitus (T2DM) is often associated with an increased risk of heart failure and cardiovascular mortality. While the reasons for this are not fully elucidated, several possible mechanisms behind it have been proposed. These include impaired cardiac high energy phosphate metabolism, coronary microvascular dysfunction, and ectopic lipid deposition. Due to the complexity of these physiological phenomena, a combination of well-established diagnostic imaging methods, such as cardiovascular magnetic resonance imaging, ultrasound, computed and positron-emission tomography have so far been traditionally used for their investigation.

Although this combination of imaging techniques is extremely powerful, very few of these methods, if any, are able to provide insights into processes taking place at a molecular level – such as some dysfunctionalities in the cardiac energy metabolism (e.g. increased fatty acid usage, decreased lactate and glucose metabolization and/or high energy phosphate metabolization). This has led researchers and clinicians to examine the possibilities offered by magnetic resonance spectroscopy methods (particularly those based on interrogating ^{1}H and ^{31}P metabolites). Such complementary techniques add an additional layer of information to the results obtained via

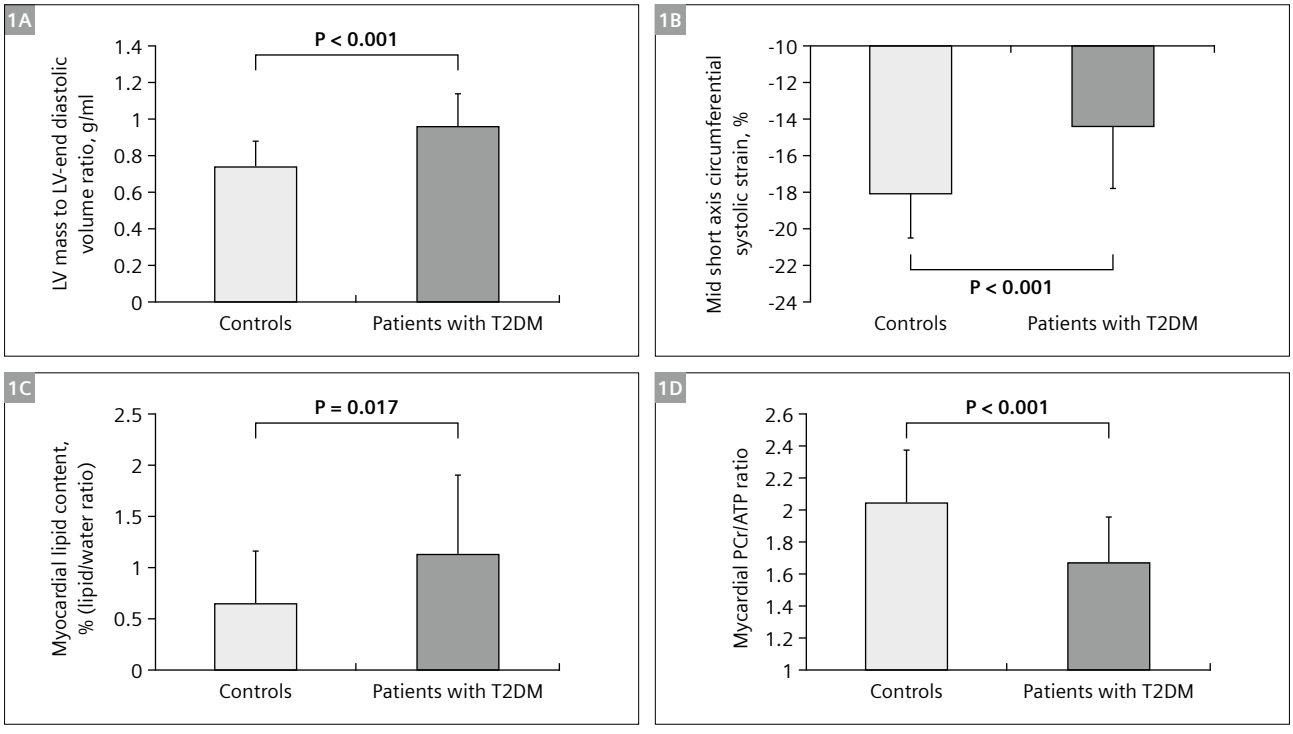

1 Differences in cardiac geometry and function between patients with T2DM and control subjects: LV-mass-to-LV-end diastolic volume (EDV) ratio (grams/millilitre) **(1A)**, systolic strain (percentage) **(1B)**, myocardial triglyceride content (percentage) **(1C)**, and myocardial energetics (PCr-to-ATP ratio) **(1D)**. *Reproduced from [2] with the author's permission.*

clinical imaging protocols. As a consequence, during the last few decades, cardiac magnetic resonance spectroscopy has started to slowly become acknowledged as being a very formidable investigation tool, useful for both early detection and disease monitoring of diabetic heart disease.

Current applications of ^{1}H and ^{31}P cardiac magnetic resonance spectroscopy in the investigation of diabetic heart disease

Ectopic adiposity and cardiovascular disease prognosis
The number of type 2 diabetes mellitus patients is rapidly rising, and this increase is partially associated to the growth in obesity. A substantial amount of evidence demonstrates that excessive ectopic adiposity is common for patients with diabetes and it considerably increases the risk of cardiovascular disease, being very likely that it contributes to non-ischemic cardiomyopathy in this patient group.

^{1}H MRS has been successfully proven to be a very effective strategy for the quantification of myocardial triglycerides [1]. Later studies have demonstrated that type 2 diabetes is associated with an increase of ~ 31% of the LV-mass-to-LV-end diastolic volume (Fig. 1A) and almost two-fold increase in myocardial triglycerides (Fig. 1C, data acquired with a custom single voxel-based method), thus demonstrating that ^{1}H cardiac magnetic resonance data can be highly predictive of LV concentric remodelling and cardiac systolic strain [2].

From a practical perspective, ^{1}H magnetic resonance spectroscopy protocols for the assessment of cardiac steatosis are typically designed to quantify the amount of lipid deposition by measuring the ratio of the integral areas of the myocardial triglycerides' resonances and that of the water resonance respectively. Thus, they are designed as a two-step process, during which the myocardial triglycerides and the water are quantified independently in a small region of interest, usually located in the interventricular septum during mid-late diastole.

The most commonly employed acquisition strategies for ^{1}H cardiac spectroscopy are single voxel methods, which rely on either spin-echo [3] or stimulated-echo [4] excitation schemes. Spin-echo approaches have the advantage of higher signal to noise ratio compared to their stimulated-echo counterparts. The longer echo times imposed by the use of refocussing pulses for signal acquisition can lead to line broadening in the case of myocardial triglycerides, (which have an inherently long transverse relaxation rate) and subsequently, to difficulties in data quantification. Additionally, the use of spin-echo based methods, due to their higher sensitivity, can lead to the results being more susceptible to signal contamination, due to motion-induced involuntary detection of water in the blood pool surrounding the interventricular septum. Stimulated-echo methods are less sensitive to signal contamination and more suitable to the detection of myocardial triglycerides, as they allow for a shorter echo time to be employed. However, due to the fact that such strategies use gradients for signal refocussing, the signal decay during the echo time is governed by T2*, as opposed to T2 in spin-echo approaches, and dephasing due phenomena such as magnetic susceptibility and chemical shift difference.

For both methods, a careful choice of acquisition parameters is essential for accurate quantification: short echo times are highly recommended, and the repetition time needs to allow for full recovery of the two resonances (~ 2 s for myocardial triglycerides and ~ 4 s for water). The voxel is typically positioned parallel to the septum and its dimensions need to be adjusted in such a way that the volume of interest is large enough to warrant a reasonable SNR value, but not as large as to increase the risk of signal contamination due to the contribution of the surrounding blood pool during cardiac motion. To ensure data is always acquired at the same point in the cardiac cycle and to mitigate the effects of breathing artifacts, these examinations are typically performed using physiological triggers [5].

Measuring cardiac energy metabolism
The most energy-consuming reactions in the heart, such as the contraction of the myofilaments or the active pump function, are fuelled by the metabolization of adenosine triphosphate, which is obtained from phosphocreatine via the creatine-kinase process occurring in the mitochondria. Diabetic heart disease is associated with inefficient energy production or utilisation, which decreases the heart's ability to adapt when subjected to an increase in workload. Myocardial energy depletion can be caused by mitochondrial disfunction, poor energy transfer to the myofibrils and impaired uptake and use of adenosine triphosphate and phosphocreatine. Thus, the phosphocreatine-to-adenosine triphosphate ratio (PCr/ATP) is a very important biomarker which can be used to diagnose and monitor cardiac diabetic disease.

^{31}P magnetic resonance spectroscopy is the only non-invasive technique which can effectively quantify the PCr/ATP ratio. Changes in the cardiac energy metabolism, reflected in the PCr/ATP ratio, can take place before any subclinical or clinical manifestation of disease are reported or observed, we believe that ^{31}P magnetic resonance spectroscopy may become an invaluable tool for prognosis and diagnosis in the future.

Studies employing ^{31}P magnetic resonance spectroscopy have shown that the PCr/ATP ratio decreases considerably in the case of diabetic patients compared to healthy controls [6] and have demonstrated that diabetes is associ-

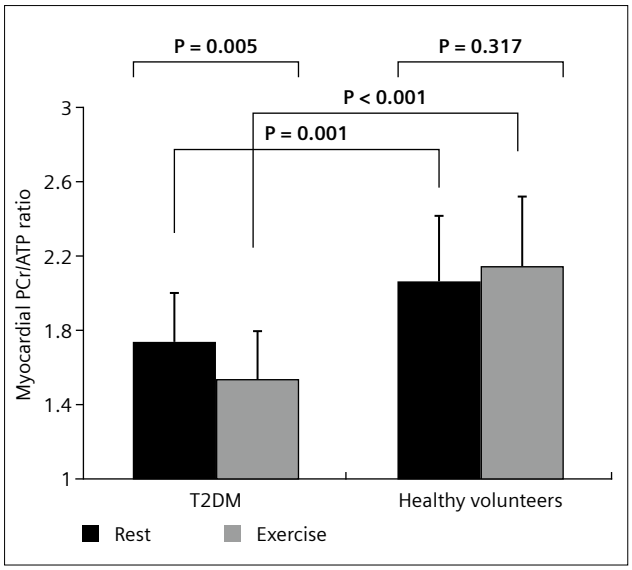

2 Differences in rest and exercise myocardial PCr/ATP ratios between controls and patients with T2DM. Bars show mean PCr/ATP ratios and error bars indicate standard deviations. *Reproduced from [7] with the author's permission.*

ated with a 17% decrease in PCr/ATP at rest compared with healthy volunteers, while a further 12% decrease was determined during exercise [7].

Our most recent research work at the University of Leeds is revolving around establishing the metabolic basis of heart disease in type 2 diabetes with a focus on exploring the role of metabolic inflexibility toward heart failure development and progression in type 2 diabetes, and the impact of diabetes on common cardiac comorbidities. We acquire ^{31}P spectroscopy data using a customised chemical shift imaging sequence, equipped with a spatially selective saturation module and a shaped excitation pulse tailored to effectively cover the full chemical shift range of interest [8]. The acquisition is ECG triggered and performed in free breathing (TR 720 ms, acquisition time ~ 9 minutes). Reproducibility is assessed by performing the same examination twice, while removing the patient from the scanner between the two consecutive scans.

Our results have confirmed the previous findings and have shown that a similar decrease in the PCr/ATP ratio is observed in type 2 diabetes patients while at rest and under stress, induced via dopamine infusion (Fig. 3).

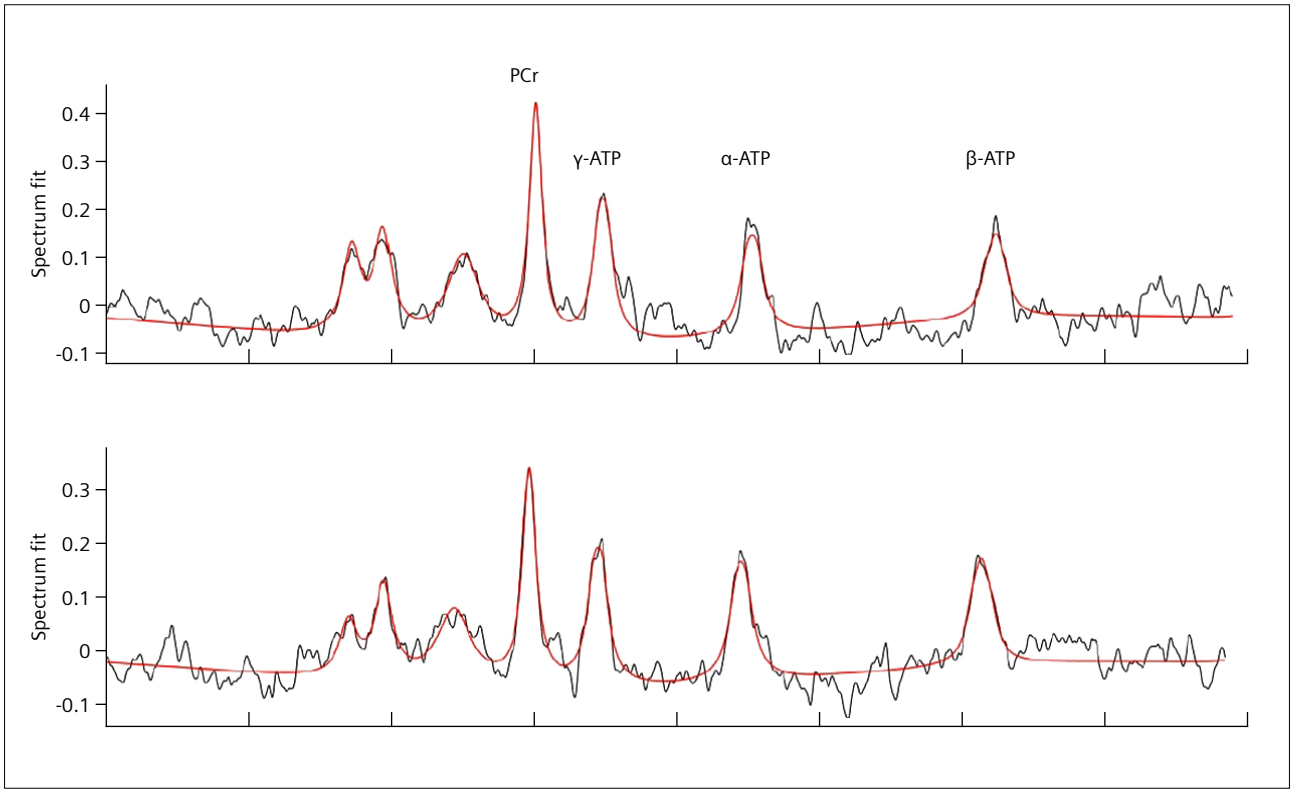

3 ^{31}P spectra acquired in the interventricular septum and the corresponding fits. The spectra have been acquired on a type 2 diabetic patient at rest (top: PCr/ATP = 2.26 ± 8.0%) and during stress (bottom: PCr/ATP = 1.79 ± 8.4%).

Challenges and outlook

Both the effectiveness and the utility of magnetic resonance spectroscopy as a tool for cardiac disease prognosis and monitoring are generally recognised, but it has yet to become a routinely used method in the clinical environment. The most significant deterrents are the need for additional input from the examiner (when compared to standard cardiac magnetic resonance imaging methods), dedicated time for the pre-scan adjustments, such as B_0 shimming, the fact that ^{1}H methods are exceptionally sensitive to cardiac and respiratory motion and the need for dedicated hardware – broadband RF amplifiers and bespoke coils – in the case of ^{31}P.

However, given the fact that magnetic resonance spectroscopy can provide essential information prior to the development of clinical symptoms and considering the recent software developments for acquisition and processing, which have considerably contributed to making spectroscopy examinations easier for the routine user. We believe that magnetic resonance spectroscopy will soon claim its place among the methods used as a gold standard for measuring cardiac disease biomarkers, allowing for prognosis, early diagnosis and treatment planning.

References

1 McGavock JM, et al. Cardiac steatosis in diabetes mellitus: a 1H-magnetic resonance spectroscopy study. Circulation 2007; 116:1170–1175.
2 Levelt E, et al. Relationship Between Left Ventricular Structural and Metabolic Remodelling in Type 2 Diabetes. Diabetes 2016; 65(1): 44-52.
3 Bottomley PA. Spatial localization in NMR spectroscopy in vivo. Ann NY Acad Sci. 1987; 508:333–348.
4 Frahm J, Merboldt et al, Localized proton spectroscopy using stimulated echoes. J Magn Reson. 1987;72:502–508.
5 Hudsmith, L E et al, Magnetic Resonance Spectroscopy in Myocardial Disease, JACC: Cardiovascular Imaging, 2009; 2(1): 87-96.
6 Shivu GN, et al, Relationship between coronary microvascular dysfunction and cardiac energetics impairment in type 1 diabetes mellitus. Circulation 2010; 121:1209–1215.
7 Levelt E, et al. Cardiac energetics, oxygenation, and perfusion during increased workload in patients with type 2 diabetes mellitus. Eur Heart J. 2016;37(46):3461-3469.
8 Robson, MD, et al, Ultrashort TE chemical shift imaging (UTE-CSI). Magnetic Resonance in Medicine 2005; 53: 267-274.

Contact

Eylem Levelt, M.D., Ph.D.
School of Medicine, Worsley Building
University of Leeds
Leeds, West Yorkshire, LS2 9JT
UK
E.Levelt@leeds.ac.uk

How to do Cardiac Single Voxel ^{1}H Spectroscopy

Morten Asp Vonsild Lund, M.D.[1–3]; Karen Kettless, B.Sc. Hons, PgD[4]; Xiaoying Cai, Ph.D.[5]; Maria-Alexandra Olaru, Dr. rer. nat.[6]

[1]Department of Cardiology, Rigshospitalet, Copenhagen University Hospital, Copenhagen, Denmark
[2]The Children's Obesity Clinic, Department of Pediatrics, Holbæk Hospital, Holbæk, Denmark
[3]Department of Biomedical Sciences, University of Copenhagen, Copenhagen, Denmark
[4]Siemens Healthineers, Ballerup, Denmark
[5]Siemens Healthineers, Boston, MA, USA
[6]Siemens Healthineers, UK

Introduction

Cardiac MR is an established method for assessing cardiac function and morphology. In the meanwhile, MR can be utilized to assess metabolism using spectroscopy, which offers many advantages compared with other imaging modalities including that it does not require additional tracer and it is free of ionizing radiation. Furthermore, in vivo spectroscopy has been used to assess cardiac energetics and myocardial metabolism. For ^{1}H spectroscopy of the heart, the commonly studied metabolites are triglycerides and creatine. Alterations in the level of these metabolites are reported in various conditions such as cardiomyopathy, heart failure, and type 2 diabetes mellitus [1, 2].

^{1}H cardiac spectroscopy can be performed using either a spin-echo (PRESS) or stimulated-echo (STEAM) excitation scheme. In this article, we describe the procedures of performing single voxel ^{1}H spectroscopy in the myocardium at our site using a MAGNETOM Aera 1.5T and a MAGNETOM Prisma 3T (Siemens Healthcare, Erlangen, Germany). The protocols we use are based on the standard PRESS sequence supplied with the Siemens Spectroscopy package and are tailored for the quantification of myocardial triglycerides content. Specifically, the integral areas of lipids and water resonance respectively are assessed via two separate scans and used to calculate the triglycerides-to-water ratio.

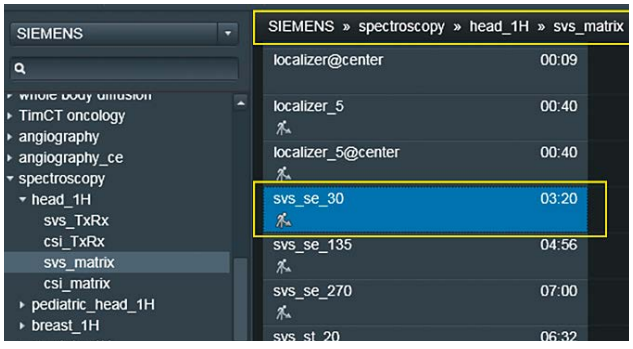

1 Location of the PRESS protocol used as the starting point to set up the desired protocols.

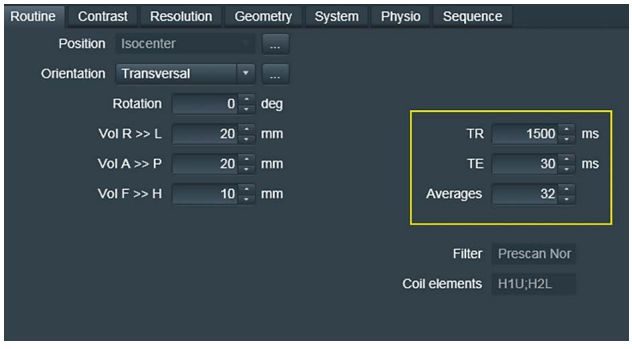

2 Routine tab of the protocol.

Protocol setup

A copy of the standard PRESS protocol (Fig. 1) is used as the starting point and modified to utilize both ECG and respiratory triggering along with changes to other acquisition parameters. Two protocols are set up with the first for assessing lipid resonances and the second for water resonance. Specific parameter selections for the lipid protocol are:

1. **Routine:** Adjust the voxel size, repetition time (TR), echo time (TE) and number of Averages (Figure 2). The voxel of interest is to be placed on the septum and approximately a size of 20 x 20 x 10 mm^3 is suitable. The choices of TR and TE need to be considered in the context of the relaxation rates of myocardial triglycerides and water, respectively. It is important to use the shortest echo time (TE) allowed by the sequence properties and a repetition time (TR) long enough to allow for full magnetization recovery. Typical parameters are TE 30 ms, TR at least 1500 ms.
2. **Contrast:** Make sure **Water sat.** is selected for water suppression (Fig. 3). With this option, a chemical shift selective (CHESS) based water suppression scheme is employed, with a typical excitation bandwidth of 35 Hz at 3T.
3. **Resolution:** Adjust the vector size to 512 for a shorter and more suitable readout duration. It is also recommended to utilize **PreScan Normalize**.
4. **Physio:** Switch on ECG triggering in **Signal1** and respiratory triggering in PACE to reduce adverse impacts of cardiac and respiratory motion to the spectrum.
5. **System:** Switch the adjustment mode to **Tune up** as the B_0 shimming will be performed via manual adjustments. Also make sure that **Adjust for water suppression** is ticked.
6. **Sequence:** Set the excitation frequency via **Delta Frequency** and adjust other parameters (Fig. 5). The frequency of the excitation pulse is centered on the interval of values corresponding to the triglyceride resonances (0.9–1.3 ppm) and it is expressed as a relative number (Delta frequency) in reference to the value corresponding to the water frequency.

After the lipid protocol is set up, the water reference protocol can be set up via:

1. Make a copy of the lipid protocol.
2. Switch water suppression off in **Contrast** tab.
3. Adjust Delta frequency to 0 ppm in **Sequence** tab.
4. Make sure the B_0 shim mode is still **Tune up**.

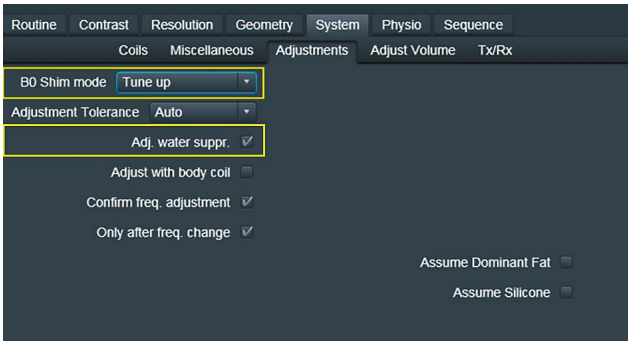

4 Parameters in System/Adjustments.

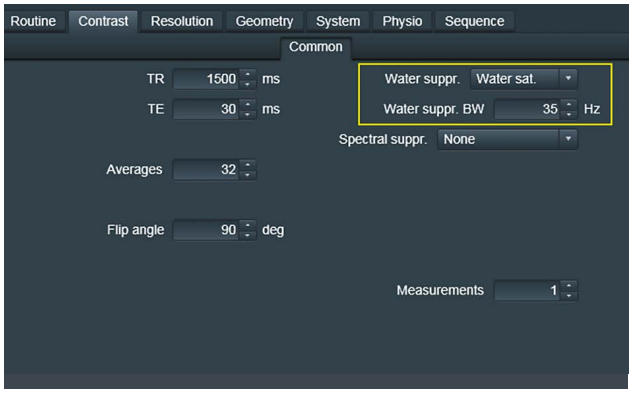

3 Contrast tab used in the protocol employed for myocardial triglyceride detection. Important parameters are Water suppr. and Water suppr. BW.

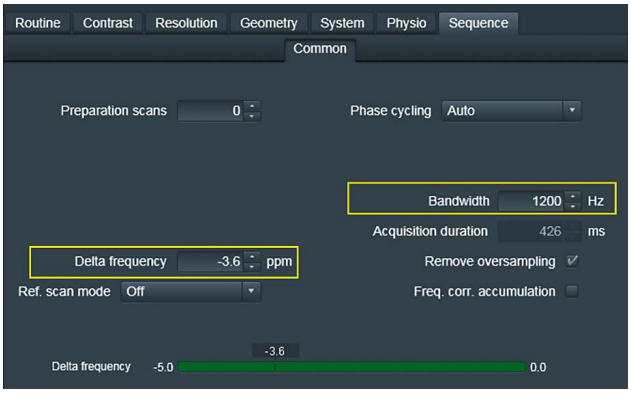

5 Parameters regarding spectroscopy acquisition in Sequence tab. For detection of triglycerides resonances, the Delta frequency should be set on the triglyceride resonance, e.g. -3.6 ppm. For water resonance, this parameter should be set 0 ppm.

Planning the acquisition

It is recommended to use the following images as reference images for planning: 3-plane localizer, short-axis stack (SAX) cine and 4-chamber cine. Planning of the voxel position and navigator can be properly using the following steps:

1. Convert the reference images to create non-distortion corrected version, as spectroscopy planning cannot be performed on images post distortion correction.
2. Load the reference images and then open the spectroscopy protocol.
3. Place the navigator (yellow box) on the liver dome and the Adjustment Volume (green) around the voxel of interest (Fig.6).
4. The voxel of interest is typically positioned in the inter-ventricular septum. The position and size of the voxel should be adjusted so that it is sufficiently large but not contaminated by the surrounding blood pool. Using as reference images (SAX) and 4-chamber cine images, position the voxel in the mid ventricular septum, avoiding the cardiac blood pool (Right-Click on LV Mid SAX: Shift to Image Plane and then make Perpendicular (Fig. 7).
5. Adjust the ECG trigger delay so that the RF pulses are trigged to end-systole. For the water reference protocol, the trigger delay is simply the time to end systole, which can be determined from the cine acquisitions. However, for the lipid protocol, the duration of water saturation needs to be taken into consideration, i.e. [trigger delay] = [time to end systole] - [water saturation duration]. The duration of water saturation train is approximately 192 ms.

B_0 shimming via manual adjustments

Optimal field homogeneity is required for successful acquisition of quality spectroscopy data. We recommend that the values of the shim currents are adjusted interactively prior to the acquisition, via the Manual Adjustments window. The B_0 shim could be performed via the following steps:

1. Set up the adjustment volume on the voxel of interest.
2. Access Manual Adjustments via the **Options** drop-down menu.
3. In 3D Shim, switch the **Sequence&Resolution** option to **GRE Cardiac** and perform shimming (Fig. 8). The GRE cardiac method is a gradient-echo based protocol optimized for cardiac magnetic resonance that allows the user to acquire field maps of the volume of interest.

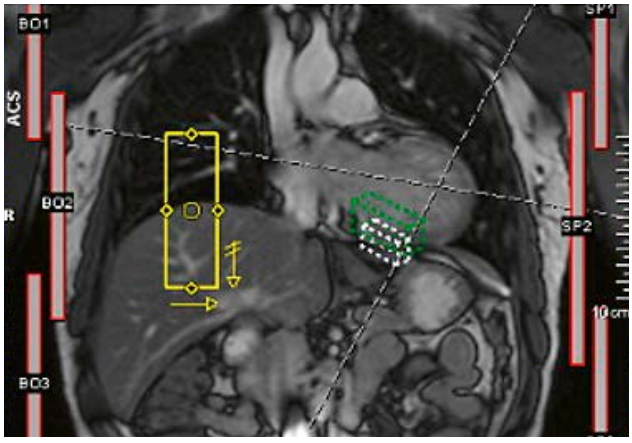

6 Positioning of the respiratory navigator.

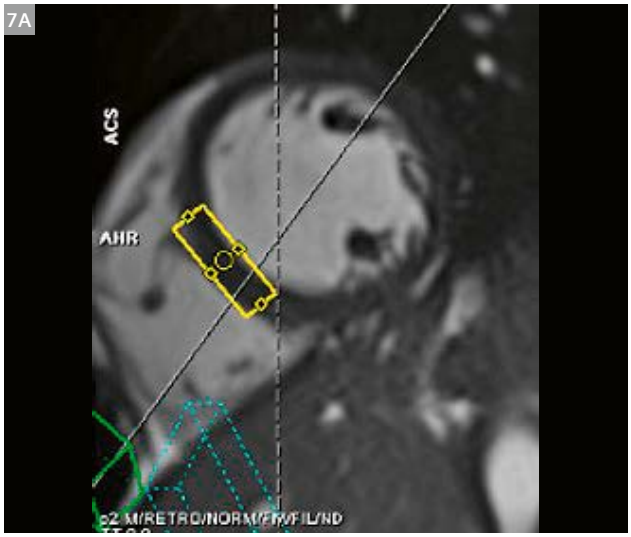

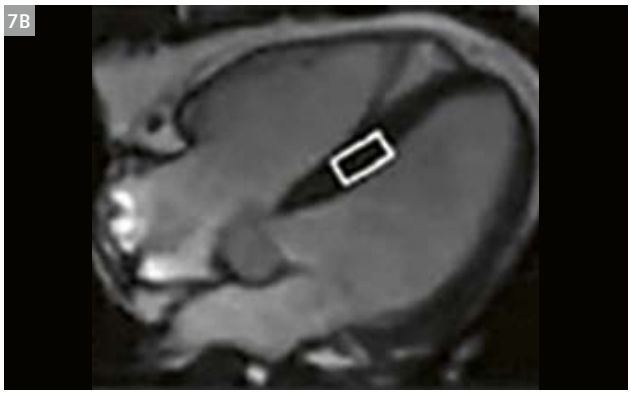

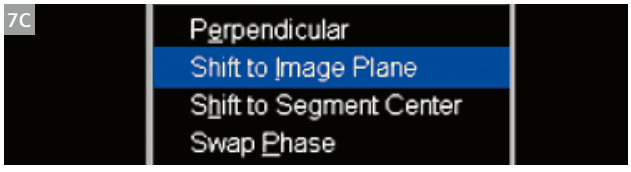

7 Voxel geometry and placement on SAX view (7A) and 4-chamber (7B) view. The **Shift to Image Plane** function can be used to facilitate voxel localization (7C).

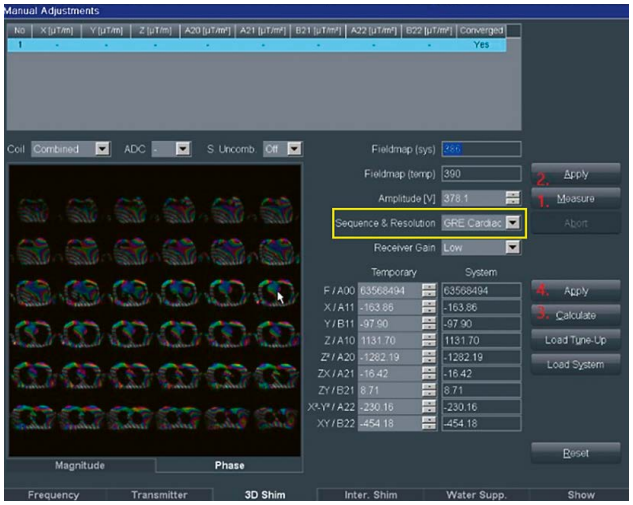

8 3D Shim steps: Measure a new field map (1), apply the field map as the current system field map (2), calculate new values for the shim currents based on the new field map (3) and apply them to the system (4).

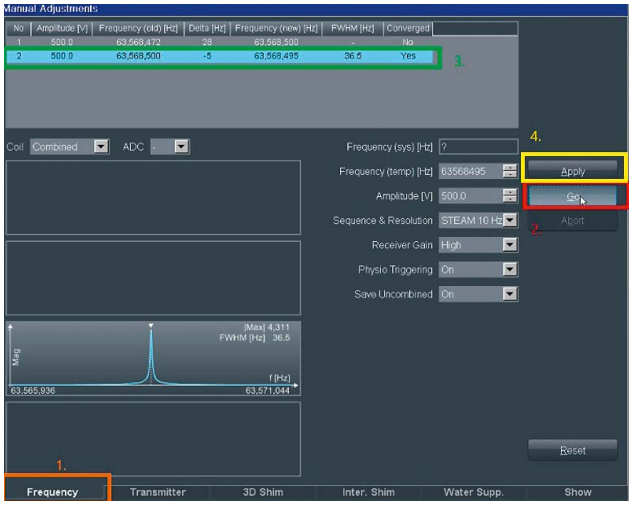

9 Assess the field inhomogeneity via (1) switching to Frequency tab and (2) measuring the current FWHM. (3) The FWHM is displayed in the table and next to the water resonance. (4) If the FWHM is acceptable, confirm/accept the current shimming.

4. Switch to Frequency tab and measure the current line width at half height (typically referred to as FWHM – Full Width at Half Max) as shown in Figure 9. The purpose is to assess the field inhomogeneity after shimming. Ideally, the FWHM should be below 25 Hz, B_0 inhomogeneities cause line broadening in the spectra.
5. If the FWHM is too high, repeat step 3 and 4. Otherwise, click **Apply** to confirm the current shimming and close the manual adjustments window.

Summary

Cardiac magnetic resonance spectroscopy can be performed with combined ECG and respiratory triggering using a standard Siemens 1.5T or 3T MR system with no additional equipment or coils required.

References:

1 McGavock JM, et al. Cardiac steatosis in diabetes mellitus: a 1H-magnetic resonance spectroscopy study. Circulation 2007; 116:1170–1175
2 Faller KME, et al. 1H-MR spectroscopy for analysis of cardiac lipid and creatine metabolism. Heart Fail Rev 2013; 18:657-668
3 Wei J, et al. Myocardial steatosis as a possible mechanistic link between diastolic dysfunction and coronary microvascular dysfunction in women. Am J Physiol Heart Circ Physiol 2016; 310: H14–H19

The .exar1 protocols for
3T MAGNETOM Prisma (software version *syngo* MR E11E) and
1.5T MAGNETOM Aera (software version *syngo* MR E11C) are available for download at:

www.siemens-healthineers.com/magnetom-world
> Clinical Corner > Protocols > Cardiovascular MRI

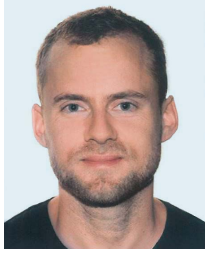

Contact

Morten Asp Vonsild Lund, M.D.
Department of Cardiology
Rigshospitalet
Copenhagen University Hospital
Blegdamsvej 9
2100 Copenhagen
Denmark
morten.lund@sund.ku.dk

3D Late Gadolinium Enhancement CMR

Patrick Pierce[1]; Xiaoying Cai, Ph.D.[1,2]; Beth Goddu[1], Rachel Davids[2]; Reza Nezafat, Ph.D.[1]

[1] Department of Medicine, Cardiovascular Division, Beth Israel Deaconess Medical Center and Harvard Medical School, Boston, MA, USA
[2] Siemens Healthineers, Malvern, PA, USA

Introduction

Late gadolinium enhancement (LGE) CMR is widely used for myocardial scar assessment. Clinically, multi-slice two-dimensional (2D) imaging is used during multiple breath-holds to cover the entire ventricle. However, 2D breath-hold imaging requires patients to perform repeated breath-holds, limits spatial resolution and coverage. Free-breathing 3D LGE imaging is an alternative technique that allows a full LV coverage in free-breathing with improved spatial resolution. Despite its potential, 3D free-breathing LGE imaging is only performed in selected clinical sites. Our laboratory at Cardiac MR Center at Beth Israel Deaconess Medical Center is among a few selected sites where free-breathing 3D LGE imaging is routinely performed in all clinical patients for nearly a decade. In this article, we describe our current practice of LGE CMR in patient scans using a 3T MAGNETOM Vida scanner (Software version: NXVA20A). Specifically, 3D LGE is performed during free-breathing with navigator-based gating and slice-tracking for respiratory motion suppression. The images are acquired on a 4-chamber slab and are reformatted to other desired planes using on-scanner tools.

Workflow

LGE acquisition is performed after injection of contrast agent and can be planned without the need for any additional localizers. As show in Figure 1, we use multi-plane localizers, 4-chamber, and short-axis images to set up the imaging volume. The setup can be performed via the following steps:

1) Copying the slice location on the 4-chamber view (Panel A);
2) Adjusting the center of the slab on the short-axis images to cover the entire left ventricle (Panel B);
3) Placing the crossed-pair navigator on the liver dome using the multi-plane localizer (Panels C-D).

It is preferred to image on 4-chamber view rather than short-axis view as imaging at 4-chamber view usually results in fewer motion artifacts.

Like segmented 2D LGE imaging, non-selective inversion is performed for magnetization preparation during systole and data acquisition is performed with segmented cartesian trajectory. The inversion time is adjusted based on the TI scout scan for proper contrast. Figures 2 and 3 show screenshots of imaging parameters

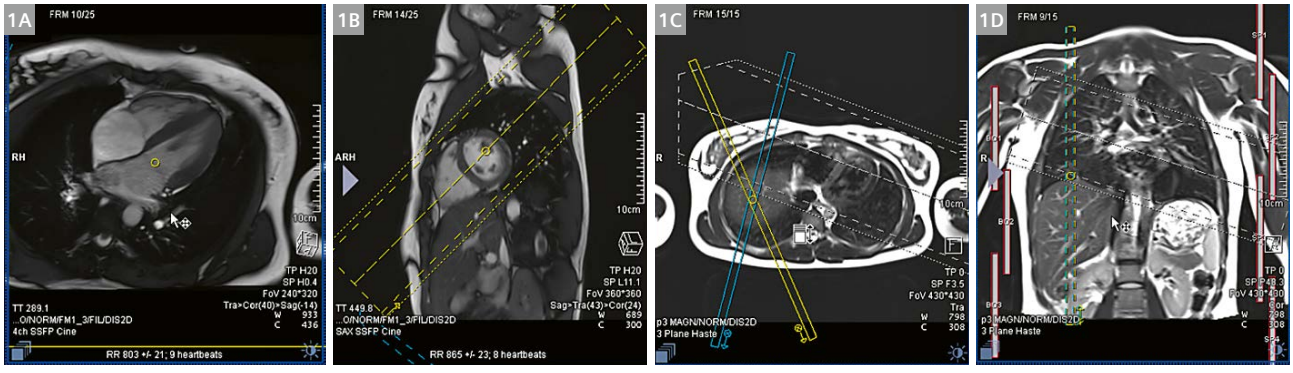

1 Illustration of image planning for 3D LGE.

in the Routine and Resolution tabs. We image a 3D slab with 40–45 slices per slab and a slice thickness of 2 mm. A large field-of-view (380 mm) is used to avoid folding artifacts in the 4-chamber plane. With an in-plane matrix size of 256 x 256, the spatial resolution is 1.5 x 1.5 x 2.0 mm^3. GRAPPA is used for an acceleration rate of two in the phase encoding direction.

The timing of acquisition is adjusted to place the read-outs during end-diastole, as shown in Figure 4. Typically, approximately 40 *k*-space lines are sampled per heartbeat depending on the heart rate. The crossed-pair navigator is used for gating and slice-tracking during the free-breathing acquisition with an acceptance window of ± 4 mm. Respiratory motion adaptation is also used to automatically locate the end-expiration position of the navigator. The acquisition time is approximately three minutes assuming a navigator efficiency of 40%.

In addition, the protocol uses "Cardio" for matrix optimization and "Cardiac B0 Shim" with the adjustment volume on the heart.

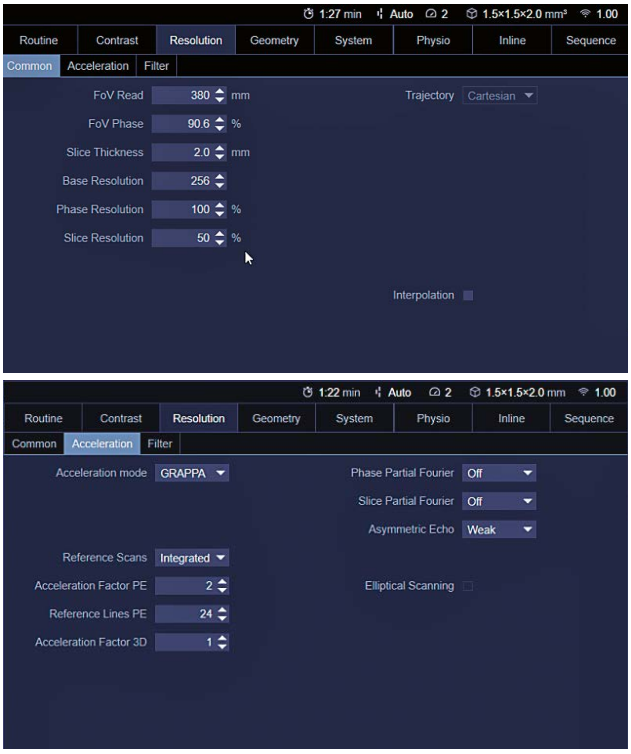

3 Screenshot shows Resolution tab of the 3D LGE protocol.

2 Screenshot shows Routine tab of the 3D LGE protocol.

4 Screenshot shows Physio tab of the 3D LGE protocol.

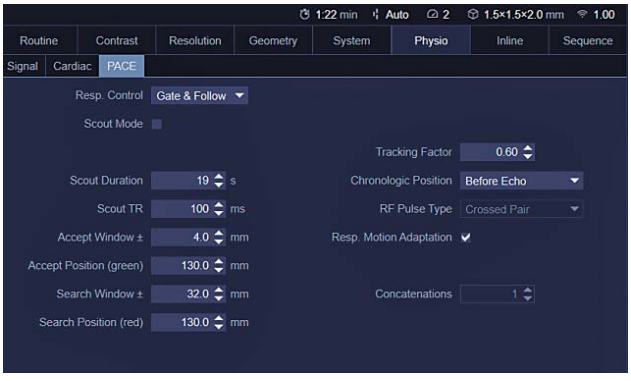

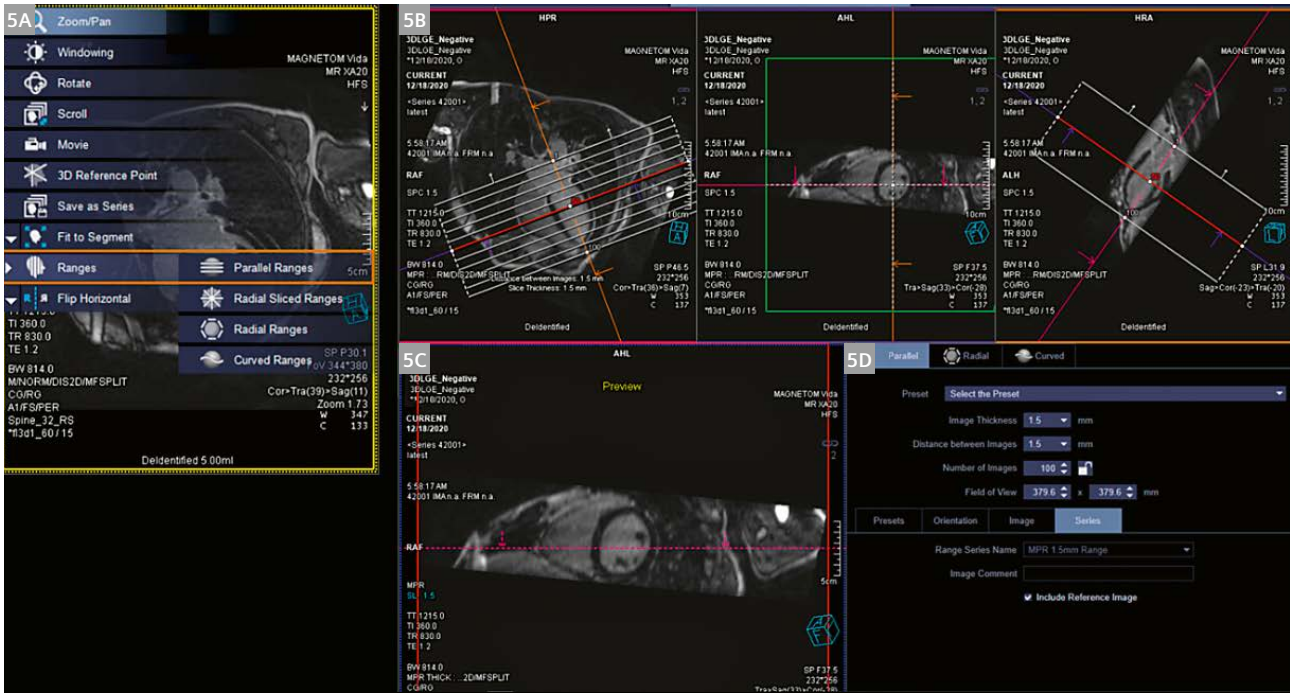

5 Illustration of reformatting the 3D LGE images to short-axis planes. **(5A)** Select "Parallel Ranges" on the source images. **(5B)** Adjust the orientation and location of the slices to be reconstructed. Short-axis views are set up in this example. **(5C)** Preview of the slices to be reconstructed. **(5D)** Parameters to adjust the coverage of the slices.

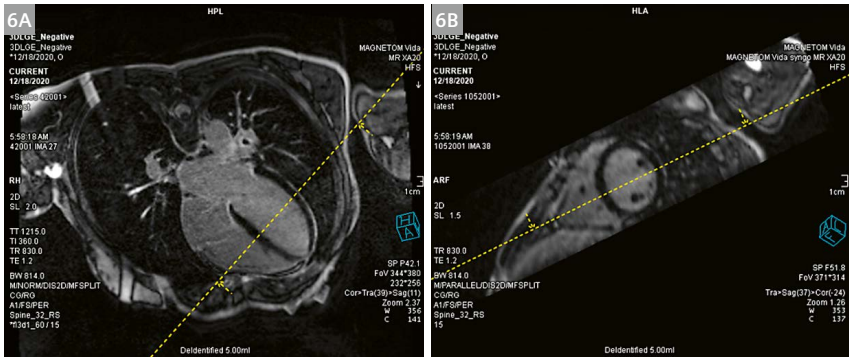

6 Exemplary images of 3D LGE acquisition in a subject with suspected cardiomyopathy. **(6A)** A 4-chamber slice. **(6B)** A short-axis slice reformatted from the 4-chamber 3D LGE images. No scar is present in this case.

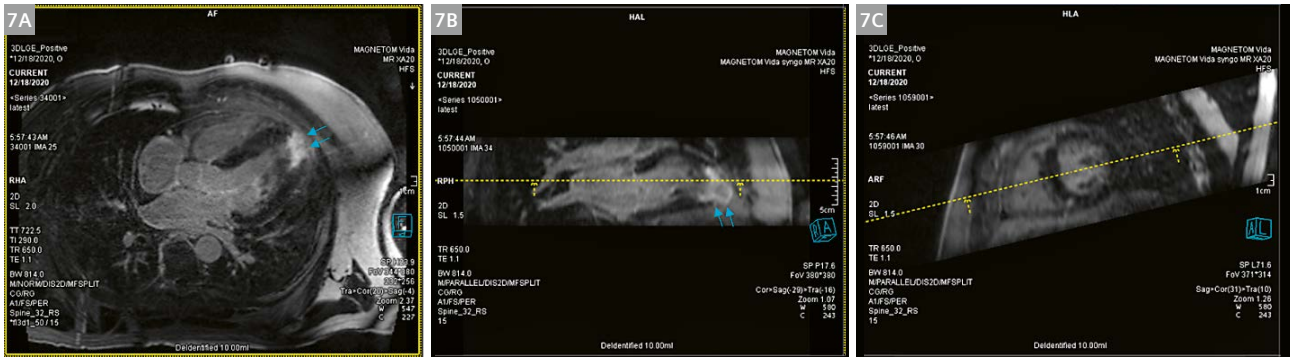

7 Exemplary images of 3D LGE acquisition in another subject. **(7A)** A 4-chamber slice. **(7B)** A 2-chamber slice reformatted from the 4-chamber 3D LGE images. **(7C)** A short-axis slice reformatted from the same dataset. Scar is present in the apical segment (arrows).

Image reconstruction

The acquisition is reconstructed inline and the images can be reformatted to short-axis and/or 2-chamber views as desired using multiplanar reconstruction. As shown in Figure 5 the reconstruction can be done in the following steps:

1) Selecting the 3D LGE series as the source images in MR View&Go or opening the series with MR View&Go.
2) Selecting "Parallel Ranges" from the upper left corner menu of the source images (Fig. 5 Panel A).
3) Adjusting the orientation, position, and coverage of the slices to be reconstructed (Fig. 5 Panel B and D).
4) Scrolling through the slices in the Preview window to check if the results are satisfactory (Fig. 5 Panel C).
5) Clicking "Start" to start the reconstruction and then "Accept" to save the output images (Fig. 5 Panel D).

Clinical examples

Figures 6 and 7 show exemplary images of 3D LGE from two clinical cases. Both the original 4-chamber view and the reconstructed short-axis or 2-chamber views are included. The first case was LGE negative with no scar present. The second case was positive showing scar in the apical area.

Discussion

In this article, we described the workflow and set up of how 3D LGE is performed at our center. With the modified protocol, we can perform high-resolution LGE imaging of the ventricle within five minutes. The workflow has been simplified to one-time setup by using 3D and free-breathing acquisition. A higher through-plane resolution is achieved compared to multi-slice 2D LGE imaging. The 3D images are acquired on 4-chamber planes but can be conveniently reformatted to other planes for flexible interpretation.

The .exar1 protocol is available for download at:
www.siemens-healthineers.com/magnetom-world
> Clinical Corner > Protocols > Cardiovascular MRI

Patrick Pierce

Beth Goddu

Contact

Reza Nezafat, Ph.D.
Cardiovascular MR Center,
Beth Israel Deaconess Medical Center
330 Brookline Ave
Boston, MA 02215
USA
rnezafat@bidmc.harvard.edu

Whole-heart High-resolution Late Gadolinium Enhancement in Clinical Routine

Solenn Toupin, Ph.D.[1]; Aurélien Bustin, Ph.D.[2,3,4]; Hubert Cochet, M.D., Ph.D.[2,3]

[1]Siemens Healthineers, Saint-Denis, France
[2]IHU LIRYC, Electrophysiology and Heart Modeling Institute, Université de Bordeaux, INSERM, Centre de recherche Cardio-Thoracique de Bordeaux, U1045, Bordeaux, France
[3]Department of Cardiovascular Imaging, Hôpital Cardiologique du Haut-Lévêque, CHU de Bordeaux, Pessac, France
[4]Department of Diagnostic and Interventional Radiology, Lausanne University Hospital and University of Lausanne, Switzerland

Introduction

Over the past two decades, late gadolinium enhancement (LGE) has become the preferred imaging technique for detecting myocardial infarction and fibrosis in various non-ischemic diseases [1–3]. LGE relies on a T1-weighted inversion-recovery gradient-echo pulse sequence acquired at least 10 minutes after gadolinium injection. The acquisition is performed during breath-hold with a conventional in-plane spatial resolution of 1.4–1.8 mm and a slice thickness of 6–8 mm [4]. Nowadays, several variants of LGE pulse sequences co-exist in clinical routine with different excitation pulses (2D or 3D), read-out schemes (FLASH or TrueFISP), acquisition strategies (segmented or single-shot), and motion compensation approaches (breath-hold or free breathing). In any case, the spatial resolution remains limited by scan time constraint, in other words by the breath-hold duration, which must stay below ~13 seconds to be acceptable in clinical routine.

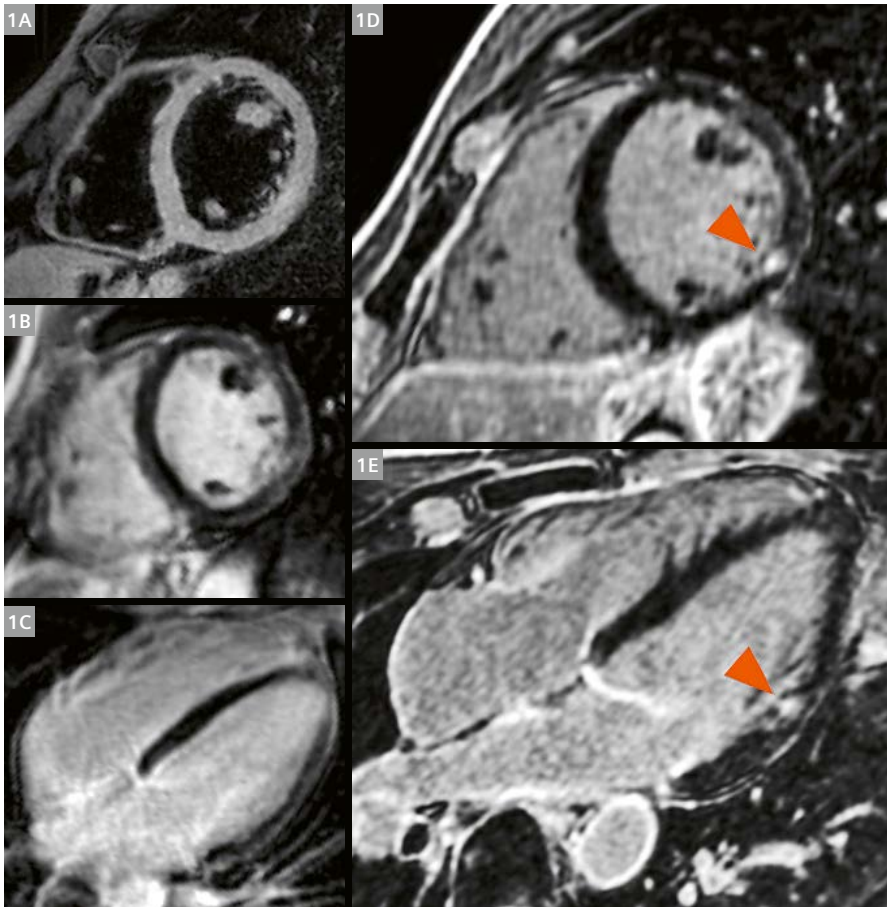

1 A 38-year-old female patient presented with typical angina and mildly elevated troponin levels. Coronary angiography showed no significant coronary artery stenosis. During the CMR exam, T2-weighted STIR **(1A)** and conventional LGE **(1B, C)** were considered negative. HR-LGE **(1D, E)** revealed focal subendocardial enhancement on the inferolateral segment, consistent with microinfarction (orange arrowheads).

Whole-heart high-resolution LGE (HR-LGE) was initially introduced to assess fibrosis in the left atrial (LA) wall, which is five times thinner than the left ventricular (LV) wall. To achieve much higher spatial resolution, breath-hold had to be replaced by free breathing with navigator gating, resulting in an extended scan time. HR-LGE gained significant momentum with the DECAAF study (Delayed-Enhancement MRI Determinant of Successful Radiofrequency Catheter Ablation of Atrial Fibrillation), which demonstrated a significant association between atrial fibrosis and arrhythmia recurrence after ablation in 15 clinical centers using Siemens Healthineers MR systems [5]. The DECAAF study extensively validated a whole-heart LGE protocol with an improved spatial resolution of 1.25 × 1.25 × 2.5 mm at 1.5T and 3T.

As DECAAF study investigators, our group has been performing HR-LGE for more than a decade and we have found clear evidence of its clinical value in both the atria and the ventricles. In this article, we share when and how we perform HR-LGE imaging daily, and how we identify patients who are likely to benefit the most from it.

Why perform whole-heart high-resolution LGE?

Firstly, HR-LGE does not have to be performed in every patient, especially when conventional LGE is sufficient to make a diagnosis. However, HR-LGE can be instrumental for several diagnoses, which we present below.

Myocardial infarction with non-obstructive coronary arteries (MINOCA)

MINOCA is a 'working diagnosis' for patients who present with acute coronary syndromes and in whom the diagnosis of myocardial infarction remains uncertain after coronary angiography. In 2020, guidelines from the European Society of Cardiology (ESC) recommend performing cardiovascular MRI (CMR) in all MINOCA patients without an obvious underlying cause [6]. Indeed, the presence and topography of LGE assessed by CMR plays a key role for the differential diagnosis of Takotsubo syndrome, myocarditis, or true myocardial infarction without obstructive coronary artery disease. However, CMR imaging is normal or inconclusive in about 25% of patients with MINOCA, creating a problem for decision-makers [7, 8]. Our group recently investigated the diagnostic value of HR-LGE in these cases [9]. After studying 172 patients with MINOCA, we showed

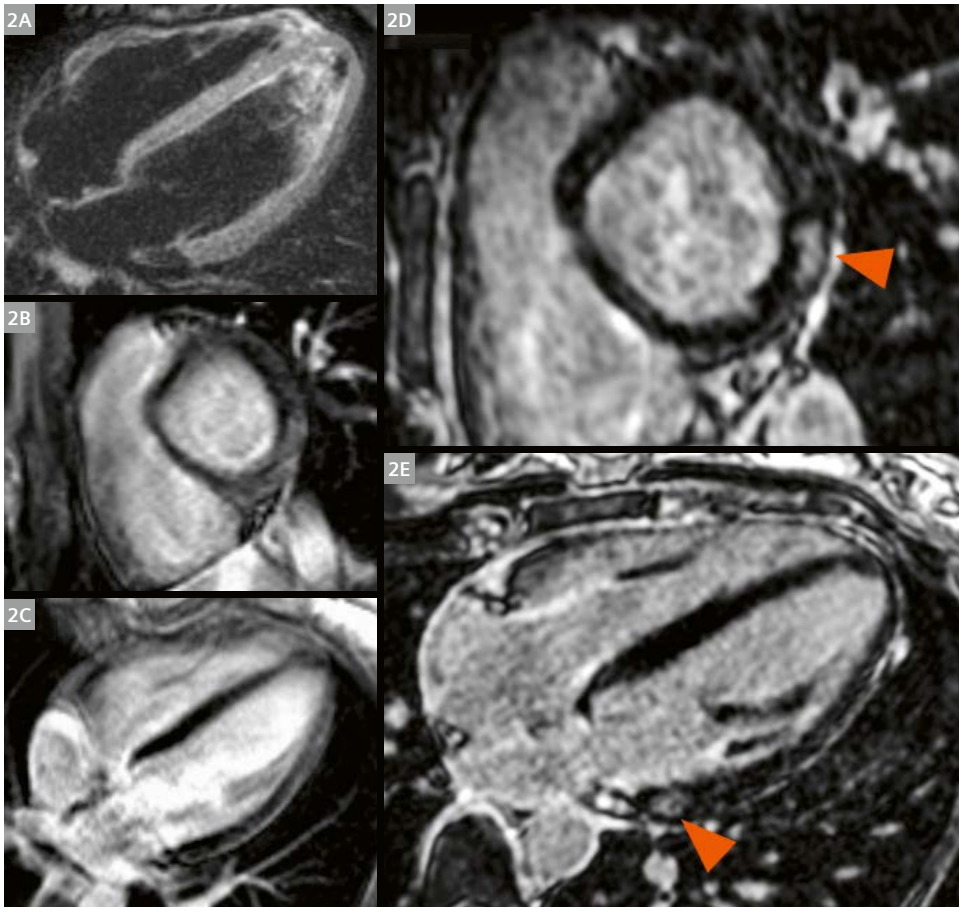

2 A 21-year-old female patient presented with atypical chest pain and elevated troponin levels. T2-weighted STIR **(2A)** and conventional LGE **(2B, C)** were considered negative. HR-LGE **(2D, E)** revealed focal subepicardial enhancement on the inferolateral segment, consistent with myocarditis (orange arrowheads).

that HR-LGE is particularly valuable when conventional LGE is negative or compatible with several diagnoses. Interestingly, it led to a change in the final diagnosis in 26% of the patients. Given that one third of these patients initially had a negative conventional LGE, these findings suggest that higher spatial resolution is of great interest. Examples of diagnoses made thanks to the addition of HR-LGE are shown in Figures 1 and 2. Improving the etiological diagnosis of MINOCA has a major impact on patient management, as it directly influences drug therapy and could motivate additional diagnostic tests to detect occult causes of myocardial infarction. This further supports the systematic use of HR-LGE in patients with MINOCA when conventional LGE is negative or inconclusive.

Diagnosis and prognosis in ventricular arrhythmia

Ventricular arrhythmias are an extremely common phenomenon. Most arrhythmias are not sustained, and therefore do not expose the patient to an increased risk of sudden death. These 'benign' ventricular arrhythmias are due to an ectopic focus most often confined to the right ventricular outflow tract. They occur in structurally normal hearts and can usually be recognized from clinical presentation and 12-lead ECG characteristics. In many cases, though, the presentation is atypical and potentially suggests a structural substrate, which can either be ruled out or diagnosed on CMR. Myocardial scars detected on LGE CMR are known to facilitate arrhythmia sustenance and therefore play a major role in arrhythmia malignancy. Besides this prognostic role, CMR is also key to establishing the diagnosis of the underlying structural heart disease. Our group investigated the value of using HR-LGE to improve the detection of focal arrhythmogenic substrates. After studying a series of 157 patients with ventricular arrhythmias, we showed that the detection rate of structural abnormalities improved two-fold with HR-LGE compared to conventional CMR methods [10]. This includes the detection of small scars on the left ventricle suggestive of occult ischemic and non-ischemic diseases, as well as the detection of right ventricular (RV) fibrosis, which can be key to diagnosing arrhythmogenic right ventricular cardiomyopathy. Indeed, although RV LGE is not part of the 2010 Task Force Criteria for the diagnosis of arrhythmogenic right ventricular cardiomyopathy, our experience suggests that in cases of borderline regional RV wall motion abnormalities, the presence of RV fibrosis on high-resolution LGE might help to confirm this challenging diagnosis (Fig. 3).

Catheter ablation guidance in scar-related ventricular arrhythmias

In patients presenting with ventricular arrhythmias, HR-LGE is also useful for guiding catheter ablation by providing precise visualization of arrhythmogenic sites [11]. Indeed, channels of surviving fibers within scar are the substrate on which scar-related re-entrant tachycardia can occur. This can be recognized on LGE images as areas of intermediate signal intensity, the so-called 'gray zones'. HR-LGE is crucial in this indication for detecting gray-zone channels on thinned walls and for appropriately rendering their 3D architecture. As shown in Figure 4, a 3D reconstruction of the different types of tissue (normal, dense scar, and gray-zone channels) can be processed from HR-LGE images using commercially available solutions. This pre-procedural analysis of the scar architecture can then be displayed in 3D electroanatomical mapping systems during the procedure, allowing the electrophysiologist to identify the best ablation strategy. It is important to mention here that in this indication, as most patients undergoing catheter ablation carry implantable cardioverter defibrillators (ICDs), the HR-LGE images acquired pre-operatively can be significantly hampered by susceptibility artifacts. Unfortunately, although wideband methods have been specifically developed to address this problem, they do not fully alleviate the image-quality issues. Our institution therefore routinely performs CMR including whole-heart high-resolution LGE before ICD implantation. This is justified by the need for accurate measurements of left ventricular ejection fraction to select patients eligible for implantation of a primary prevention ICD, and by the need to obtain detailed and

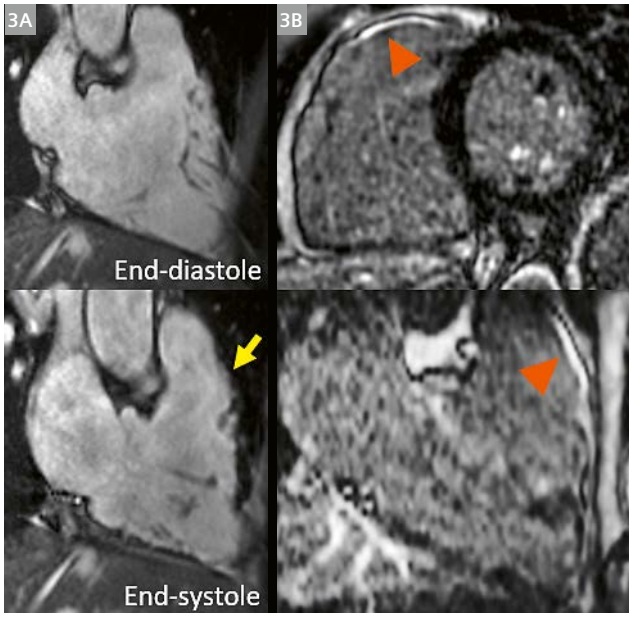

3 A 45-year-old male patient was referred for evaluation due to a recent family history of sudden cardiac death. CMR showed right ventricular dilatation and borderline wall motion abnormality in the right ventricular outflow tract (**3A,** yellow arrow). HR-LGE showed focal fibrosis in the outflow tract (**3B,** orange arrowheads). The finding of focal LGE on an area of borderline wall motion was instrumental in retaining the diagnosis of arrhythmogenic right ventricular cardiomyopathy.

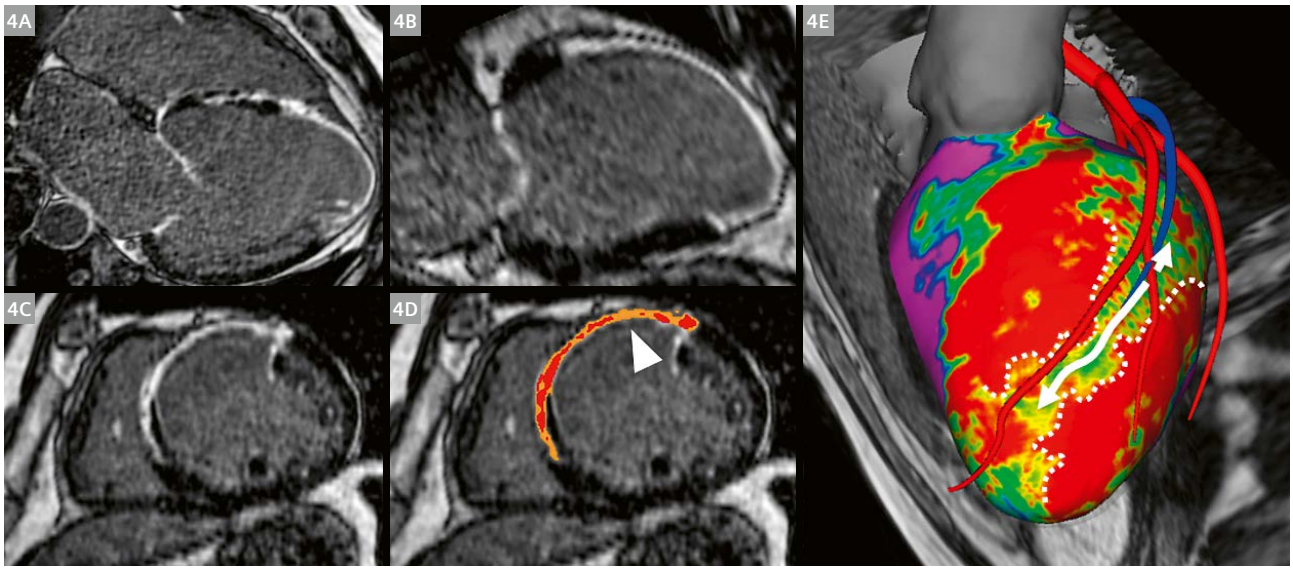

4 HR-LGE is segmented based on the signal intensity **(4A–D)** to reconstruct the complex scar architecture of this patient **(4E)**: violet (normal tissue), blue-green-yellow (gray zone), and red (dense scar). A conducting channel (**4D,** white arrowhead; and **4E,** white arrow) could be identified inside the dense scar area. This 3D rendering was useful for guiding the ventricular tachycardia ablation by integrating the image into electroanatomical systems.

high-quality HR-LGE images of the scar, which may be useful in the future if the patient comes back with ICD shocks requiring catheter ablation.

High-resolution 3D whole-heart LGE: how we do it

Sequence parameters and positioning

The sequence parameters are presented in Table 1. HR-LGE is a 3D inversion-recovery spoiled gradient-echo (FLASH) pulse sequence. The voxel size is 1.25 × 1.25 × 2.5 mm^3, reconstructed to 0.63 × 0.63 × 1.25 mm^3. All desired views can be reconstructed from the 3D volume, which is of particular interest compared to conventional breath-hold LGE. For that reason, the interpolation allows a better image quality for multi-planar reconstructions. Spectral fat saturation is used to remove epicardial fat signal and to facilitate the visualization of epicardial LGE. The volume is strictly transversal and positioned on free-breathing localizer images (Fig. 5). A margin is kept in head-feet direction to avoid cropping the ventricle. While this may at first seem counter-intuitive, the phase-encoding direction is set in left-right direction in order to minimize residual artifacts caused by breathing. To reduce the fold-over artifact from the arms, two saturation bands are positioned over the arms (see Fig. 5). A third band is positioned over the chest to also reduce ghosting artifacts and subcutaneous fat signal.

3D whole-heart HR-LGE	
Sequence type	3D spoiled gradient-echo
Motion compensation	Diaphragmatic navigator gating (acceptance window: 3 mm)
TR/TE	5.2/2.50 ms
Field of view	360 x 360 x 120 mm
Matrix	288 x 288 pixels
Acquired voxel size	1.25 x 1.25 x 2.5 mm
Reconstructed voxel size	0.63 x 0.63 x 1.25 mm
Flip angle	19°
Bandwidth	255 Hz/pixel
Fat suppression	Spectral fat saturation
Phase encoding direction	Right-left
Phase oversampling	20 %
Slice oversampling	16.7 %
Acceleration method	Parallel imaging (GRAPPA)
Acceleration factor	2
Number of heartbeats	295
Number of segments per heartbeat	35
Acquisition window	156 ms

Table 1: High-resolution 3D whole-heart LGE sequence parameters

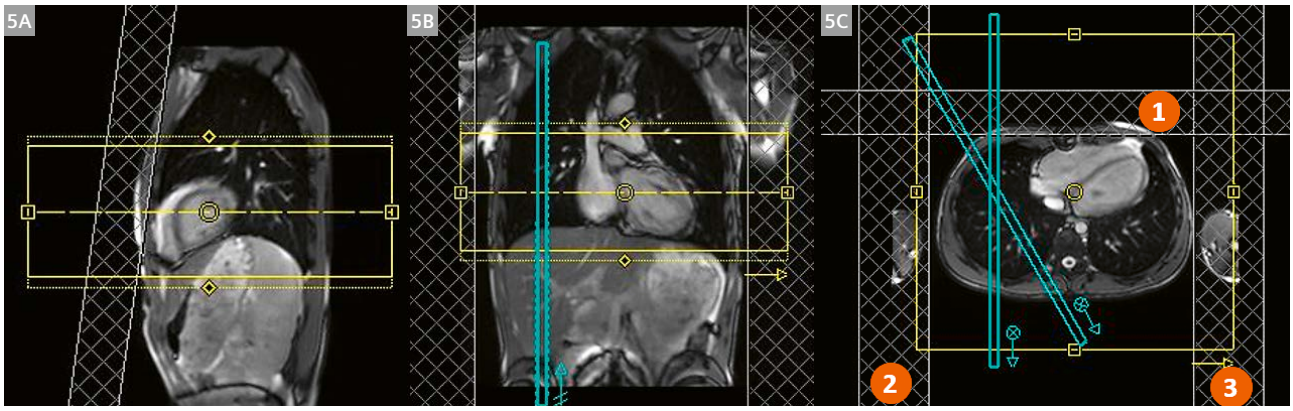

5 **Sequence positioning on the MR console:** The volume (yellow box) is positioned in strict transversal orientation to cover the ventricles on free-breathing localizers: sagittal **(5A)**, coronal **(5B)**, and transversal **(5C)**. The intersection of the crossed pair of the navigator is positioned on the liver dome (blue boxes). Three saturation bands are positioned on the patient's chest (1) and arms (2 and 3) to reduce fold-over artifacts in the right-left direction (phase encoding direction, depicted by the yellow arrow).

6 **Navigator settings:** The sequence is first run with 'Scout Mode' selected (**6A,** orange rectangle) so that the navigator data is displayed in the 'Online Display' window **(6B)**. This window shows the navigator line through the lung (hyposignal) and the liver (hypersignal). The expiratory phase is automatically detected and indicated as 'Mode' (**6B,** orange rectangle). The green box represents the acceptance window of ± 3 mm, in which data will be accepted. The scan efficiency is shown as a percentage next to 'Accept'. The 'Mode' value has to be entered manually into the 'Search Position (red)' field **(6C)** to center both the green and red boxes on this position. 'Scout Mode' is then deselected to run the real scan **(6C)**. During the scan, the navigator is displayed in the 'Inline Display' window, so that it can be checked by the technologist **(6D)**. The remaining data to be acquired is indicated as a percentage to the right of 'Ima', and the scan efficiency is still indicated as 'Accept'. As 'Resp. Motion Adaptation' is selected **(6C)**, the acceptance position (green box) will be dynamically adapted over time to account for breathing drift.

Gadolinium injection and timing
HR-LGE is acquired 15 to 30 minutes after injection of gadolinium-based contrast agent (double dose) [12]. The inversion time (TI) must be set to null the normal myocardium signal. An off-set of 20–30 ms at 1.5T and of 50–80 ms at 3T must be added to account for gadolinium wash-out during the scan. This off-set must be determined empirically by each center and depending on their habits.

Navigator positioning and setting
A spectrally selective crossed-pair navigator is used to dynamically track the respiratory motion. The cross section of the two planes must be positioned on the liver dome at the interface between the lung and the diaphragm (Fig. 5). The navigator should not cross any anatomy of interest. The sequence is first run for ~20 seconds to check the quality of the navigator and enter the expiratory phase position (in mm). For this, 'Scout Mode' is selected in the 'Physio/PACE' section of the sequence settings (Fig. 6A). The navigator data will be displayed over time in the 'Inline Display' window as a line through the liver (hypersignal) and the lung (hyposignal) (Fig. 6B). The green box shows the positions in which data acquisition is permitted. In our protocol, the acceptance window (green-box thickness) is set to ± 3 mm. The ideal accepted position is automatically detected by the system and indicated as 'Mode'. This value must be entered manually in the 'Search Position (red)' field, so that both red and green boxes are centered on this position (Fig. 6C). Scout Mode should be unchecked before validating the sequence. During the scan, the navigator data is displayed in the 'Inline Display' window (Fig. 6D). The scan efficiency is indicated as a percentage ("Accept 33%" in the example in Fig. 6). This value should remain above 30% to maintain a reasonable scan time. To ensure good scan efficiency, the patient should have the shallowest breathing pattern, which is not always easy to obtain. The 'Respiratory Motion Adaptation' feature allows the position of the green box to be dynamically adapted in case of breathing drift during the scan. However, if the drift is too severe, the scan efficiency will be preserved, but the image quality might be impaired. Note that the 'Search Position (red)' box is not updated during the scan.

ECG triggering
HR-LGE is electrocardiogram (ECG)-triggered in the end-diastolic phase every heartbeat. The number of segments determines the number of acquired lines per heartbeat, and therefore the total acquisition time. The longer the cardiac cycle, the longer the diastolic resting phase. With this in mind, we adapt the number of segments to the patient's heart rate, following Table 2. That way, the scan time is less dependent on the patient's heart rate. The repetition time (TR) is set below the cardiac cycle (e.g., TR = 680 ms for RR = 800 ms) to allow for potential changes in heart rate during the scan. In patients with arrhythmia, the TR is decreased to the shortest cardiac cycle encountered in the patient.

Heart rhythm (beats per minute)	Cardiac cycle (ms)	Number of segments	TR (ms)
120	500	18	440
100	600	22	520
86	700	26	600
75	800	29	680
67	900	33	760
55	1000	37	840

Table 2: Physio settings for high-resolution 3D whole-heart LGE

Future technical developments of high-resolution LGE

Despite promising results, the main problem with HR-LGE is the scan time, which is not compatible with all clinical workflows. Efforts are currently underway to accelerate this sequence, either by improving the navigator efficiency or by further under-sampling *k*-space data.

Data acquisition is currently restricted to an acceptance window of ± 3 mm at end expiration, resulting in a limited scan efficiency of 30–60%. This efficiency can further decrease in the case of irregular breathing and lead to long and unpredictable scan times. In addition, the complex motion of the heart is not taken into account, as a simplified linear correlation with the diaphragm is used. Novel image-based navigators (iNAV) have recently been introduced to directly track the heart and compensate for non-rigid motion during image reconstruction. This improves scan efficiency to 95–100%, reduces the scan time, and makes it predictable. The technique has shown promising results for whole-heart HR-LGE [13, 14].

k-space under-sampling is another way of accelerating HR-LGE by acquiring less data. Conventional HR-LGE is usually under-sampled by a factor of two using parallel imaging with generalized autocalibrating partially parallel acquisitions (GRAPPA). Higher acceleration rates are hindered by the inherent loss of signal-to-noise ratio and by parallel-imaging artifacts. As an alternative, compressed-sensing acceleration has been proposed to further accelerate whole-heart LGE sequences using incoherent *k*-space under-sampling followed by iterative non-linear reconstruction. Initial implementations showed scan time acceleration without compromising image quality in the atria and the ventricles [15–17]. However, iterative recon-

struction is time-consuming and requires powerful reconstruction systems equipped with graphics processing units (GPU). Hence, artificial intelligence with fast deep-learning reconstruction might play a role in further developing the clinical availability of HR-LGE in the future [18].

Conclusion

High-resolution 3D whole-heart LGE improves the sensitivity of CMR for the detection and characterization of structural heart diseases. Preliminary experience, particularly in the context of MINOCA and ventricular arrhythmias, indicates that HR-LGE goes far beyond the current state-of-the-art breath-hold LGE imaging. Knowing the diagnostic and prognostic value of LGE, the method has the potential to significantly impact clinical decision-making in many domains of cardiology. Although the extended scan time remains a significant limitation, the combination of under-sampling and better scan efficiency might soon bring HR-LGE closer to widespread clinical use.

References

1 Kim RJ, Fieno DS, Parrish TB, Harris K, Chen E-L, Simonetti O, et al. Relationship of MRI Delayed Contrast Enhancement to Irreversible Injury, Infarct Age, and Contractile Function. Circulation. 1999;100(19):1992–2002.

2 Mahrholdt H, Wagner A, Judd RM, Sechtem U, Kim RJ. Delayed enhancement cardiovascular magnetic resonance assessment of non-ischaemic cardiomyopathies. Eur Heart J. 2005;26(15):1461–74.

3 Kuruvilla S, Adenaw N, Katwal AB, Lipinski MJ, Kramer CM, Salerno M. Late Gadolinium Enhancement on Cardiac Magnetic Resonance Predicts Adverse Cardiovascular Outcomes in Nonischemic Cardiomyopathy: A Systematic Review and Meta-Analysis. Circ Cardiovasc Imaging. 2014;7(2):250–8.

4 Kramer CM, Barkhausen J, Bucciarelli-Ducci C, Flamm SD, Kim RJ, Nagel E. Standardized cardiovascular magnetic resonance imaging (CMR) protocols: 2020 update. J Cardiovasc Magn Reson. 2020;22(1):17.

5 Marrouche NF, Wilber D, Hindricks G, Jais P, Akoum N, Marchlinski F, et al. Association of Atrial Tissue Fibrosis Identified by Delayed Enhancement MRI and Atrial Fibrillation Catheter Ablation: The DECAAF Study. JAMA. 2014;311(5):498–506.

6 Collet J-P, Thiele H, Barbato E, Barthélémy O, Bauersachs J, Bhatt DL, et al. 2020 ESC Guidelines for the management of acute coronary syndromes in patients presenting without persistent ST-segment elevation. Eur Heart J. 2020;ehaa575.

7 Pasupathy S, Air T, Dreyer RP, Tavella R, Beltrame JF. Systematic Review of Patients Presenting With Suspected Myocardial Infarction and Nonobstructive Coronary Arteries. Circulation. 2015;131(10):861–70.

8 Dastidar AG, Baritussio A, De Garate E, Drobni Z, Biglino G, Singhal P, et al. Prognostic Role of CMR and Conventional Risk Factors in Myocardial Infarction With Nonobstructed Coronary Arteries. JACC Cardiovasc Imaging. 2019;12(10):1973–82.

9 Lintingre P-F, Nivet H, Clément-Guinaudeau S, Camaioni C, Sridi S, Corneloup O, et al. High-Resolution Late Gadolinium Enhancement Magnetic Resonance for the Diagnosis of Myocardial Infarction With Nonobstructed Coronary Arteries. JACC Cardiovasc Imaging. 2020;13(15)1135–1148. Epub 2020 Jan 15.

10 Hennig A, Salel M, Sacher F, Camaioni C, Sridi S, Denis A, et al. High-resolution three-dimensional late gadolinium-enhanced cardiac magnetic resonance imaging to identify the underlying substrate of ventricular arrhythmia. Europace. 2018;20(FI2):f179–91.

11 Yamashita S, Sacher F, Mahida S, Berte B, Lim HS, Komatsu Y, et al. Image Integration to Guide Catheter Ablation in Scar-Related Ventricular Tachycardia: Image Integration-Guided VT Ablation. J Cardiovasc Electrophysiol. 2016;27(6):699–708.

12 Siebermair J, Kholmovski EG, Marrouche N. Assessment of Left Atrial Fibrosis by Late Gadolinium Enhancement Magnetic Resonance Imaging. JACC Clin Electrophysiol. 2017;3(8):791–802.

13 Munoz C, Bustin A, Neji R, Kunze KP, Forman C, Schmidt M, et al. Motion-corrected 3D whole-heart water-fat high-resolution late gadolinium enhancement cardiovascular magnetic resonance imaging. J Cardiovasc Magn Reson. 2020;22(1):53.

14 Bratis K, Henningsson M, Grigoratos C, Dell'Omodarme M, Chasapides K, Botnar R, et al. 'Image-navigated 3-dimensional late gadolinium enhancement cardiovascular magnetic resonance imaging: feasibility and initial clinical results'. J Cardiovasc Magn Reson. 2017;19(1):97.

15 Akçakaya M, Rayatzadeh H, Basha TA, Hong SN, Chan RH, Kissinger KV, et al. Accelerated Late Gadolinium Enhancement Cardiac MR Imaging with Isotropic Spatial Resolution Using Compressed Sensing: Initial Experience. Radiology. 2012;264(3):691–699.

16 Basha TA, Akçakaya M, Liew C, Tsao CW, Delling FN, Addae G, et al. Clinical performance of high-resolution late gadolinium enhancement imaging with compressed sensing. J Magn Reson Imaging. 2017;46(6):1829–38.

17 Kamesh Iyer S, Tasdizen T, Burgon N, Kholmovski E, Marrouche N, Adluru G, et al. Compressed sensing for rapid late gadolinium enhanced imaging of the left atrium: A preliminary study. Magn Reson Imaging. 2016;34(7):846–54.

18 El-Rewaidy H, Neisius U, Mancio J, Kucukseymen S, Rodriguez J, Paskavitz A, et al. Deep complex convolutional network for fast reconstruction of 3D late gadolinium enhancement cardiac MRI. NMR Biomed [Internet]. 2020 Jul [cited 2020 Nov 29];33(7). Available from: https://onlinelibrary.wiley.com/doi/abs/10.1002/nbm.4312

Contact

Professor Hubert Cochet
Department of Cardiovascular Imaging
Hôpital Cardiologique du Haut-Lévêque
CHU de Bordeaux
Avenue de Magellan
33604 Pessac
France
hubert.cochet@chu-bordeaux.fr

3D Coronary MRA Integrated in a Fast and Comprehensive Free-breathing CMR Exam

Juliano Lara Fernandes, M.D., Ph.D., M.B.A.[1]; Karl P. Kunze, Ph.D.[2]; Claudia Prieto, Ph.D.[3]; Rene Botnar, Ph.D.[3]

[1]Cardiovascular Department, Radiologia Clinica de Campinas, Jose Michel Kalaf Research Institute, Campinas, SP, Brazil
[2]MR Research Collaborations, Siemens Healthineers, Frimley, UK
[3]Department of Biomedical Engineering, King's College London, UK

Introduction

Coronary artery disease (CAD) evaluation is one of the cornerstones of cardiovascular imaging. Cardiovascular magnetic resonance (CMR) has been shown to have many advantages in the assessment of the disease, and multiple randomized multi-center trials have demonstrated its diagnostic and prognostic capabilities [1–4]. The evaluation of CAD by CMR has mostly focused on identifying relevant functional information regarding myocardial perfusion, and associating that evidence with left ventricular global and regional function, as well as with scar data from late gadolinium enhancement (LGE) images. Most studies have used qualitative assessment of myocardial perfusion as an indication of significant coronary stenosis, but more recently automated quantitative stress perfusion has been made available for routine clinical workflows [5].

Despite the important functional information provided by CMR, the increased availability of, and clinical results from studies using coronary computed tomography angiography (CCTA), as well as recent findings in the ISCHEMIA trials, have raised questions about whether an anatomical or functional test is better for assessing CAD [6,7]. While a more thorough discussion of the debate is beyond the scope of this manuscript, recent ESC guidelines for stable CAD have been revised to incorporate anatomical evaluation as a first-line diagnostic test, especially in patients with a low-to-intermediate likelihood of obstructive disease [8].

The role for CMR in the assessment of CAD in this ever-changing environment will require further critical developments given these recent clinical findings. On

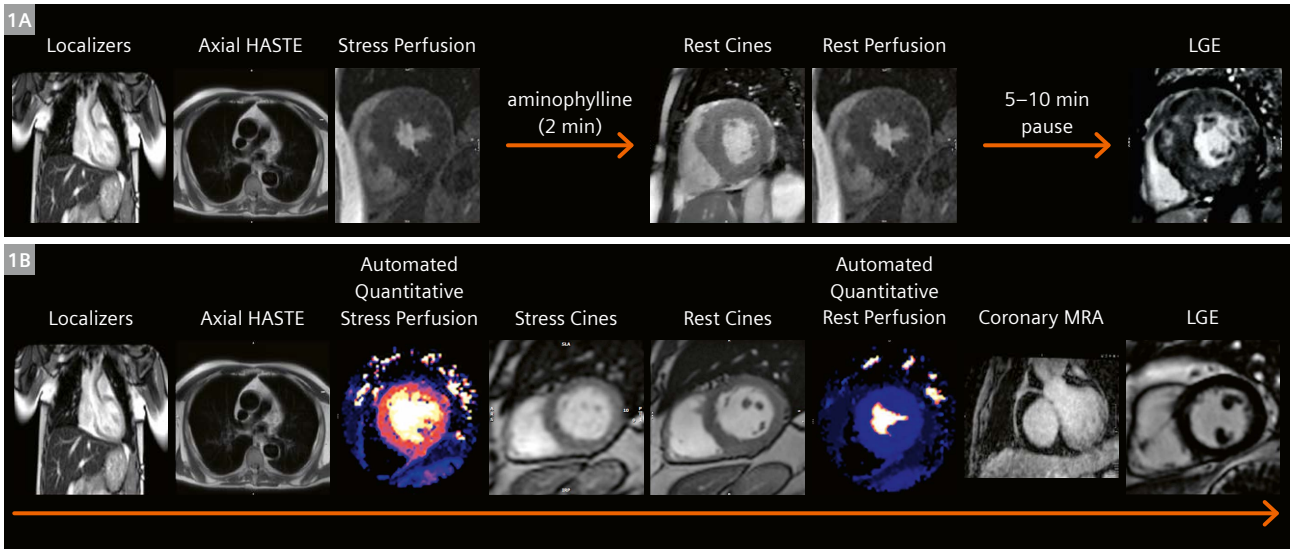

1 **(1A)** The first routine free-breathing (FB) protocol used in 2017, which did not incorporate quantitative perfusion data or coronary magnetic resonance angiography (MRA); **(1B)** the latest version of the protocol with the quantitative perfusion data, plus the stress cine images and coronary MRA included in the temporal gaps of the first protocol, with limited time penalty. The whole stress protocol takes around 30 minutes to complete.

the one hand, we have a technique that has many unique features, robust clinical evidence of effectiveness, and an advantageous cost-effectiveness ratio in CAD evaluation [9]. On the other hand, the modality remains under-utilized in most parts of the world [10], is still considered a time-consuming imaging exam, and so far offers limited evidence for providing routine clinical assessment of coronary anatomy. 3D coronary magnetic resonance angiography (CMRA) has been available for more than two decades [11], but limited spatial resolution and heart coverage, long unpredictable (due to respiratory gating), and associated image degradation due to respiratory motion acquisition times have prevented its more widespread use [12]. Recent technical developments in free-breathing whole-heart CMRA including the use of artificial intelligence (AI), faster acquisition sequences, and motion-compensated reconstruction have made it possible to provide images that are clinically useful within a clinical environment [13]. Integrating the newer anatomical data provided by these sequences to the already established functional CMR exam is still a challenge. In the following, we try to provide a framework which we believe can help CMR to overcome some of the hurdles involved in this integration and offer a truly comprehensive approach to provide both anatomical and quantitative functional data for CAD in a relatively short time slot while still maintaining its cost-effectiveness.

A complete free-breathing protocol

In 2017, we started using a free-breathing (FB) protocol routinely in our clinical scans with a MAGNETOM Verio 3T scanner [14], which we later upgraded to a MAGNETOM Skyra^{fit}. The initial FB protocol is shown in Figure 1A. In summary, it contained routine orthogonal and cardiac axis localizers, an axial black-blood T1-weighted half-Fourier single-shot turbo spin echo (HASTE) sequence, a multi-slice FLASH perfusion sequence, a prototype compressed sensing cine bSSFP sequence with sparse sampling and iterative reconstruction, and a prototype respiratory motion-corrected bSSFP averaged phase-sensitive inversion recovery sequence (MOCO-PSIR-LGE) that was reconstructed in-line using the Gadgetron framework [15, 16]. Spatial and temporal resolution of the FB sequences matched clinically used breath-hold protocols. The FB protocol allowed us to perform a cardiac scan in 21.0 ± 5.1 minutes (range 14 to 27 minutes) with comparable image quality to routine breath-hold protocols.

As technology development occurred, we were able to further improve image quality and information gathered during the FB exam by incorporating new sequences that, while providing the same speed of acquisition and FB capabilities, also included new automated features using AI or faster, cloud-based post-processing. The current protocol uses a dual sequence perfusion protocol with in-line, fully automated analysis within a 2-minute reconstruction time [17]. This quantitative approach has been validated against PET perfusion and provides a comprehensive evaluation of ventricular perfusion with no additional acquisition time or manual post-processing [18]. The ability to have quantitative data without the need to change the usual single infusion workflow by using the dual sequence approach, makes this sequence very practical without the need to change any of our routine setup.

In addition to that, we are now able to acquire a full dataset of cine images during vasodilatory stress, comprising a total of 15 slices (three 4-chamber, three 2-chamber, and nine short-axis slices) in less than 1 minute while aminophylline is being administered to the patient. This sequence uses real-time cine images with non-linear reconstruction to provide rapid acquisition times with the high temporal resolution necessary for evaluating possible regional dysfunction during stress [19]. After stress reversal, we can now move on to acquire high-resolution cine images that require more computational power and use a distributed cloud-based solution within the Gadgetron framework [20]. This sequence uses a re-binning scheme from multiple real-time images, which are motion-corrected and averaged to provide a high signal-to-noise ratio as well as high temporal resolution [21]. The additional quantitative perfusion, stress cines, and binning rest cines provide a significant improvement in image quality and quantitative information without adding to the total exam time.

Coronary MRA – the missing link

Despite now having a full FB protocol that provided us with most of the functional data for CAD evaluation, the protocol still included 5 to 10 minutes of dead time after the second contrast infusion for the first-pass rest perfusion while waiting for the LGE acquisitions. In our view, this was the perfect time slot to acquire a coronary MRA that would add anatomical information to the functional information already available.

Twenty years ago, a seminal paper by Kim et al. demonstrated the first true clinical application for coronary MRA [11]. Despite never having really fulfilled its original promise, the use of coronary MRA has significantly evolved over the last few years with the development of many new technical advances that use a combination of faster imaging, more robust respiratory motion correction, and enhanced reconstruction methods to boost both spatial resolution and whole-heart coverage [13]. This has paved the way for the development of new sequences that provide isotropic < 1 mm resolution, simplified 3D scan planning, and reasonable reconstruction times, giving

coronary MRA a true shot at competing with other modalities, especially cardiac CTA [22].

The addition of coronary MRA to perfusion analysis has generated mixed results in recent years [23–25]. The lack of added value for coronary MRA stems partly from earlier technical limitations of the sequences, unpredictable scan time [26], and their particular use in intermediate- to high-risk populations where functional information seems more important. Using more recent techniques, Zhang et al. showed that contrast-enhanced coronary MRA performed at 3T significantly improved sensitivity and diagnostic accuracy versus perfusion/LGE CMR alone [27]. This is in line with work in computed tomography that has shown that the combination of functional and anatomical information can provide results that are superior to either type of data on its own [28].

Coronary MRA – inclusion into FB protocol

In order to take advantage of recently developed rapid FB CAD CMR protocol, we used a coronary MRA prototype WIP sequence[1] developed in collaboration with King's College London that acquires a full coronary 3D dataset within the 5–10 minute window prior to the LGE image acquisition. The sequence uses a 2D image-based navigation (iNAV) [29], a two-point Dixon acquisition with bipolar readout gradients for improved fat suppression [30] and a variable density spiral-like Cartesian (VD-CASPR) trajectory [31, 32] with non-rigid motion-compensated reconstruction [33]. Basic scan parameters on our MAGNETOM Skyra^{fit} scanner included a 3D spoiled gradient echo sequence, FOV 320 x 320 x 90–130 mm for an isotropic spatial resolution of 1.0 mm^3, bandwidth 967 Hz/px, subject specific acquisition window of 70–100 ms, and a 2D iNAV preceding the VD-CASPR acquisition [32]. Undersampling between 5x and 10x was chosen to maintain an acquisition time of around 5–8 minutes, depending on the patient's heart rate. A predictable scan time and 100% respiratory scan efficiency is achieved using a non-rigid motion-compensated iterative reconstruction that is performed in-line on the MARS computer. An example of the sequence setup is shown in Figure 2. The radiographer has to determine the extent of the transversal slab in the coronal plane to include the whole heart, and position the iNAV window within the left ventricle and two saturation bands to cover the arms. Minimum preparation is required for the acquisition beyond these steps. The sequence then outputs four image datasets (Fig. 3): an in-phase, an out-of-phase, a water, and a fat volume.

In order to choose a quiet cardiac phase to acquire the CMRA, we use another prototype[1] for AI-based resting phase detection on a 4-chamber FB CINE prior to the coronary acquisition. The AI algorithm is able to detect and track the motion of the right coronary artery (RCA) located at the atrio-ventricular junction in that cine image [34]. The sequence then generates a graphic motion curve of the RCA throughout the cycle, automatically detecting the best resting phase(s). The time and length of the scan window can be manually edited by adjusting the trigger delay visually, making it a highly customizable option if one chooses to use a systolic or diastolic phase, for example. In Figure 4, an example of the RCA tracking at diastole and systole plus the motion curve and detected resting phases as displayed in the 3D protocol is shown.

Given the ability to perform sequence setup and acquisition in less than 10 minutes, we routinely included this sequence in all our protocols where the information regarding coronary anatomy would be clinically valuable, using the interval prior to LGE imaging in order to avoid extending the exam unnecessarily (Fig. 1B).

[1] *Work in progress: the application is currently under development and is not for sale in the U.S. and in other countries. Its future availability cannot be ensured.*

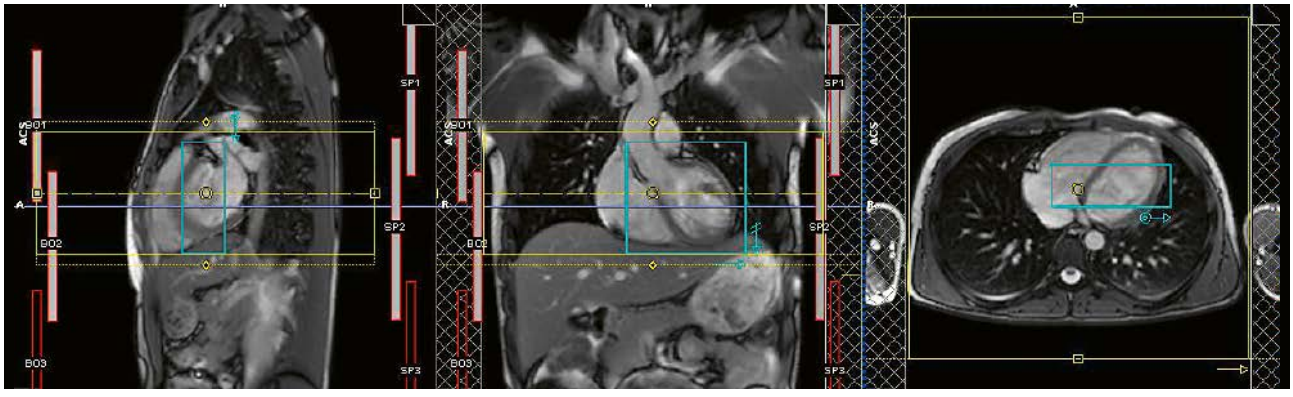

2 A typical whole-heart 3D coronary magnetic resonance angiography (MRA) setup; in yellow, the field of view can be seen with saturation slabs on the arms for signal suppression; at 3T and using the Cartesian spoiled gradient echo acquisition, no specific shim box needs to be established, with coverage of the whole slab; in blue, the 2D image-based navigation (iNAV) tracking in both read and phase directions over the left ventricle.

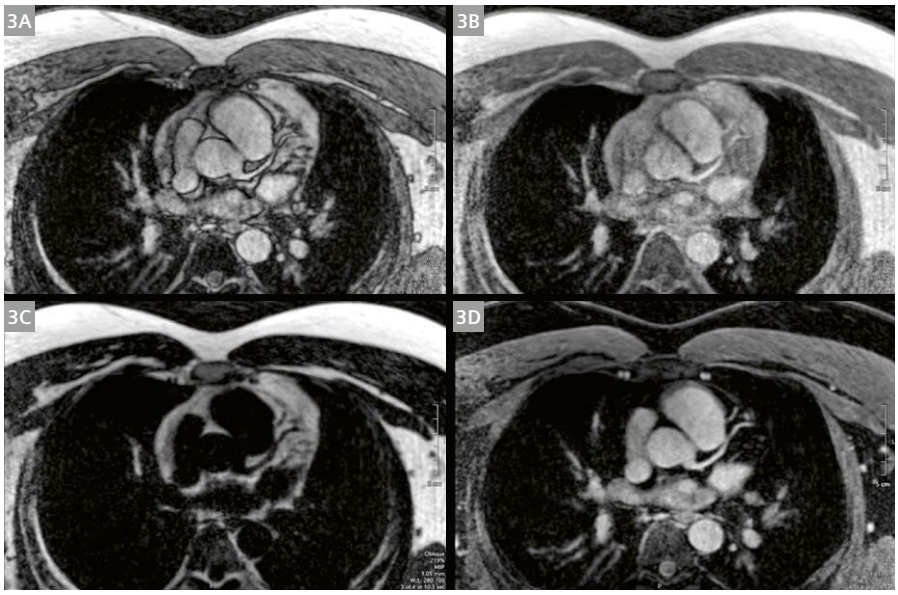

3 The output from the 3D whole-heart coronary magnetic resonance angiography (MRA) sequence used in this study:
(3A) out-of-phase images;
(3B) in-phase images;
(3C) fat-reconstructed images;
(3D) water-reconstructed images.
Most of the time, reading of the coronary MRA was performed only with the water-reconstructed dataset, although the other images may also be used to check for potential artifacts or other anatomical areas of interest outside the coronary tree.

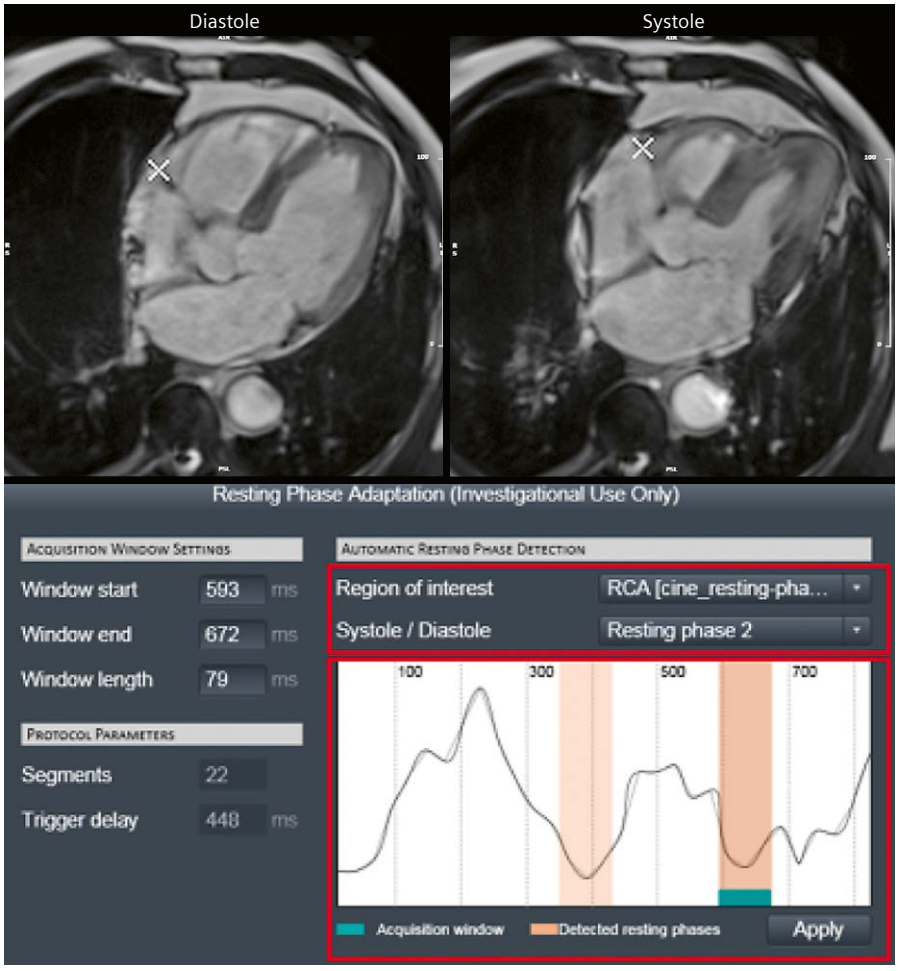

4 The AI-based resting phase detection for static cardiac imaging output is shown after acquiring a free-breathing cine in the 4-chamber long-axis view. The algorithm detects the right coronary artery location and tracks its movement during the cardiac phase (identified in X). It then generates a curve graph depicting the movement and automatically suggests the optimal phase and window length for the best resting phase(s) of the coronary images. This can be manually edited and the user can configure whether to image in systole or diastole, and can set the temporal resolution of the acquisition. Shorter window lengths increase the exam time but shortens the scan-window within one heart-beat, while longer window lengths decrease the total exam time.

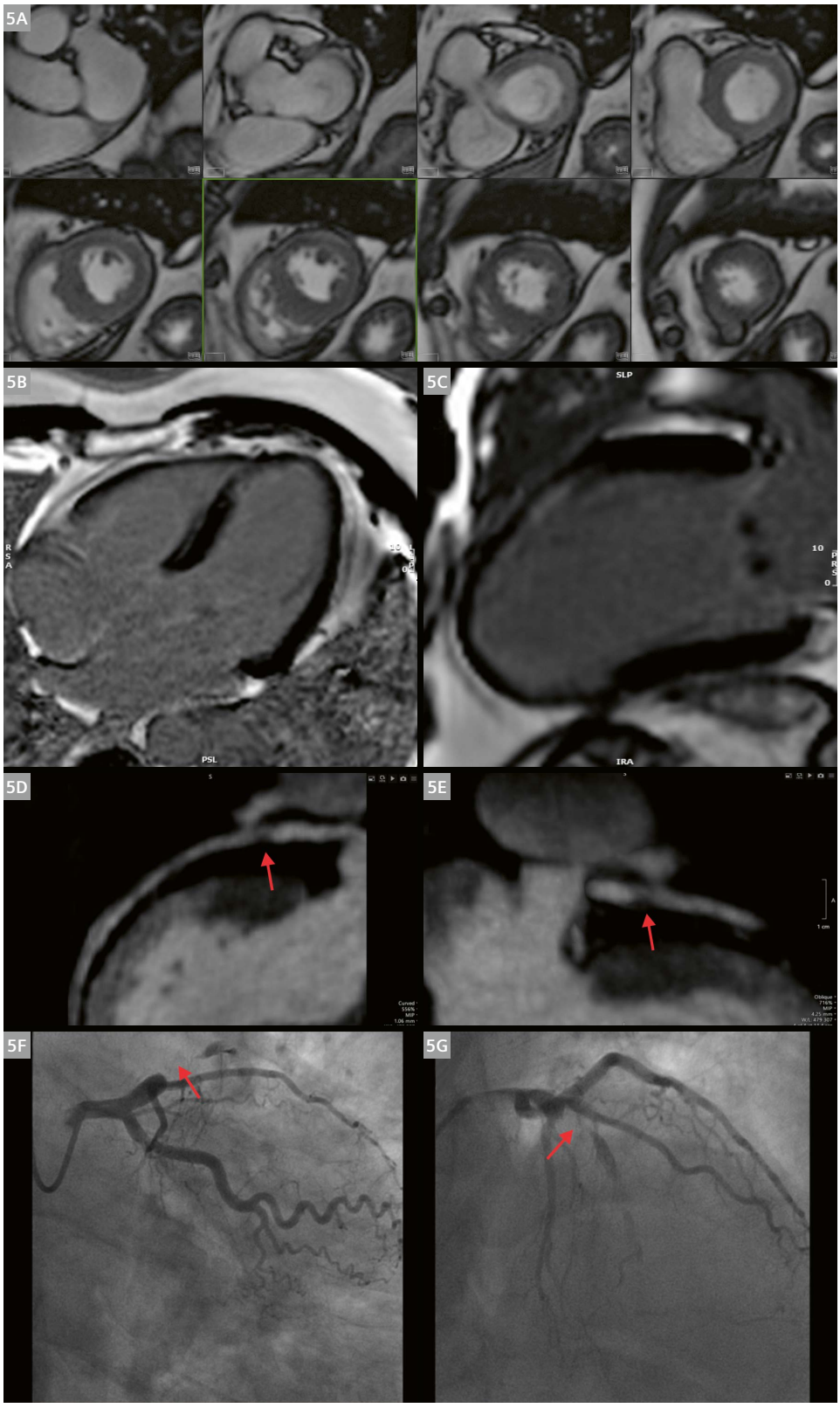

5 **(5A)** In the systolic frame of a short-axis binning FB cine, where one can identify the antero-septal mid-apical segmental hypocontractility; **(5B and C)** show late gadolinium enhanced (LGE) images with a subendocardial infarct in the same segments; **(5D and E)** the left anterior descending (LAD) artery shows a severe obstructive lesion identified in the proximal segment of the artery (red arrows); **(5F and G)** reveal the subsequent invasive angiogram that identified an occluded proximal LAD (red arrows), confirming the findings from the coronary magnetic resonance angiography MRA.

Clinical uses of the integrated FB CMR exam

Since the integration of the Whole-Heart CMRA WIP[1] in our protocol in May 2020, we were able to scan over 350 patients using the integrated FB protocol in a heterogeneous population comprising CAD evaluation, cardiomyopathies, arrythmia investigation, and myocarditis. A more in-depth analysis of the clinical utility, effectiveness, and quality obtained with this protocol is underway, but we believe some examples presented here will help other centers to further explore the possibilities that are opening up with these new techniques.

The first case is a 56-year-old male patient who underwent CMR evaluation for recent onset of typical chest pain associated with a segmental deficit identified on a rest echocardiography. CMR confirmed the akinesia in the antero-septal mid-apical segments of the left ventricle (LV), and LGE revealed a subendocardial infarct in areas with viable myocardium (Fig. 5). Coronary MRA suggested a significant lesion in the proximal segment of the left anterior descending artery (LAD) with preserved distal segments of the artery. After the exam, the patient underwent an invasive angiography that confirmed an occluded proximal LAD, that was treated percutaneously.

The second example is a 77-year-old woman who presented with recent shortness of breath, and had a normal exercise ECG test and global LV function by echocardiography. She underwent a CMR exam for further evaluation of her symptoms and to rule out CAD (Fig. 6).

Her stress first-pass perfusion exam showed a mild defect in the infero-septal wall throughout the whole extension of the LV, although there was some doubt regarding whether the finding represented a true defect. LGE images demonstrated an inferior infarct in the apical segment, comprising 50–75% of the area of that segment. The complementary coronary MRA revealed a dominant left circumflex artery with a significant proximal lesion. The LAD artery was normal (not shown). Coronary MRA confirmed that the perfusion defect was indeed a true defect, and the patient subsequently underwent invasive angiography that confirmed the CMR findings, and was treated accordingly.

The third example is a 32-year-old man, for whom a CMR was requested to investigate the hypothesis of myocarditis after episodes of chest pain and raised serum troponin. His initial native T1 values in a long-axis view (Fig. 7) were normal in the septal region but decreased in the basal portion of the infero-lateral wall (1232 ms and 1057 ms respectively, at 3T). LGE images did not reveal a pattern typical of myocarditis, but they did show a transmural lesion with a dark center compatible with a recent infarct with areas of no-reflow. The coronary MRA images obtained further supported these results, better depicting the area of no-reflow shown in the LGE images. Coronary evaluation revealed a normal right coronary artery (RCA) and LAD, and a significant lesion in the mid portion of the circumflex artery just after the take-off of the first left marginal branch. CMR findings excluded the hypothesis of myocarditis and the patient was treated accordingly.

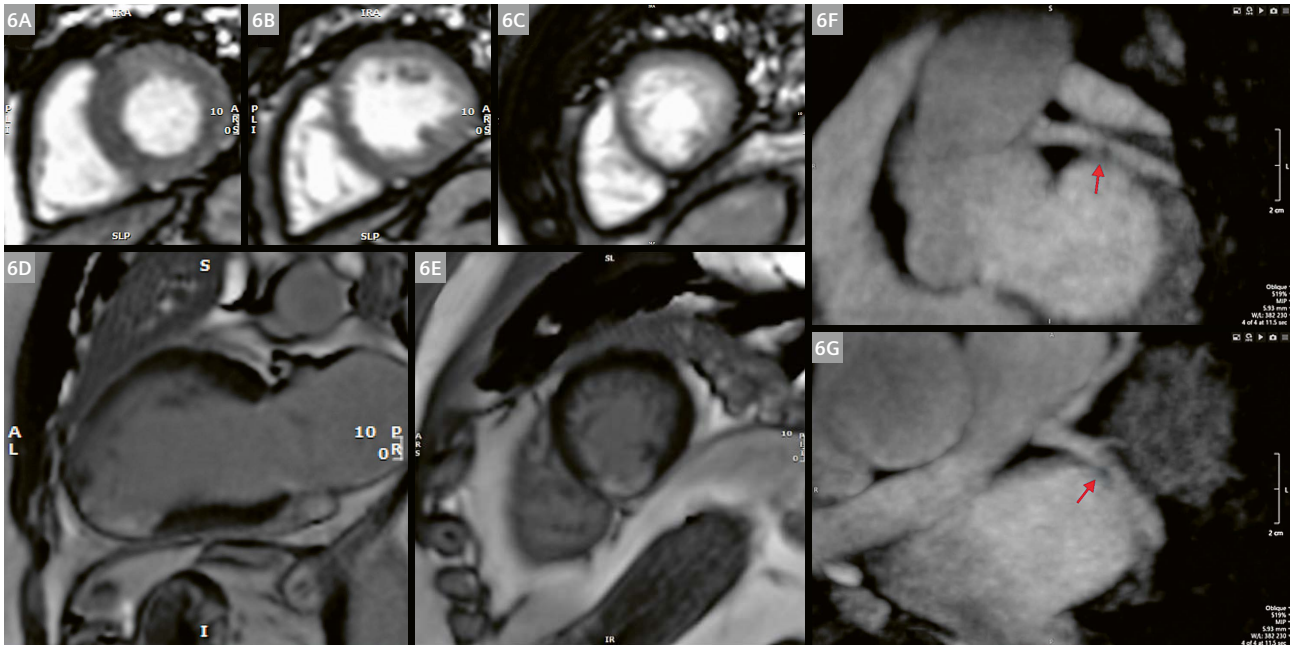

6 First-pass stress perfusion images of the basal **(6A)**, mid **(6B)**, and apical **(6C)** segments suggested reduced perfusion in the infero-septal wall along the full extension of the left ventricle, but some questions were raised about whether the defect represented true perfusion defects; **(6D and E)** corresponding LGE images that identified an inferior apical infarct; **(6F and G)** show the coronary MRA images of the dominant left circumflex artery with a significant proximal obstruction corroborating the findings from both the perfusion and LGE images.

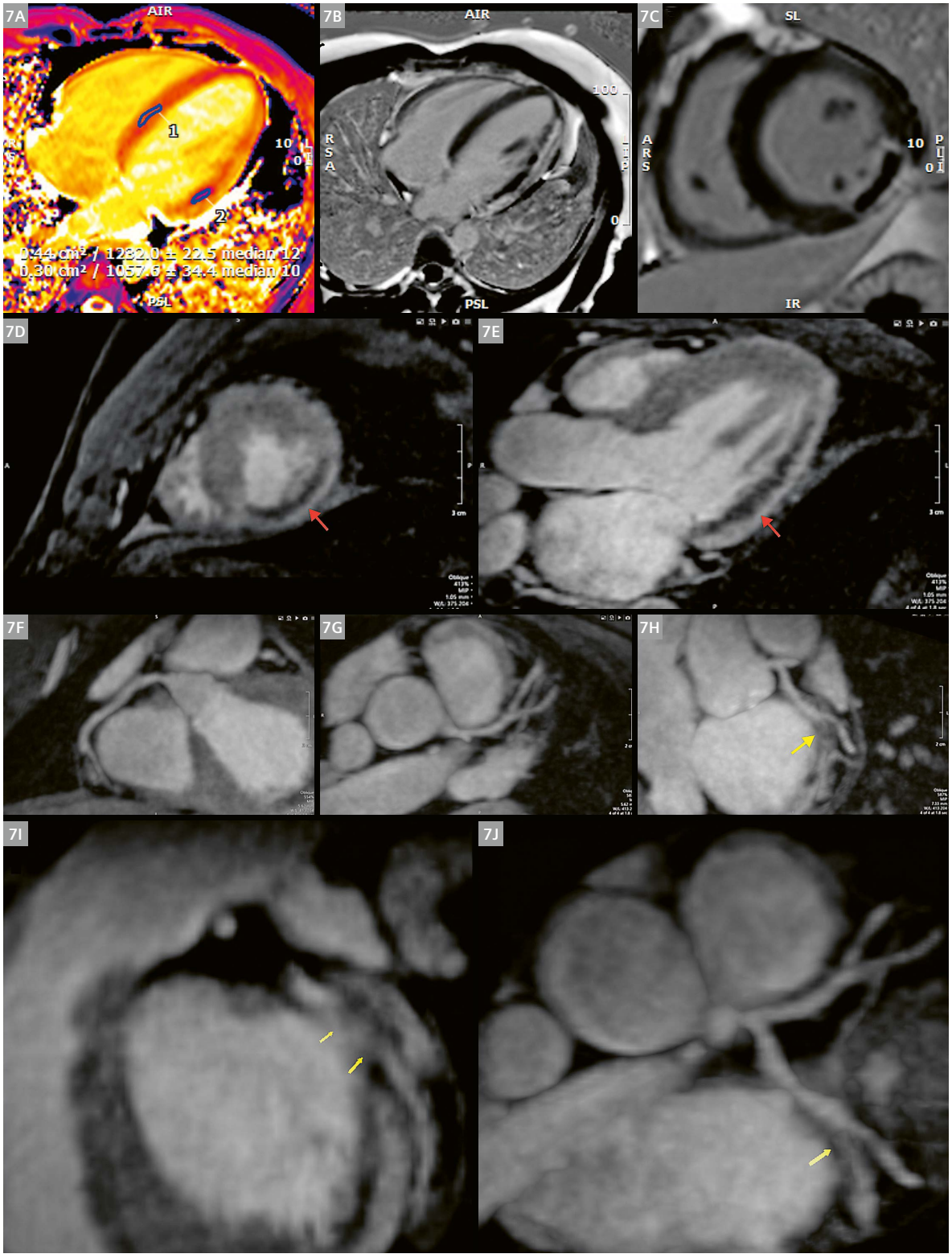

7 In a patient studied to rule out myocarditis, native T1 images **(7A)** identified a lower T1 value in the lateral wall of the basal segment of the left ventricle (10577 ms at 3T); **(7B and C)** LGE images showing an area of transmural scar in the infero-lateral wall of the left ventricle with a dark center corresponding to an area of no-reflow; **(7D and E)** better identified of the region of no-reflow using the water-reconstructed image from the coronary MRA dataset (red arrows); the right coronary artery **(7F)** and left anterior descending artery **(7G)** were normal; the left circumflex artery **(7H–J)** was occluded in its mid-segment after the take-off of the first marginal branch (yellow arrows).

The final example is shown in Figure 8: a 70-year-old woman who underwent CMR for suspected CAD due to diffusely inverted T waves in her resting ECG and an apparently normal echocardiography. In the cine images, we already observed apical hypertrophy that was probably missed by echo. Quantitative stress perfusion revealed reduced absolute perfusion in the subendocardial portion of the apical segments, co-localized with the hypertrophic regions seen in the cine images. LGE did not demonstrate any fibrosis. The coronary MRA images showed normal coronary arteries, confirming that the perfusion defects observed were due to microcirculatory deficits common in hypertrophic cardiomyopathies, and not a result of epicardial obstruction of the coronary arteries. The patient then underwent a coronary CTA, which confirmed the findings from the coronary MRA.

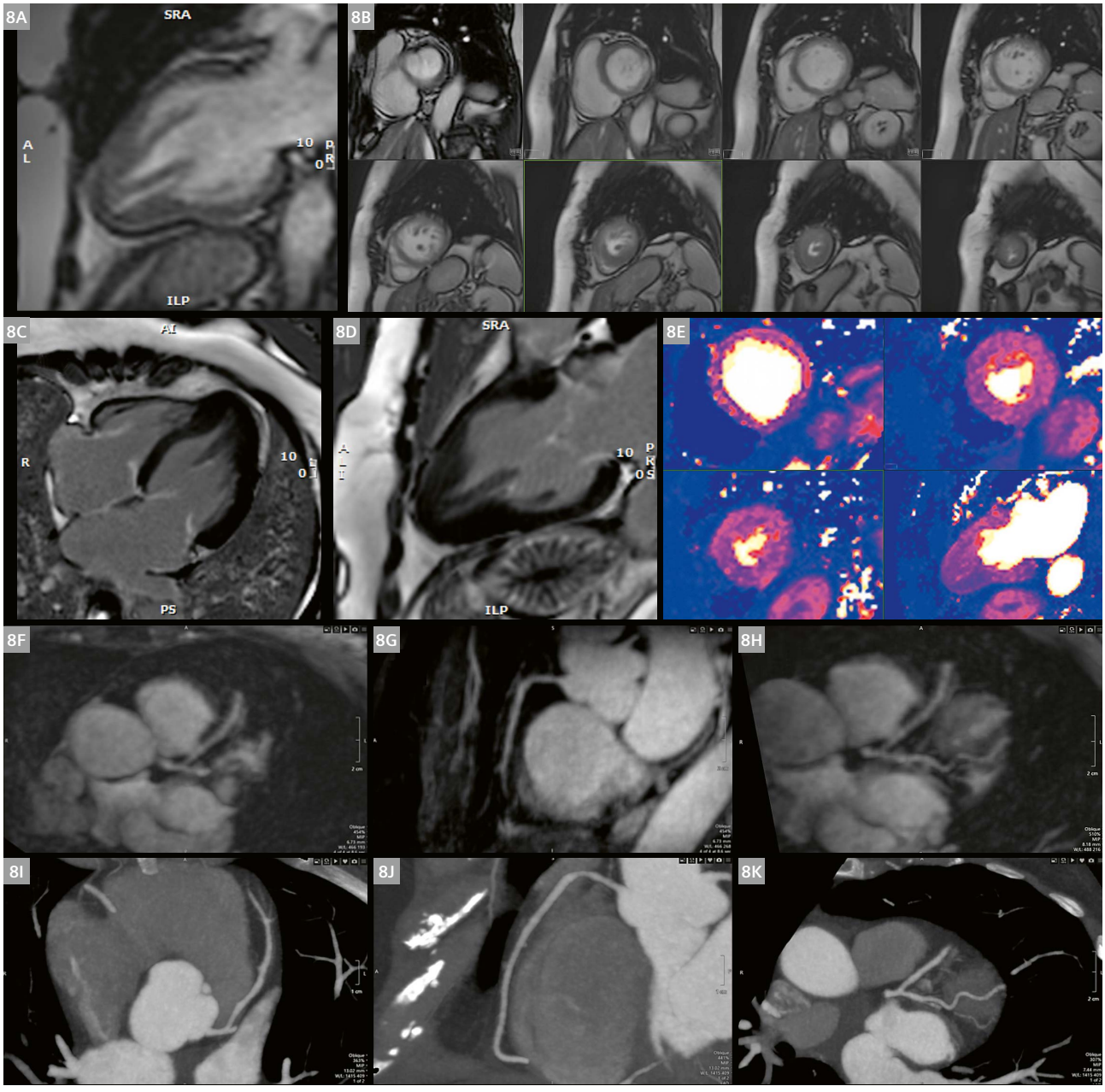

8 Cine images **(8A and B)** illustrate the apical hypertrophy of the left ventricle in a 2-chamber and short-axis view; **(8C and D)** long-axis LGE images confirm the hypertrophy but did not identify any associated scars in those segments; **(8E)** quantitative first-pass stress perfusion shows mild reduction in myocardial blood flow in the subendocardial areas of the hypertrophic segments, but the coronary MRA images of the left anterior descending artery **(8F)**, right coronary artery **(8G)**, and left circumflex **(8H)** did not identify any significant lesions, attributing the perfusion findings to microcirculatory impairment found in the primary cardiomyopathy; **(8I–K)** the patient underwent a further coronary computed tomography angiography (CTA) that confirmed the coronary MRA findings.

Standalone coronary MRA exams

Apart from integrating the coronary MRA with other routine CMR sequences, we also explored the possibility of using the sequence as a standalone exam for coronary MRA anatomical evaluation per se. Our center performs a high number of coronary CTAs and it is not uncommon to find patients who have that exam ordered, but either do not consent to receiving contrast or have a significant contraindication to the exam (a history of severe allergic reactions or high-risk kidney disease, for example). In cases where the pre-test likelihood for CAD was low but the CTA exam was requested anyway, we believe that coronary MRA can be of value, especially in young patients[2], even when performed alone and without the other information gathered in a routine CMR exam.

The protocol used in our center for these cases was to initially perform a non-contrast CT exam for calcium score in patients with the aforementioned history. If the calcium score was zero, revealing a very low probability of obstructive coronary disease given the already low pre-test clinical probability, the patient would undergo a coronary MRA without the use of contrast. We have performed 17 of these cases since the installation of the sequence, and no coronary CTA with contrast was subsequently requested in any of them, suggesting that this can be a valid alternative in this setting, providing further evidence.

In these cases, the objective of the coronary MRA is to rule out obstructive CAD in patients with low probability of the disease. The CMR protocol requires only localizers and use of the AI-based resting phase detection based on FB 4-chamber CINE followed by the whole-heart MRA. As this is a dedicated exam with more time available in the scanner, we perform two separate acquisitions in both systole and diastole, in order to improve the accuracy of the exam and eliminate artifacts that may be caused by coronary motion in either cardiac phase. Figure 9 shows the example of a 38-year-old woman who had suffered a severe allergic reaction to iodinated contrast prior to her coronary CTA request. She first underwent a non-contrast CT exam, which showed a calcium score of zero. She then underwent a coronary MRA with images obtained both in systole and diastole, ruling out significant obstructive CAD.

Limitations and future developments

The current WIP sequences[1] used in the last six months allowed us to perform coronary MRAs in a busy clinical routine without significant impact on examination time. We believe that, coupled with the use of a full FB CMR protocol and quantitative perfusion analysis, the anatomical and functional data provided by this comprehensive exam can be very competitive in providing the most useful clinical information in a relatively short exam time and with no radiation, singling out CMR as the only imaging modality that can offer this possibility. The current implementation of the whole-heart coronary MRA technique allows the sequence to become truly usable in clinical routine. While the current spatial resolution is not yet matching that of coronary CTA technology, the CMR alternative is a genuine option for ruling out coronary disease, as we have experienced in these initial cases.

A few challenges still remain, and we list them here so that other centers can collaborate in further developing what is now a very mature option for anatomical coronary assessment. First, in all the exams we performed, no particular attention was given to optimizing the coronary exam using either nitrates or beta-blockers. The goal was to test-drive the sequence in a real clinical environment and under any possible circumstances, including cases involving arrhythmias, obesity, tachycardia, etc. While the benefits of both drugs in coronary CTA are well known, the experience in CMR is very limited [35]. Exploring the possible benefits of using these drugs for coronary MRA is necessary for accurately comparing the findings of this technique with coronary CTA. The second question regards the influence of contrast agents on SNR. In our cases, most patients were studied after having received contrast so possibly the current SNR/CNR observed is influenced by the protocol design. Having said that, in the cases of isolated coronary MRAs, no contrast was used and we did not observe a significant change in signal compared to the contrast enhanced exams (visual observation). But, again, this is another issue that merits further investigation as it has an important impact on the workflow.

Another possible use of these sequences is in children[2], since it can prevent any use of ionizing radiation and contrast injection. Given that most coronary evaluations in children are not intended to assess atherosclerotic obstructions, which require higher spatial resolution, this particular coronary sequence can be very useful as it provides a full FB acquisition with 100% respiratory efficacy and predictable scan time. Finally, the current implementation of whole-heart coronary MRA still cannot help us answer questions concerning patients with stents or bypass grafts, as most of these cases involve metal artifacts. What is more, we also observed some lower image quality when assessing the distal segments of the RCA, especially the posterior descending artery branch and posterior ventricular artery branch. Finally, atherosclerotic evaluation and the determination of coronary plaques are emerging as key elements for establishing the patient's prognosis and guiding clinical treatment. Current CMRA sequences only provide limited information with regard to coronary plaque. This is one of the reasons why we opted

[2]MR scanning has not been established as safe for imaging fetuses and infants less than two years of age. The responsible physician must evaluate the benefits of the MR examination compared to those of other imaging procedures.

to add a CT calcium score in patients that underwent a standalone anatomical coronary study. Reducing the current spatial resolution to something closer to 0.5 mm^3 is still desirable as long as acquisition time can still be kept below 10 minutes.

Conclusions

In conclusion, our current experience with integrating coronary anatomical information into a full FB CMR protocol has been very positive, adding very little overhead in terms of exam time while providing us with new information to support our clinical diagnosis and therapeutic decisions. The current 3D whole-heart sequences could be incorporated in a busy clinical service and also provided an alternative imaging option to patients who did not consent or had a contraindication to an iodinated contrast exam. However, there are many questions that remain despite this initial experience. We encourage other centers to engage in this development, as the impact of coronary anatomical evaluation in clinical practice is rapidly being revisited with the growing use of CTA. CMR has potential for incorporating that information in addition to all the unique functional data that it already provides, especially if more centers contribute to the advancement of this technique.

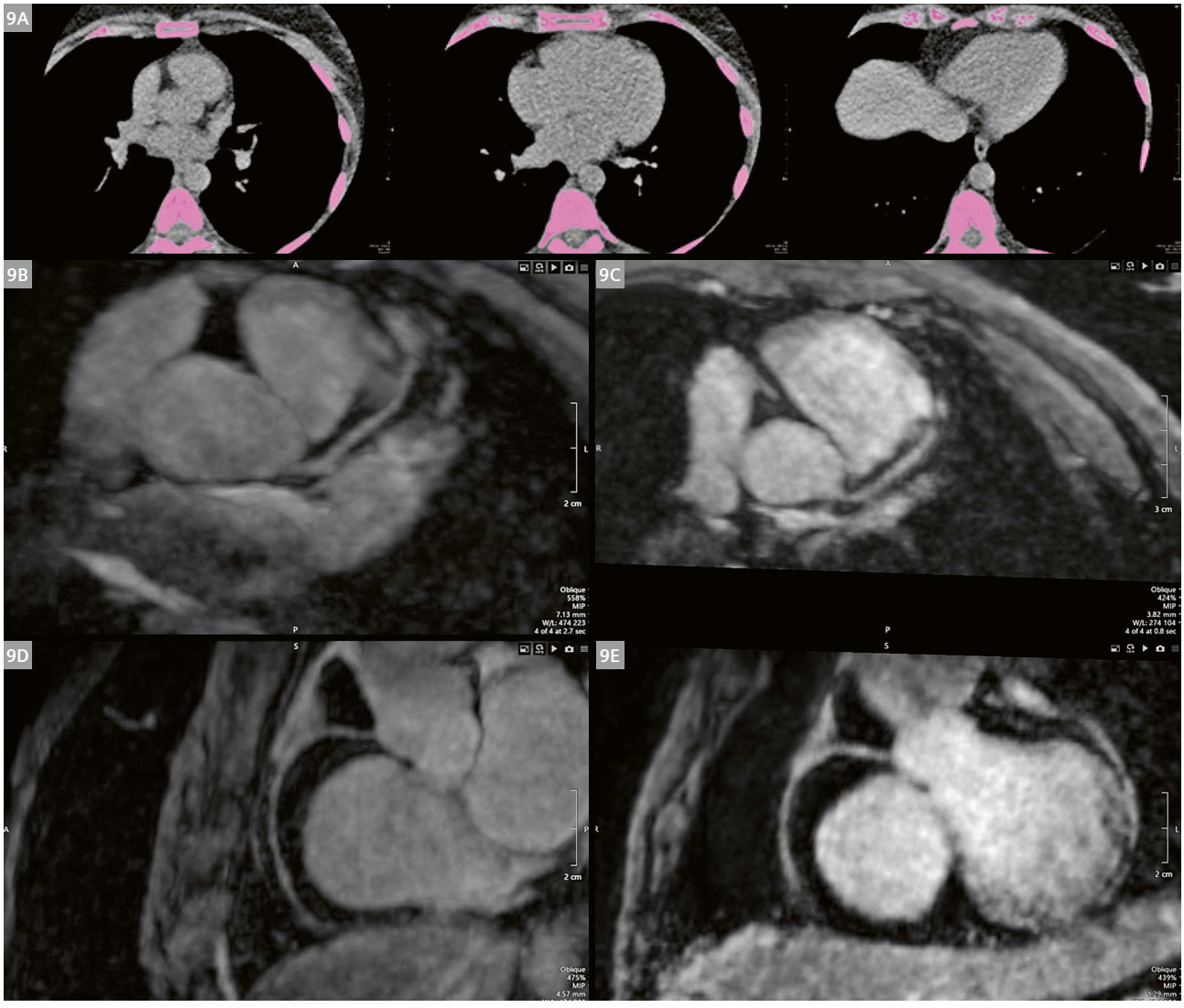

9 A patient with contra-indications for a contrast coronary CTA underwent a non-contrast calcium score exam with a score of zero **(9A, part of the dataset)**; she then underwent a non-contrast coronary MRA that revealed normal coronary arteries with no significant obstructions, ruling out significant coronary artery disease; **(9B and D)** the left anterior descending artery and right coronary artery were imaged during diastole; **(9C and E)** the same arteries imaged during systole; both datasets were obtained in order to increase the accuracy of the interpretation and rule out potential artifacts; this strategy is also used when reading coronary CTAs, especially when patients are arrhythmic and an increased acquisition window is used.

Acknowledgments

The Siemens Healthineers Whole-Heart team for development and setup of the free-breathing whole-heart CMRA sequence.

Peter Kellman and Hui Xue (Medical Signal and Image Processing Program at the NHLBI, USA) for setting up and providing the cine, LGE, and quantitative perfusion FB sequences used in the protocols described within the Gadgetron framework.

References

1 Kwong RY, Ge Y, Steel K, Bingham S, Abdullah S, Fujikura K, Wang W, Pandya A, Chen YY, Mikolich JR, Boland S, Arai AE, Bandettini WP, Shanbhag SM, Patel AR, Narang A, Farzaneh-Far A, Romer B, Heitner JF, Ho JY, Singh J, Shenoy C, Hughes A, Leung SW, Marji M, Gonzalez JA, Mehta S, Shah DJ, Debs D, Raman SV, Guha A, Ferrari VA, Schulz-Menger J, Hachamovitch R, Stuber M, Simonetti OP. Cardiac Magnetic Resonance Stress Perfusion Imaging for Evaluation of Patients With Chest Pain. J Am Coll Cardiol. 2019;74:1741-1755.

2 Nagel E, Greenwood JP, McCann GP, Bettencourt N, Shah AM, Hussain ST, Perera D, Plein S, Bucciarelli-Ducci C, Paul M, Westwood MA, Marber M, Richter WS, Puntmann VO, Schwenke C, Schulz-Menger J, Das R, Wong J, Hausenloy DJ, Steen H, Berry C, Investigators M-I. Magnetic Resonance Perfusion or Fractional Flow Reserve in Coronary Disease. N Engl J Med. 2019;380:2418-2428.

3 Ullah W, Roomi S, Abdullah HM, Mukhtar M, Ali Z, Ye P, Haas DC, Figueredo VM. Diagnostic Accuracy of Cardiac Magnetic Resonance Versus Fractional Flow Reserve: A Systematic Review and Meta-Analysis. Cardiol Res. 2020;11:145-154.

4 Greenwood JP, Ripley DP, Berry C, McCann GP, Plein S, Bucciarelli-Ducci C, Dall'Armellina E, Prasad A, Bijsterveld P, Foley JR, Mangion K, Sculpher M, Walker S, Everett CC, Cairns DA, Sharples LD, Brown JM, Investigators C-M. Effect of Care Guided by Cardiovascular Magnetic Resonance, Myocardial Perfusion Scintigraphy, or NICE Guidelines on Subsequent Unnecessary Angiography Rates: The CE-MARC 2 Randomized Clinical Trial. JAMA. 2016;316:1051-60.

5 Knott KD, Fernandes JL, Moon JC. Automated Quantitative Stress Perfusion in a Clinical Routine. Magn Reson Imaging Clin N Am. 2019;27:507-520.

6 Maron DJ, Hochman JS, Reynolds HR, Bangalore S, O'Brien SM, Boden WE, Chaitman BR, Senior R, Lopez-Sendon J, Alexander KP, Lopes RD, Shaw LJ, Berger JS, Newman JD, Sidhu MS, Goodman SG, Ruzyllo W, Gosselin G, Maggioni AP, White HD, Bhargava B, Min JK, Mancini GBJ, Berman DS, Picard MH, Kwong RY, Ali ZA, Mark DB, Spertus JA, Krishnan MN, Elghamaz A, Moorthy N, Hueb WA, Demkow M, Mavromatis K, Bockeria O, Peteiro J, Miller TD, Szwed H, Doerr R, Keltai M, Selvanayagam JB, Steg PG, Held C, Kohsaka S, Mavromichalis S, Kirby R, Jeffries NO, Harrell FE, Jr., Rockhold FW, Broderick S, Ferguson TB, Jr., Williams DO, Harrington RA, Stone GW, Rosenberg Y, Group IR. Initial Invasive or Conservative Strategy for Stable Coronary Disease. N Engl J Med. 2020;382:1395-1407.

7 Saraste A, Barbato E, Capodanno D, Edvardsen T, Prescott E, Achenbach S, Bax JJ, Wijns W, Knuuti J. Imaging in ESC clinical guidelines: chronic coronary syndromes. Eur Heart J Cardiovasc Imaging. 2019;20:1187-1197.

8 Knuuti J, Wijns W, Saraste A, Capodanno D, Barbato E, Funck-Brentano C, Prescott E, Storey RF, Deaton C, Cuisset T, Agewall S, Dickstein K, Edvardsen T, Escaned J, Gersh BJ, Svitil P, Gilard M, Hasdai D, Hatala R, Mahfoud F, Masip J, Muneretto C, Valgimigli M, Achenbach S, Bax JJ, Group ESCSD. 2019 ESC Guidelines for the diagnosis and management of chronic coronary syndromes. Eur Heart J. 2020;41:407-477.

9 Ge Y, Pandya A, Steel K, Bingham S, Jerosch-Herold M, Chen YY, Mikolich JR, Arai AE, Bandettini WP, Patel AR, Farzaneh-Far A, Heitner JF, Shenoy C, Leung SW, Gonzalez JA, Shah DJ, Raman SV, Ferrari VA, Schulz-Menger J, Hachamovitch R, Stuber M, Simonetti OP, Kwong RY. Cost-Effectiveness Analysis of Stress Cardiovascular Magnetic Resonance Imaging for Stable Chest Pain Syndromes. JACC Cardiovasc Imaging. 2020;13:1505-1517.

10 Kramer CM. Potential for Rapid and Cost-Effective Cardiac Magnetic Resonance in the Developing (and Developed) World. J Am Heart Assoc. 2018;7:e010435.

11 Kim WY, Danias PG, Stuber M, Flamm SD, Plein S, Nagel E, Langerak SE, Weber OM, Pedersen EM, Schmidt M, Botnar RM, Manning WJ. Coronary magnetic resonance angiography for the detection of coronary stenoses. N Engl J Med. 2001;345:1863-9.

12 Kato Y, Ambale-Venkatesh B, Kassai Y, Kasuboski L, Schuijf J, Kapoor K, Caruthers S, Lima JAC. Non-contrast coronary magnetic resonance angiography: current frontiers and future horizons. MAGMA. 2020;33:591-612.

13 Hajhosseiny R, Bustin A, Munoz C, Rashid I, Cruz G, Manning WJ, Prieto C, Botnar RM. Coronary Magnetic Resonance Angiography: Technical Innovations Leading Us to the Promised Land? JACC Cardiovasc Imaging. 2020;13:2653-2672.

14 Fernandes JL, Fioravante LA, Zenge MO, Forman C, Schmidt M, Nadar MS, Mazo PE, Greiser A, Speier P, Staeb D, Xue H, Hansen MS, Kellman P, Strecker R. A Comprehensive Free-Breathing Protocol for Cardiovascular Magnetic Resonance Imaging of Ischemia and Cardiomyopathies: a Feasibility Study. Journal of Cardiovascular Magnetic Resonance. 2016;18:P313.

15 Hansen MS, Sorensen TS. Gadgetron: an open source framework for medical image reconstruction. Magn Reson Med. 2013;69:1768-76.

16 Ledesma-Carbayo MJ, Kellman P, Hsu LY, Arai AE, McVeigh ER. Motion corrected free-breathing delayed-enhancement imaging of myocardial infarction using nonrigid registration. J Magn Reson Imaging. 2007;26:184-90.

17 Kellman P, Hansen MS, Nielles-Vallespin S, Nickander J, Themudo R, Ugander M, Xue H. Myocardial perfusion cardiovascular magnetic resonance: optimized dual sequence and reconstruction for quantification. J Cardiovasc Magn Reson. 2017;19:43.

18 Engblom H, Xue H, Akil S, Carlsson M, Hindorf C, Oddstig J, Hedeer F, Hansen MS, Aletras AH, Kellman P, Arheden H. Fully quantitative cardiovascular magnetic resonance myocardial perfusion ready for clinical use: a comparison between cardiovascular magnetic resonance imaging and positron emission tomography. J Cardiovasc Magn Reson. 2017;19:78.

19 Xue H, Kellman P, Larocca G, Arai AE, Hansen MS. High spatial and temporal resolution retrospective cine cardiovascular magnetic resonance from shortened free breathing real-time acquisitions. J Cardiovasc Magn Reson. 2013;15:102.

20 Xue H, Inati S, Sorensen TS, Kellman P, Hansen MS. Distributed MRI reconstruction using Gadgetron-based cloud computing. Magn Reson Med. 2015;73:1015-25.

21 Cross R, Olivieri L, O'Brien K, Kellman P, Xue H, Hansen M. Improved workflow for quantification of left ventricular volumes and mass using free-breathing motion corrected cine imaging. J Cardiovasc Magn Reson. 2016;18:10.

22 Greenwood JP, Maredia N, Younger JF, Brown JM, Nixon J, Everett CC, Bijsterveld P, Ridgway JP, Radjenovic A, Dickinson CJ, Ball SG, Plein S. Cardiovascular magnetic resonance and single-photon emission computed tomography for diagnosis of coronary heart disease (CE-MARC): a prospective trial. Lancet. 2012;379:453-60.
23 Heer T, Reiter S, Hofling B, Pilz G. Diagnostic performance of non-contrast-enhanced whole-heart magnetic resonance coronary angiography in combination with adenosine stress perfusion cardiac magnetic resonance imaging. Am Heart J. 2013;166:999-1009.
24 Klein C, Gebker R, Kokocinski T, Dreysse S, Schnackenburg B, Fleck E, Nagel E. Combined magnetic resonance coronary artery imaging, myocardial perfusion and late gadolinium enhancement in patients with suspected coronary artery disease. J Cardiovasc Magn Reson. 2008;10:45.
25 Bettencourt N, Ferreira N, Chiribiri A, Schuster A, Sampaio F, Santos L, Melica B, Rodrigues A, Braga P, Teixeira M, Leite-Moreira A, Silva-Cardoso J, Portugal P, Gama V, Nagel E. Additive value of magnetic resonance coronary angiography in a comprehensive cardiac magnetic resonance stress-rest protocol for detection of functionally significant coronary artery disease: a pilot study. Circ Cardiovasc Imaging. 2013;6:730-8.

Contact

Juliano Lara Fernandes, M.D., Ph.D., M.B.A.
Cardiovascular Department
Radiologia Clinica de Campinas
Jose Michel Kalaf Research Institute
Av Jose de Souza Campos 840
Campinas, SP, Brazil 13092-123
jlaraf@terra.com.br

26 Hamdan A, Doltra A, Huppertz A, Wellnhofer E, Fleck E, Kelle S. Comparison of coronary magnetic resonance and computed tomography angiography for prediction of cardiovascular events. JACC Cardiovasc Imaging. 2014;7:1063-5.
27 Zhang L, Song X, Dong L, Li J, Dou R, Fan Z, An J, Li D. Additive value of 3T cardiovascular magnetic resonance coronary angiography for detecting coronary artery disease. J Cardiovasc Magn Reson. 2018;20:29.
28 Celeng C, Leiner T, Maurovich-Horvat P, Merkely B, de Jong P, Dankbaar JW, van Es HW, Ghoshhajra BB, Hoffmann U, Takx RAP. Anatomical and Functional Computed Tomography for Diagnosing Hemodynamically Significant Coronary Artery Disease: A Meta-Analysis. JACC Cardiovasc Imaging. 2019;12:1316-1325.
29 Henningsson M, Koken P, Stehning C, Razavi R, Prieto C, Botnar RM. Whole-heart coronary MR angiography with 2D self-navigated image reconstruction. Magn Reson Med. 2012;67:437-45.
30 Munoz C, Cruz G, Neji R, Botnar RM, Prieto C. Motion corrected water/fat whole-heart coronary MR angiography with 100% respiratory efficiency. Magn Reson Med. 2019;82:732-742.
31 Bustin A, Ginami G, Cruz G, Correia T, Ismail TF, Rashid I, Neji R, Botnar RM, Prieto C. Five-minute whole-heart coronary MRA with sub-millimeter isotropic resolution, 100% respiratory scan efficiency, and 3D-PROST reconstruction. Magn Reson Med. 2019;81:102-115.
32 Prieto C, Doneva M, Usman M, Henningsson M, Greil G, Schaeffter T, Botnar RM. Highly efficient respiratory motion compensated free-breathing coronary MRA using golden-step Cartesian acquisition. J Magn Reson Imaging. 2015;41:738-46.
33 Cruz G, Atkinson D, Henningsson M, Botnar RM, Prieto C. Highly efficient nonrigid motion-corrected 3D whole-heart coronary vessel wall imaging. Magn Reson Med. 2017;77:1894-1908.
34 Yoon SS, Hoppe E, Schmidt M, Forman C, Chitiboi T, Sharma P, Tillmanns C, Maier A, Wetzl JA. Robust Deep-Learning-based Automated Cardiac Resting Phase Detection: Validation in a Prospective Study. Proc Intl Soc Mag Reson Med. 2020;28:2210.
35 Hajhosseiny R, Bustin A, Rashid I, Cruz G, Radhouene N, Kunze K, Ismail TF, Rajani R, Masci PG, Prieto C, Botnar RM. 3D whole heart CMRA using an image-navigator framework – a clinical comparison study with CCTA and diaphragmatic navigators. ISMRM 2020. 2020:Abstract 2142.32

Clinical Implementation of 4D Flow MRI in a Large Cardiovascular Imaging Practice: Motivation, Strategies, and Initial Experience

Ryan J. Avery, M.D.[1]; Bradley D. Allen, M.D., M.S.[1]; Fei Fei Gong, M.D.[2]; Rachel Davids, B.S.R.T.(R)(MR)MRSO(MRSC)[3]; Marci Messina, RT(R)(MR)MRSO(MRSC)[1]; Kelvin Chow, Ph.D.[3]; James C. Carr, M.D.[1]; Michael Markl, Ph.D.[1]

[1]Department of Radiology, Northwestern University, Chicago, IL, USA
[2]Bluhm Cardiovascular Institute, Northwestern University, Chicago, IL, USA
[3]Cardiovascular MR R&D, Siemens Medical Solutions, USA Inc., Chicago, IL, USA

Like most sites during the initial onset of the COVID-19 pandemic, we sought to reduce exposure by dramatically reducing our dedicated clinical and research MRI scanning to a low quantity, resulting in both outpatient and research scanning being markedly reduced. During this period, our staff took this opportunity to set-up a working group in order to advise on scanner efficiency regarding our current cardiovascular MRI (CMR) scanning protocols. Given that our institution performs a high volume of CMR scans that utilize multiple 2-dimensional phase-contrast sequences to evaluate the flow across both the aortic and pulmonic valves and throughout the course of the aorta, our group decided that a concerted effort to fully implement four-dimensional phase-contrast imaging (hereafter referred to as 4D Flow) could improve scanner efficiency and perhaps provide more consistent flow quantification. This goal was implemented with the expectation that overall MR operations would be streamlined by both eliminating the numerous breath-hold 2D phase-contrast image acquisitions and decreasing technologist sequence planning time, while simultaneously improving patient comfort with the free-breathing 4D Flow sequence in cases requiring vascular flow evaluation.

Heterogeneity all around

Previous considerations of clinical implementation of 4D Flow proved daunting, given the difficulty of uniformly setting up a sequence notable for requiring a longer (~10 min) acquisition time, unique spatial planning, and balancing multiple parameters including velocity encoding, phase oversampling, and field of view (FOV), and the time necessary for inline reconstruction of the large volume of data involved. These factors were further complicated by an additional order of complexity, since many different MR scanners are utilized for CMR at our institution. For instance, our hospital has multiple 1.5T and 3T MR scanners, but we currently perform 4D Flow only on 1.5T

1 A screenshot of the scanner workstation interface during the planning of the 4D Flow sequence: The three images are from the 3-plane TrueFISP localizer. Notice that the yellow acquisition box has a coronal orientation with complete inclusion of the thoracic aorta. On the axial image (far left), it is evident that the main pulmonary artery and its right branch are included in the acquisition.

scanners, reducing the complexity of our implementation by a single level. However, a uniform implementation of this sequence on multiple different types of 1.5T scanners was still a challenge. While the 1.5T scanners that we utilize for cardiovascular imaging with 4D Flow are all manufactured by Siemens Healthineers, we were still faced with a heterogeneous installation since our institution routinely utilizes 3 different models of scanners: MAGNETOM Sola, MAGNETOM Aera, and MAGNETOM Avanto. Since the MAGNETOM Sola and MAGNETOM Aera are the most recent types of scanners, we will limit the discussion of our installation to these scanners, given that we expect most readers will be working on a similar platform. Furthermore, our work with this implementation of 4D Flow on the older MAGNETOM Avanto MR scanners utilized techniques that may not be widely able for implementation by our current audience, so further discussions of the Avanto will not be included.

Uniformity across different platforms

Our previous 4D Flow pulse sequences used an earlier version of the 4D Flow works-in-progress (WIP)[1] that was prospectively ECG-gated. While this version was useful for detecting peak velocities, prospective gating is suboptimal for flow analysis, because a portion of diastole is not acquired, thus limiting certain analyses such as mitral regurgitation quantification. For this project, our MAGNETOM Sola and MAGNETOM Aera scanners were both updated to a newer version of the 4D Flow WIP[1] pulse sequence, allowing us to perform a retrospective ECG-gated sequence providing complete analysis of the cardiac cycle and the flow of the associated vascular structures. Since this sequence was available for both our MAGNETOM Sola and MAGNETOM Aera scanners, it provided a unique opportunity to improve sequence acquisition uniformity. Our goal was to provide a complete phase-contrast evaluation of the cardiac cycle across our MR platforms with the expectation of a uniform dataset that would be comparable regardless of patient pathology or scanner type. Given that our previous use of 4D Flow was dictated by the clinical indication for the exam, sequence spatial coverage had previously been set up in order to interrogate specific vascular structures (e.g., a sagittal oblique volumetric slab performed with complete coverage of the aorta). However, indication-based FOV selection can too often lead to errors related to coverage planning or miscommunication in regard to the indication for the exam. In order to simplify set-up and reduce the chances of spatial acquisition errors or incomplete evaluation of vessels, our team agreed that our goal would be to perform a sequence that could be uniformly applied to all patients and was acceptable regardless of the anatomic structure being evaluated. With these constraints in mind, we agreed that acquisition of a coronal slab, which could be quickly and relatively easily planned by the technologist using the 3-plane localizer sequences (Fig. 1), would provide an ideal solution. The slab would be planned with the primary objective of covering the entire aorta while limiting the slab to exclude the sternum anteriorly and avoiding the soft tissues posterior to the descending thoracic aorta. This consistent target would simplify the planning for our technologists and provide a uniform anatomic assessment for easier post-processing and analysis (Figs. 2A, B).

[1] Work in progress: the application is currently under development and is not for sale in the U.S. and in other countries. Its future availability cannot be ensured.

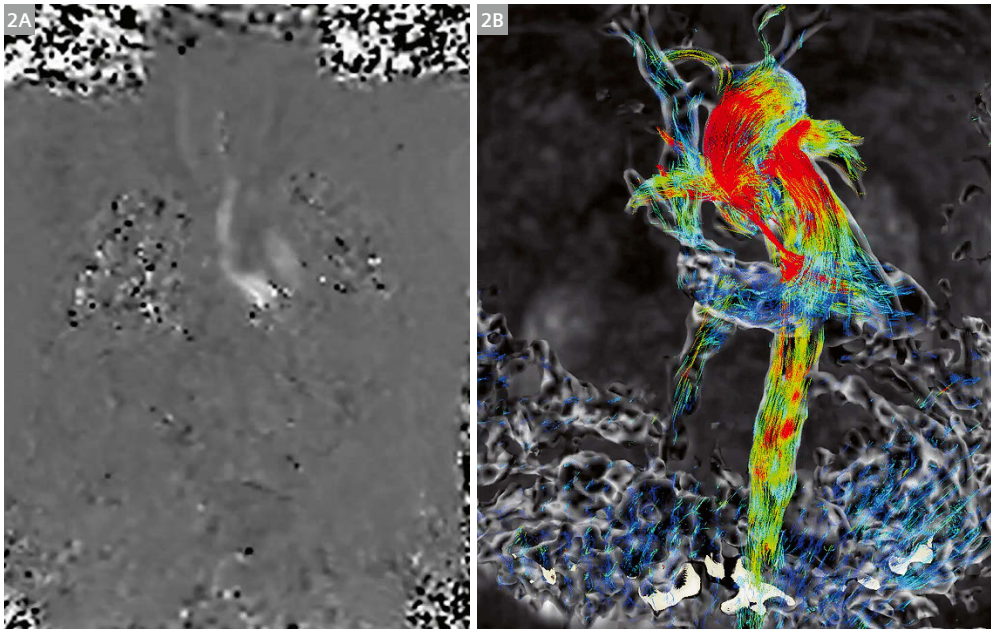

2 **(2A)** Image from one of the three phase-encoding directions acquired from the coronal slab 4D Flow acquisition;
(2B) Uncropped view of the 4D Flow coronal slab after post-processing; the image demonstrates the complete visualization of flow in all thoracic vasculature, including complete coverage of the thoracic aorta, major pulmonary arteries, vena cava, and cardiac chambers.

The slab

Clinically, the spatial planning of a single coronal slab of the chest satisfied our primary goal of acquiring complete thoracic aorta coverage and ensuring that each exam would enable a comprehensive evaluation of the entire thoracic aorta that could be used for all aortic pathologies commonly encountered (Fig. 3). An additional advantage of routinely implementing 4D Flow via this approach is that it gives us the opportunity for post-hoc flow evaluation of both the aorta and the aortic valve, which could provide quantitative analysis of any previously undiagnosed aortic pathology without requiring a priori planning. Additionally, the coronal slab spatial acquisition generally includes the entire main pulmonary artery and its branch vessels, pulmonary veins, and vena cavae, which could be used for verification of consistent flows throughout the left and right cardiac chambers, and their respective great vessels, and for verification of these flows relative to volumetric stroke volume analysis from cine data, to better calculate valvular insufficiency or shunt (Fig. 4). Also, given the emerging use of 4D Flow for intracardiac pathology evaluation, this coverage plan would be able to routinely investigate the atrioventricular valves and the left ventricular outflow tract (Fig. 5).

While our primary goal for spatial planning was to achieve both appropriate and uniform anatomic coverage, we elected to also simplify the approach by limiting additional parameters that should be considered during image planning. To simplify planning by our technologist, our group decided that coronal orientation would always be used with no adjustment to the orientation, such as a coronal oblique orientation. Furthermore, we established a FOV that would not be adjusted in order to maintain a 2.6 x 2.6 mm in-plane spatial resolution that would be acceptable for accurate diagnostic quantification of vascular flow. In order to avoid spatial aliasing in larger patients with wide shoulders, we implemented 20% phase-encoding oversampling to the sequence. While ECG gating is necessary to maintain temporal resolution, our group evaluated the necessity to alleviate breathing-related motion artifacts via respiratory navigation (Fig. 6). Since the coronal view is less susceptible to motion artifacts, we tested the sequence without respiratory navigation. The images without respiratory navigation suffered from no appreciable motion artifacts and did not have the area of signal loss in the right chest that occurs due to the navigator slice. Given that this approach provided a clinically acceptable sequence while further streamlining set-up by foregoing technologist planning of the navigator slice, and faster image acquisition since images could be acquired continuously (without navigator efficiency limitations), we felt this was an acceptable trade-off. However, we do acknowledge that this technique will require further data analysis to confirm accuracy.

3 Cropped view of the 4D Flow coronal slab after post-processing demonstrates pathline visualization of flow throughout the thoracic aorta.

4 Post-processed view of the 4D Flow coronal slab, including cropping and segmentation to allow visualization of flow via pathlines within the main pulmonary artery and its left and right branch vessels.

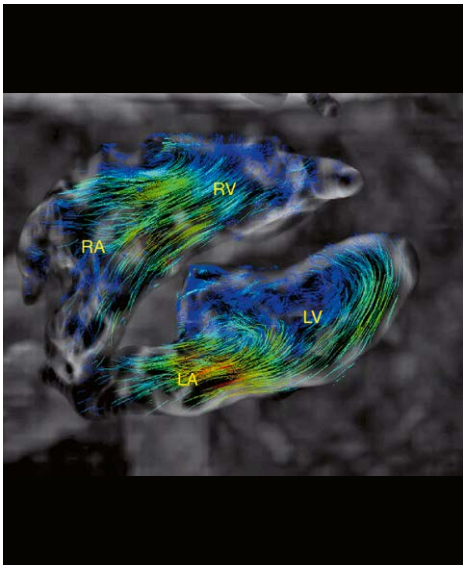

5 Post-processed view of the 4D Flow coronal slab after cropping and angulation orientated to the 4-chamber view of the heart: Pathlines demonstrate flow during ventricular diastole. Note the passive filling of the ventricles, with flow leaving the atria and crossing the atrioventricular valves.

6 During 4D Flow acquisition, our protocol utilizes a technique that does not require use of the respiratory navigator. In the Physio card on the scanner, the Respiratory Control setting has been set to Off.

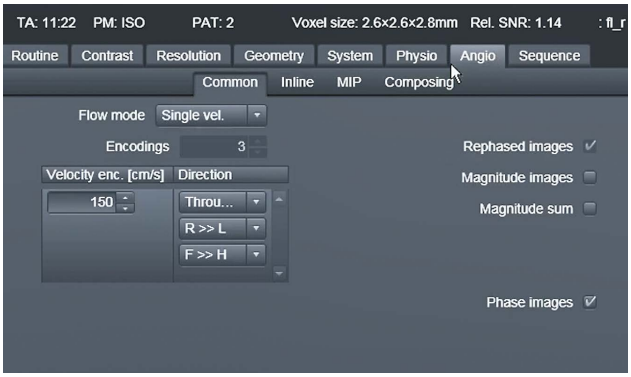

7 The technologist is responsible for working with the physician-provided protocol to designate if this is routine flow evaluation, set to a velocity encoding of 150 cm/s. More severe cases are often set to 300 cm/s, but depending on history or expectations, they could be set higher prior to 4D Flow acquisition.

As simple as possible, but no more

For planning, our technologists and physicians would routinely have to evaluate three independent parameters during planning. Since it was agreed that the FOV was to not be changed and that the 20% phase oversampling was acceptable for most patients' habitus, the technologist was primarily responsible for modifying slice thickness of the 4D Flow acquisition. We agreed that a slice thickness of 2.5 mm in the anteroposterior direction would be optimum in order to balance appropriate coverage, image acquisition time, and spatial resolution. To ensure appropriate coverage for larger patients, we advised our technologist to increase slice thickness in increments of 0.1 mm and to use 3.0 mm as a maximum slice thickness with the caveat that slice thickness could also be slightly increased if times became unacceptably long (our goal is ~10 minutes). Velocity encoding was the second parameter that required planning prior to image acquisition. While the variety of valvular and stenosis-related pathologies can be expected to extend across a spectrum of different flow ranges, we elected to encourage a velocity encoding of 150 cm/s for patients undergoing routine evaluation, and 300 cm/s for patients with a known or highly suspected history of significant stenosis. Although our group considered a velocity-encoding scout, our goal was to be able to uniformly evaluate multiple types of pathologies. The need for multiple phase-encoding scouts for the various pathologies (e.g., aortic disease vs. pulmonary disease) would therefore be counter to our objective, so this option was not pursued. In our experience, the two settings for velocity encoding have succeeded in the majority of cases. In more severe cases of stenosis, alias unwrapping using our post-processing software was able to correct the problem. The third parameter that the technologist had to set for sequence planning was the flip angle. Since not all of our cardiovascular cases would require intravenous administration of gadolinium-based contrast, we instructed our technologist to use a flip angle of 15° for scans performed with contrast, and 7° for non-contrast scans (Fig. 7). While the parameters had been reduced to three main options, a final decision that our group had to make was whether or not to utilize the Compressed Sensing (CS) version of the WIP.

Compressed Sensing working overtime

Compressed Sensing (CS) retrospective ECG-gated 4D Flow has been a very promising approach for faster acquisition of this pulse sequence, which can often take approximately 12 minutes to acquire. With CS, it was expected that we could reduce our 4D Flow acquisition time approximately by half, allowing for faster patient turnaround, given that it is customarily run as the last sequence in our protocols. While our CS sequence does reduce acquisition time, it was found to require a significant amount of inline reconstruction on the scanner workstation. While the GPU provided with the MAGNETOM Sola scanner was able to provide an acceptable inline sequence construction time of approximately six minutes, the GPU of our older MAGNETOM Aera unit took longer and was found to not be acceptable. From a workflow perspective, we found that despite the differences in GPU capabilities on the MAGNETOM Sola and Aera platforms, the average was approximately 12 minutes from the start of the sequence acquisition to the completion of the inline reconstruction. While the shorter acquisition time provided by CS was felt to be better for the patient, since the scan would be completed about six minutes earlier, there is also still some debate as to how phase-contrast data fidelity is impacted by aggressive acceleration techniques. Therefore, we have so far opted to not utilize CS approaches in favor of acquisition and data uniformity across all scanner platforms.

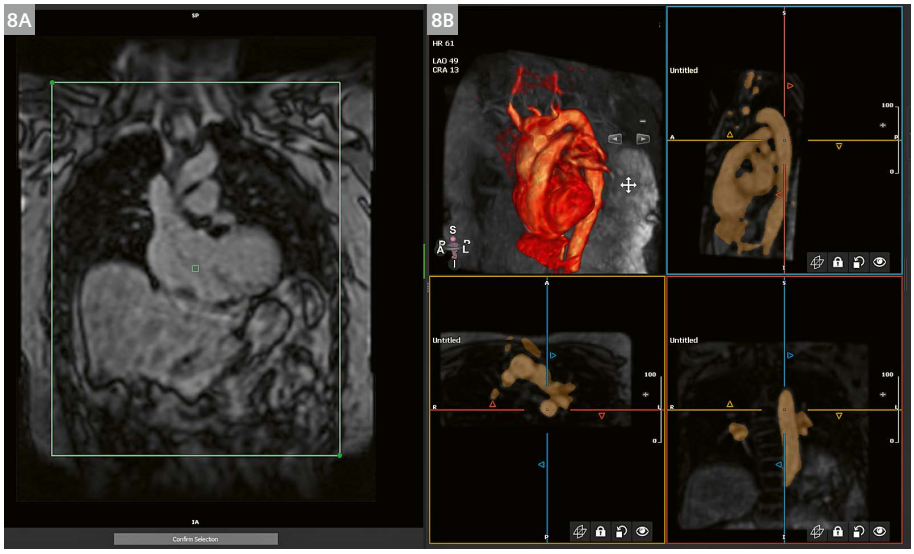

8 Post-processing of 4D Flow data: **(8A)** Raw data is displayed in post-processing software and **(8B)** initial segmentation of the acquired image.

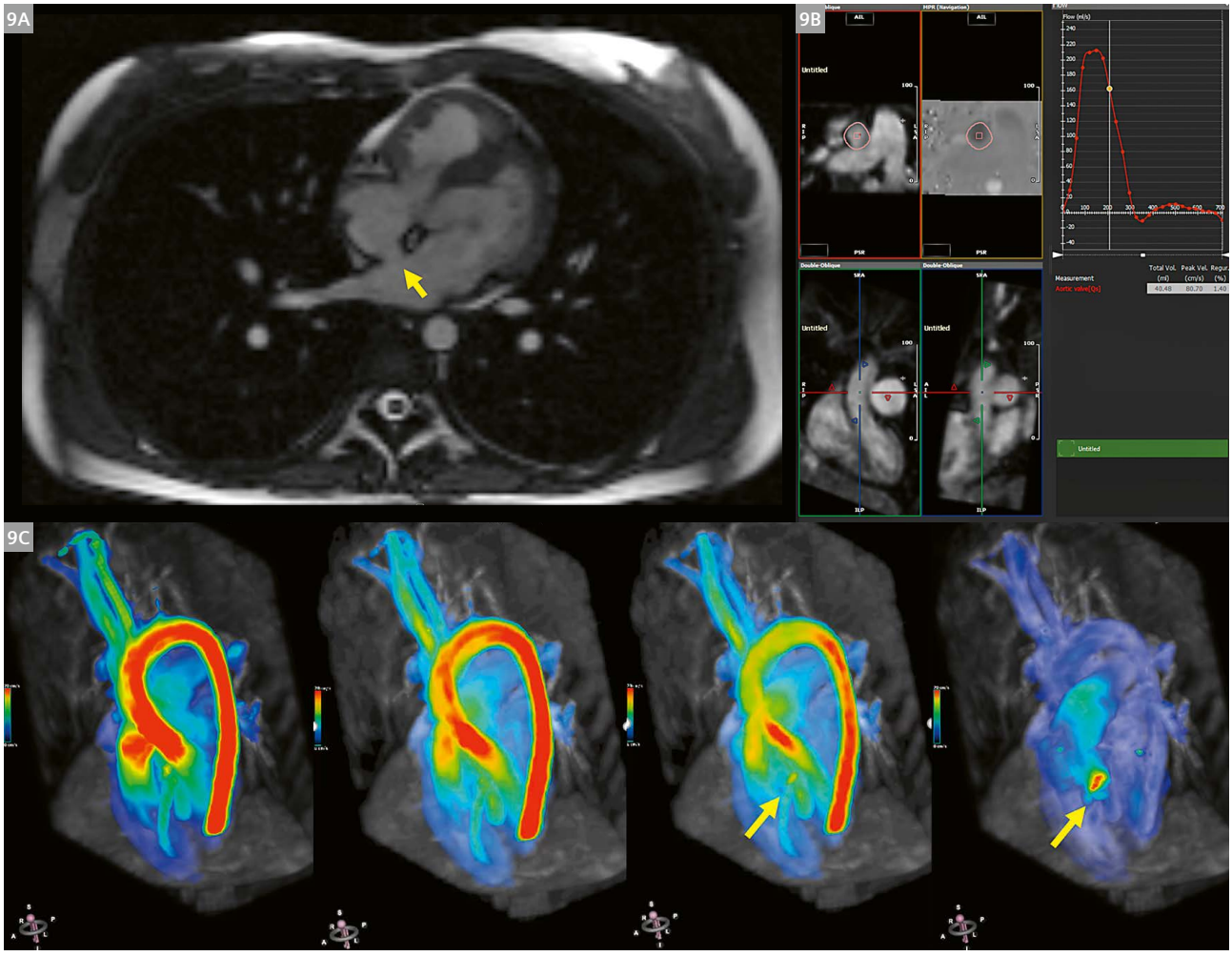

9 Cardiac MRI performed for quantification of pulmonary-to-systemic flow ratio (Qp:Qs): **(9A)** A secundum atrial septal defect is shown in the four-chamber view (yellow arrow); **(9B)** a double-oblique imaging plane is placed above the aortic valve, and the region of interest is traced throughout the cardiac cycle to obtain a flow-time curve and Qs quantification; **(9C)** 4D Flow visualization shows high velocity flow transiting the aorta from early to late systole (left to right) with visualization of the left-to-right intracardiac shunt across the atrial septal defect (yellow arrow) during latter systole. In this case, Qp:Qs calculated by 4D Flow was 1.8, indicating hemodynamic significance.

Making a diagnosis

One of the most important aspects of CMR is the ability to accurately quantify cardiac and valvular function, and, at least at our institution, there is now increasing demand for comprehensive aortic hemodynamic evaluation. As 4D Flow has become increasingly available, many software vendors now provide tools to post-process the data, generate 3D cine flow images, and perform flow quantification by placing 2D planes orthogonal to flow features of interest. Usually, some degree of background offset correction, eddy current correction, and occasionally anti-aliasing are required, and different software vendors address these needs in different ways. Once the data is ready for visualization, we often begin by reviewing velocity maximum intensity projections (for example, Fig. 9C), which allow for bulk flow visualization that can be helpful for plane placement and visualization of intracardiac and valvular jets. For most cases, it is best practice to evaluate flow through the aortic valve and main pulmonary artery, which allows for comparison with right and left ventricular stroke volume, and to validate internal consistency in the flow data. Research has shown [1] that flow quantification accuracy can be limited by areas of increased vorticity, which is why we often use streamline visualization (Fig. 10B) to identify areas of flow complexity that may impact quantification prior to final analysis plane placement.

We have multiple examples of 4D Flow "saving" our flow and velocity quantification in cases of poor 2D plane selection. Moreover, the ability to retrospectively analyze all the major vasculature in the chest, including pulmonary and systemic veins, provides multiple opportunities to check for internal consistency and to more accurately quantify valvular insufficiency or shunts (Fig. 9).

As adult congenital heart disease has become an increasing part of our practice, it is clear that the 4D Flow is far superior for flow quantification from an efficiency standpoint for these patients. For example, a repaired Tetralogy of Fallot patient might require 2D phase contrast imaging at the aortic valve, pulmonic valve, and left and right pulmonary arteries, which all require specialized planning sequences and expertise in vascular anatomy. 4D Flow in a coronal slab brings this acquisition much closer to being a "one-click" solution. We also have a large bicuspid aortic valve clinical service, so we tend to encounter many patients with aortic coarctation or repaired coarctations (Fig. 10). 2D plane placement on

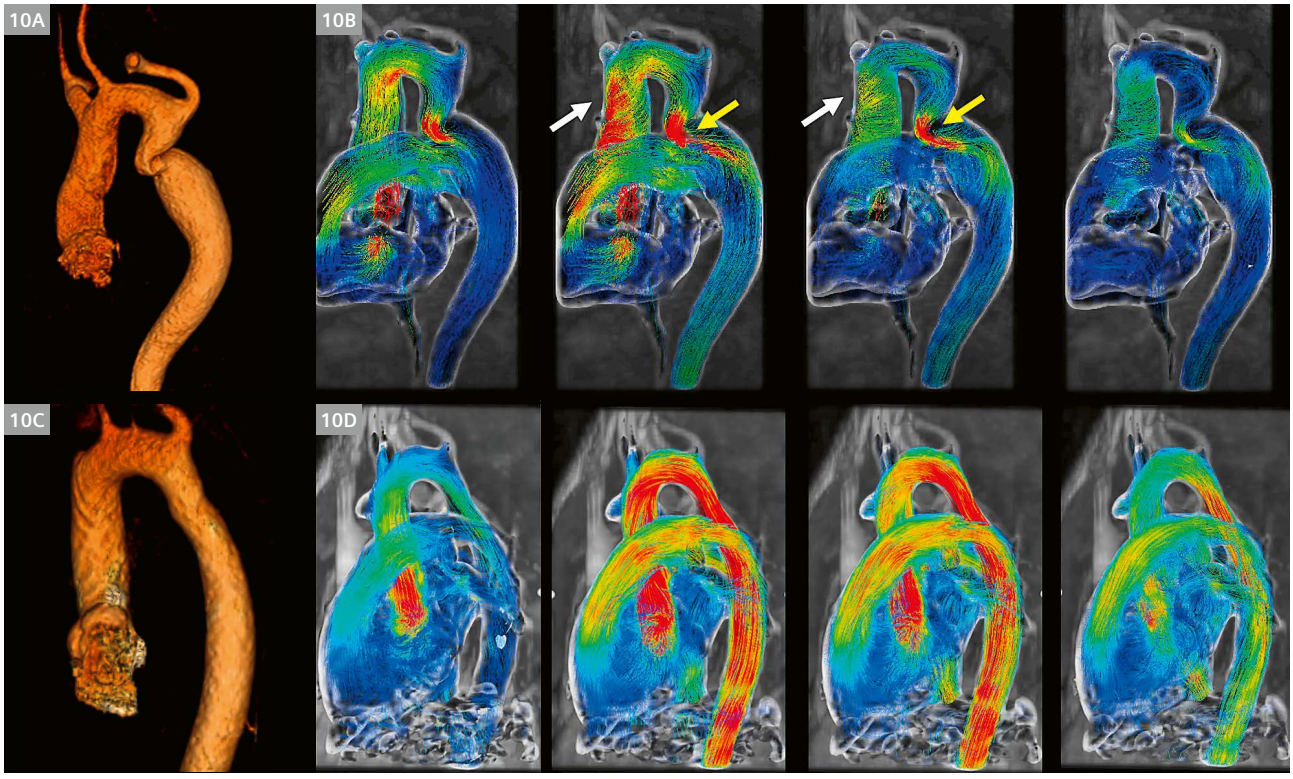

10 3D streamlines allow visualization of velocities in the aorta: **(10A)** 3D reconstruction of the thoracic aorta in a patient with bicuspid aortic valve and coarctation with **(10B)** streamlines showing helical flow patterns (white arrow) and flow acceleration at the coarct (yellow arrow) during early to late systole (left to right); **(10C)** 3D reconstruction of the thoracic aorta in a separate patient after coarctation repair, with **(10D)** now smoother streamlines indicative of substantial normalization of flow and sheer stress during early to late systole (left to right).

the scanner for evaluation of a tortuous coarctation can be particularly challenging, but 4D Flow makes the acquisition straightforward.

Conclusions

We have designed and implemented a clinical 4D Flow protocol for vascular flow evaluation with CMR that functions across multiple scanner platforms from Siemens Healthineers and is easy to perform for CMR technologists of all experience levels. Anecdotally, we believe this approach improves the patient experience and also provides the interpreting physicians with more consistent data for visualization and quantification. Moreover, this addition to our protocol not only allows for routine flow and velocity measurements of the great vessels at multiple sites, but also creates opportunities for advanced analysis such as aorta wall-shear stress and pulse wave velocity measurements, direct mitral valve flow quantification, and flow stasis mapping in the left atrium and false lumen of aortic dissection. These are currently under investigation and may become important diagnostic tools in the near future.

Reference

1 Contijoch FJ, Horowitz M, Masutani E, Kligerman S, Hsiao A. 4D Flow Vorticity Visualization Predicts Regions of Quantitative Flow Inconsistency for Optimal Blood Flow Measurement. Radiol Cardiothorac Imaging. 2020;2(1):e190054. doi: 10.1148/ryct.2020190054.

Contact

Ryan J. Avery, M.D.
Associate Professor of Radiology
(Nuclear Medicine)
Northwestern University
NMH/Arkes Family Pavilion Suite 800
676 N Saint Clair
Chicago, IL 60611
USA
ravery@northwestern.edu

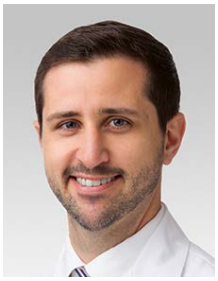

Bradley D. Allen, M.D., M.S.
Assistant Professor of Radiology
(Chest Imaging and Cardiovascular Imaging)
Northwestern University
NMH/Arkes Family Pavilion Suite 800
676 N Saint Clair
Chicago, IL 60611
USA
bdallen@northwestern.edu

4D Flow MRI for the Evaluation of Aortic Endovascular Graft

Davide Capra[1]; Caterina Beatrice Monti[1]; Francesco Secchi[1,2]

[1]Department of Biomedical Sciences for Health, Università degli Studi di Milano, Milano, Italy
[2]Unit of Radiology, IRCCS Policlinico San Donato, San Donato Milanese, Milano, Italy

Introduction

Since its introduction, four-dimensional (4D) flow magnetic resonance imaging (MRI) has been established as the in-vivo reference standard for non-invasive hemodynamic assessment [1]. 4D Flow is usually performed using spoiled gradient-echo sequences with short repetition time (TR), and electrocardiographic and respiratory gating, for a recommended total scan time of 5–8 minutes [2]. This technique allows a volumetric assessment of blood flow over the entire vessel of interest, along with volumetric quantification and retrospective analysis of blood flow through any plane [2], thus providing a full functional evaluation which can be then combined with anatomical information derived from other sequences. Indeed, 4D Flow already proved useful in the assessment of many clinical conditions, from aortic valve diseases [3] to complex congenital heart pathologies [4]. In all such cases, 4D Flow allows both a qualitative assessment of blood flow dynamics, i.e. discerning helical and vortical flow from laminar flow, and a quantitative assessment, deriving from the encoded velocities parameters such as jet angles [5] and wall shear stress [6].

4D Flow in aortic endografts

Recently, the potential role of 4D Flow in the follow up of endovascular aortic repair (EVAR) has been explored with encouraging results. Indeed, EVAR requires a lifelong postoperative surveillance, as it could be affected by long-term complications, such as endoleaks [7], which are defined as a persistent blood flow outside the stent and within the vessel walls, stent collapse, stent infection, and stent migration. Furthermore, computational fluid dynamics studies showed how hemodynamic factors could exert relevant drag force on the stent, possibly leading to stent migration or failure [8]. Initially, Hope et al. [9] first proposed the use of 4D Flow for the identification of endoleaks after EVAR in a case report, then Rengier et al. [10] and Bunk et al. [11] demonstrated the feasibility of in-stent flow visualization in phantom studies, establishing that the stent presence does not undermine flow measurements. More recently, Sakata et al. [12] characterized each type of endoleak after EVAR by its flow appearance, describing a superior sensitivity than computed tomography angiography in endoleaks detection. Subsequently, the same team investigated the predictive power of 4D Flow analysis of type 2 endoleaks, suggesting that it could be useful for the prediction of sac expansion after EVAR [13]. Furthermore, Ravesh et al. [14] reported how 4D Flow allowed to measure relevant hemodynamic parameters, namely blood flow velocity and wall shear stress in a patient with a folded endograft following thoracic EVAR (TEVAR).

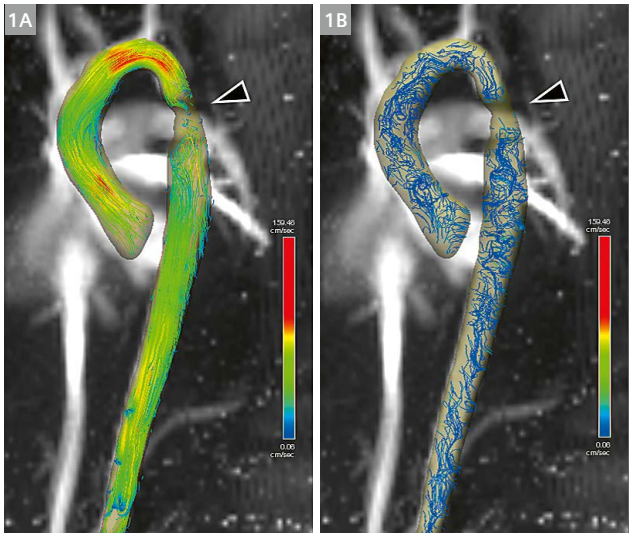

1 10-year-old female patient treated for aortic coarctation (black arrowhead). Maximum intensity projection image of flow speed, 3D streamlines visualization. **(1A)** Peak systolic phase. **(1B)** Diastolic phase. In correspondence of the luminal narrowing there is a reduction in flow signal. Nonetheless, flow evaluation is feasible proximally and distally from the stent, and an acceleration of the blood flow is visible in the aortic arch.

In our institution, a relevant number of aortic endovascular treatments are performed each year, hence we decided to explore the clinical usefulness of 4D Flow MRI for patients undergoing thoracic aorta endovascular treatment at our institution.

Materials and methods

We evaluated 10 patients (2 female), with a mean (± standard deviation) age of 61 ± 20 years, undergoing MRI for follow-up after endovascular aortic treatment. All patients underwent EVAR except one, who had an intravascular stent therapy for isthmic coarctation. All 4D Flow examinations were performed using a 1.5T system (MAGNETOM Aera, Siemens Healthcare, Erlangen, Germany) using a 48-channel surface phased-array coil, placed over the thorax of the patient in supine position. In addition to the standard examination protocol, a 4D flow sensitive 3D spatial-encoding, time-resolved, phase-contrast prototype sequence[1] with retrospective electrocardiogram gating and respiratory gating was acquired. This package supports the acquisition of volumetric phase contrast data with velocity vector encoding. Compared to the current product sequences for phase contrast flow imaging, a 3D spatial encoding option was integrated, and a navigator as known from the product coronary imaging protocols was included. To minimize the time during the cardiac cycle used for the navigator acquisition, the duration of the navigator module was reduced to < 20 msec. From a sequence design standpoint, phase contrast flow quantification was integrated into a sequence derived from the object-oriented cardiovascular sequence. Acquisition parameters were: TE 2.3–3.1 ms, echo spacing 5.1 ms, flip angle 8°, segment number 2, temporal resolution 40.6–43.4 ms, bandwidth 490 Hz/pixel, FOV 340–232 mm^2, 3D acquired resolution 3.5 × 2.4 × 3.9 mm, and VENC 100 cm/s. Images were acquired in a sagittal plane, yielding 40 to 52 slices depending on the patient size. For the post-processing, we used 4D Flow Demonstrator Version 2.4[1], a prototype software package that allows the qualitative and quantitative analysis of blood flow using time-resolved phase-contrast MRI datasets. We also evaluated the presence of artifacts.

Results

Among our cases, flow evaluation was feasible in all patients, although in 3 out of 10 patients we observed some artifacts. Indeed, three individuals displayed a reduced signal within the vessel lumen where the endograft was placed, while other presented with turbulent or increased flow.

Concerning reduced flows, in the first case (Fig. 1), a 10-year-old girl treated with a stent for aortic coarctation, a flow reduction may be observed where the aortic lumen tightens. This may be due to the fact that the narrowing causes an acceleration of the flow over the velocity encoding, which is set a priori, or to alterations in the magnetic field induced by the stent. The second and the third case, respectively an 82-year-old woman and an 81-year-old man with EVAR, presented a reduced flow in the aortic lumen likely attributable to difficult ECG trigger or stent-induced artifacts.

Concerning patients with blood flow turbulence, we observed a vortical flow in the ascending aorta of one 60-year-old male patient that underwent EVAR for aortic dissection (Fig. 2). This patient showed an accelerated flow right above the aortic valve in peak systole, contributing to the generation of a vortex towards the late systolic phase. The accelerated flow was situated at the proximal insertion of the endograft, and thus the acceleration could be attributed to the lumen and wall change that it generates.

Three patients presented aortic flow accelerations. In particular, a 70-year-old male patient that underwent TEVAR for aortic aneurysm showed an acceleration of the aortic flow in the distal section of the endograft (Fig. 3); a 53-year-old male patient with repaired dissection displayed

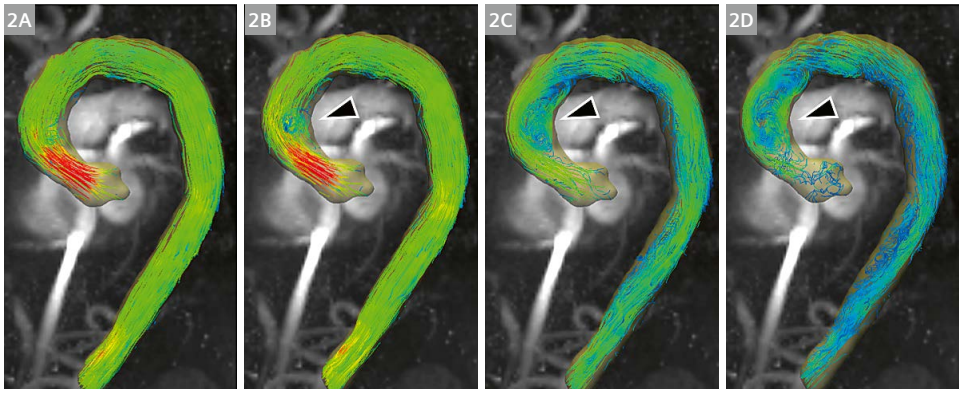

2 60-year-old man with EVAR for aortic dissection. Maximum intensity projection image of flow speed, 3D streamlines visualization. **(2A)** Peak systolic phase. The flow is accelerated at the aortic valve level. **(2B)** Mid-systolic phase. A vortex starts forming in the ascending aorta (black arrowhead). **(2C, D)** The vortex grows towards the late systolic phases (black arrowheads).

[1]*Work in progress: the application is currently under development and is not for sale in the U.S. and in other countries. Its future availability cannot be ensured.*

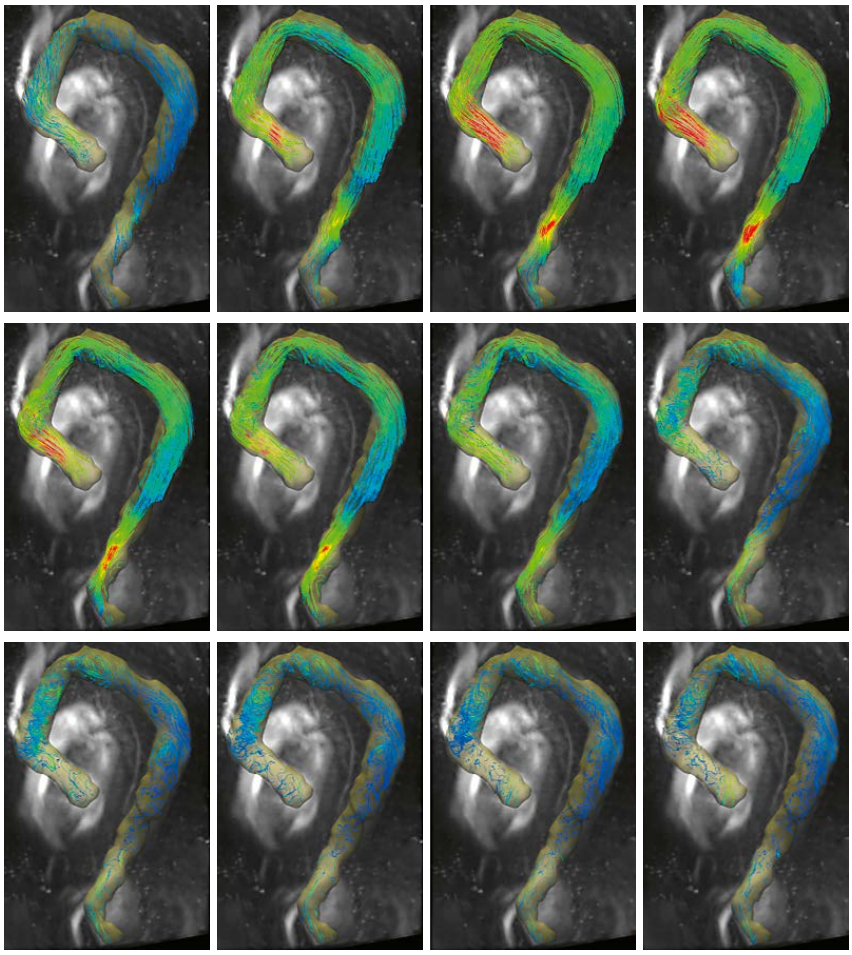

3 70-year-old male patient with TEVAR for aortic aneurysm. Maximum intensity projection image of flow speed, 3D streamlines visualization. The sequence of the cardiac circle shows the development of an abnormal helical flow in the ascending aorta towards the late systolic phases, and an increased velocity in the distal part of the endograft caused by a narrowing of the lumen.

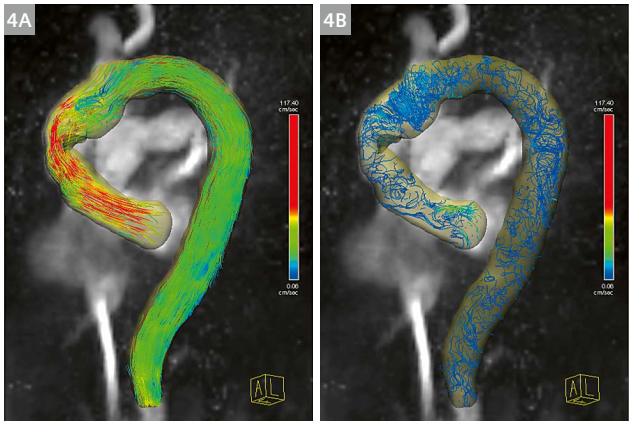

4 53-year-old male patient with repaired dissection. Maximum intensity projection image of flow speed, 3D streamlines visualization. **(4A)** Peak systolic phase, the streamlines show a complex flow pattern due to the tortuosity of the ascending aorta. **(4B)** Diastolic phase.

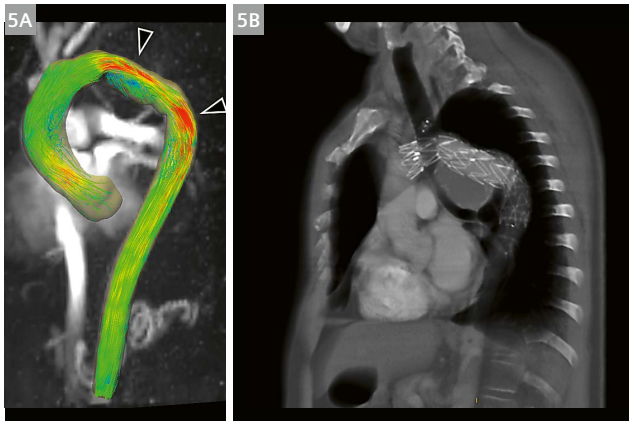

5 51-year-old male patient with TEVAR. **(5A)** Maximum intensity projection image of flow speed. The 3D streamlines show increased velocity in correspondence with the graft's bends (black arrowheads). **(5B)** Computed tomography scan showing the position of the endograft.

accelerated and turbulent flow in a tortuous ascending aorta, proximally to the endograft (Fig. 4); and a 51-year-old male patient with a repaired aneurysm of the aortic arc presented flow accelerations in correspondence with endograft bends (Fig. 5).

Nevertheless, in all the other patients, the flow signal magnitude was unaltered throughout the graft lumen, granting a complete representation of the flow. For instance, in a 53-year-old patient that underwent aortic reparation after traumatic rupture, the flow was laminar in all the visualized aortic segments, and an acceleration was visible at aortic valve level (Fig. 6).

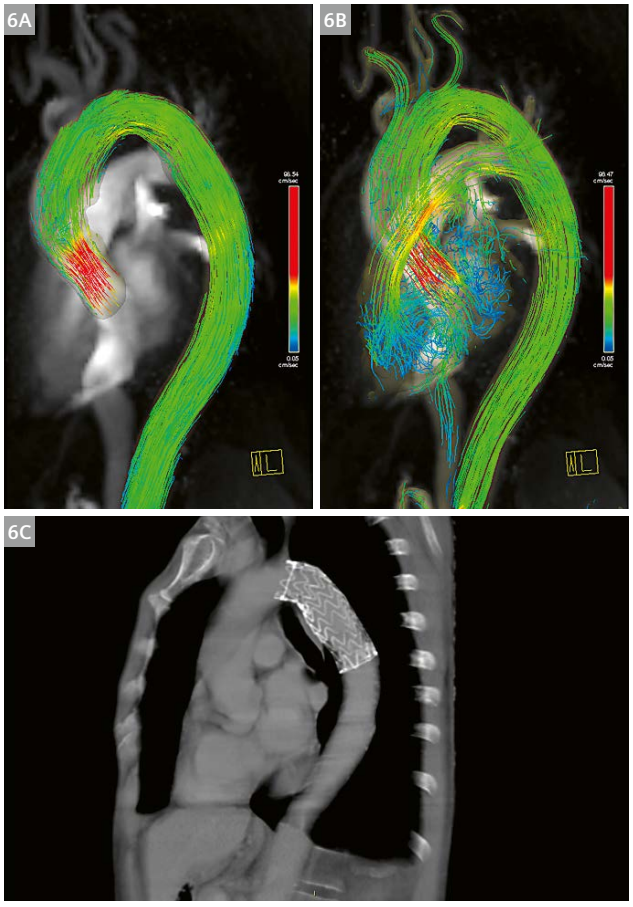

6 53-year-old male patient treated with endograft for traumatic aortic rupture. **(6A)** Maximum intensity projection image of flow speed. Hemodynamics of peak systolic phase. Streamlines display increased velocity at aortic valve level, and a regular flow throughout the visualized aorta. Note that flow velocity is also evaluable in endovascular graft. **(6B)** Pulmonary and supra-aortic branches flows. **(6C)** Computed tomography scan showing the position of the endograft.

Future perspectives

Currently, CT imaging is the cornerstone for the post-operative follow-up of EVAR. Nevertheless, 4D Flow MRI offers the unique advantage of a comprehensive analysis of blood flow in the repaired aorta. The ability to visualize different flow patterns and derive dynamic parameters such as wall shear stress might provide new insight on the risk of post-operative complications. Indeed, computational fluid dynamics revealed that aortic segments presenting low wall shear stress are linked to thrombus formation, whereas increased wall shear stress is related to the propagation of aortic dissection [15]. 4D Flow MRI may thus allow an in-vivo assessment of such features, without radiation exposure or administration of contrast agent.

Moreover, currently, the management of type II endoleaks is decided upon the growth of aneurysmatic sac [16]. In this regard, 4D Flow analysis of endoleaks flow patterns such as flow direction, volume and velocity might allow a more timely detection of endoleak complications leading to a more tailored treatment [12].

Conclusions

The presence of an aortic endograft does not necessarily hinder the visualization of blood flow through 4D Flow sequences, although in some cases flow artifacts could be generated by the graft. The introduction of a hemodynamic evaluation for aortic endovascular treatments follow up in everyday clinical practice could possibly provide insights on the flow changes after EVAR, spotlighting their impact on the procedure success. Prospective studies are warranted to assess the prognostic value of 4D Flow for the follow up after aortic endovascular treatment.

References

1 Catapano F, Pambianchi G, Cundari G, Rebelo J, Cilia F, Carbone I, Catalano C, Francone M, Galea N. 4D flow imaging of the thoracic aorta: is there an added clinical value? Cardiovasc Diagn Ther 2020;10:1068–1089.
2 Dyverfeldt P, Bissell M, Barker AJ, Bolger AF, Carlhäll CJ, Ebbers T, Francios CJ, Frydrychowicz A, Geiger J, Giese D, Hope MD, Kilner PJ, Kozerke S, Myerson S, Neubauer S, Wieben O, Markl M. 4D flow cardiovascular magnetic resonance consensus statement. J Cardiovasc Magn Reson 2015;17:1–19.
3 Blanken CPS, Farag ES, Boekholdt SM, Leiner T, Kluin J, Nederveen AJ, Ooij P, Planken RN. Advanced cardiac MRI techniques for evaluation of left-sided valvular heart disease. J Magn Reson Imaging 2018;48:318–329.
4 Geiger J, Markl M, Jung B, Grohmann J, Stiller B, Langer M, Arnold R. 4D-MR flow analysis in patients after repair for tetralogy of Fallot. Eur Radiol 2011;21:1651–1657.

5 Sigovan M, Hope MD, Dyverfeldt P, Saloner D. Comparison of four-dimensional flow parameters for quantification of flow eccentricity in the ascending aorta. J Magn Reson Imaging 2011;34:1226–1230.
6 Rodríguez-Palomares JF, Dux-Santoy L, Guala A, Kale R, Maldonado G, Teixidó-Turà G, Galian L, Huguet M, Valente F, Gutiérrez L, González-Alujas T, Johnson KM, Wieben O, García-Dorado D, Evangelista A. Aortic flow patterns and wall shear stress maps by 4D-flow cardiovascular magnetic resonance in the assessment of aortic dilatation in bicuspid aortic valve disease. J Cardiovasc Magn Reson 2018;20:28.
7 Riambau V, Böckler D, Brunkwall J, Cao P, Chiesa R, Coppi G, Czerny M, Fraedrich G, Haulon S, Jacobs MJ, Lachat ML, Moll FL, Setacci C, Taylor PR, Thompson M, Trimarchi S, Verhagen HJ, Verhoeven EL, et al. Editor's Choice – Management of descending thoracic aorta diseases. Eur J Vasc Endovasc Surg 2017;53:4–52.
8 Fung GSK, Lam SK, Cheng SWK, Chow KW. On stent-graft models in thoracic aortic endovascular repair: A computational investigation of the hemodynamic factors. 2008;38:484–489.
9 Hope TA, Zarins CK, Herfkens RJ. Initial experience characterizing a type I endoleak from velocity profiles using time-resolved three-dimensional phase-contrast MRI. YMVA 2009;49:1580–1584.
10 Rengier F, Delles M, Frederik T, Böckler D, Ley S, Kauczor H, Tengg-kobligk H Von. In vitro validation of flow measurements in an aortic nitinol stent graft by velocity-encoded MRI. Eur J Radiol 2011;80:163–167.
11 Bunck AC, Jüttner A, Kröger JR, Burg MC, Kugel H, Niederstadt T, Tiemann K, Schnackenburg B, Crelier GR, Heindel W, Maintz D. 4D phase contrast flow imaging for in-stent flow visualization and assessment of stent patency in peripheral vascular stents – A phantom study. Eur J Radiol 2012;81:e929–e937.
12 Sakata M, Takehara Y, Katahashi K, Sano M, Inuzuka K, Yamamoto N, Sugiyama M, Sakahara H, Wakayama T, Alley MT, Konno H, Unno N. Hemodynamic analysis of endoleaks after endovascular abdominal aortic aneurysm repair by using 4-dimensional flow-sensitive magnetic resonance imaging. Circ J 2016;80:1715–1725.
13 Katahashi K, Sano M, Takehara Y, Inuzuka K, Sugiyama M, Alley MT, Takeuchi H, Unno N. Flow dynamics of type II endoleaks can determine sac expansion after endovascular aneurysm repair using four-dimensional flow-sensitive magnetic resonance imaging analysis. J Vasc Surg 2019;70:107-116.e1.
14 Salehi Ravesh M, Langguth P, Pfarr JA, Schupp J, Trentmann J, Koktzoglou I, Edelman RR, Graessner J, Greiser A, Hautemann D, Hennemuth A, Both M, Jansen O, Hövener JB, Schäfer JP. Non-contrast-enhanced magnetic resonance imaging for visualization and quantification of endovascular aortic prosthesis, their endoleaks and aneurysm sacs at 1.5 T. Magn Reson Imaging 2019;60:164–172.
15 Munshi B, Parker LP, Norman PE, Doyle BJ. The application of computational modeling for risk prediction in type B aortic dissection. J Vasc Surg 2020;71:1789-1801.e3.
16 Wanhainen A, Verzini F, Van Herzeele I, Allaire E, Bown M, Cohnert T, Dick F, van Herwaarden J, Karkos C, Koelemay M, Kölbel T, Loftus I, Mani K, Melissano G, Powell J, Szeberin Z, ESVS Guidelines Committee, de Borst GJ, et al. Editor's Choice – European Society for Vascular Surgery (ESVS) 2019 clinical practice guidelines on the management of abdominal aorto-iliac artery aneurysms. Eur J Vasc Endovasc Surg 2019;57:8–93.

Contact

Caterina Beatrice Monti
Department of Biomedical Sciences for Health
Università degli Studi di Milano
Via Mangiagalli 31
20133 Milano
Italy
Tel.: +39-02-52774468
Fax: +39-02-52774925
caterina.monti@unimi.it


Caterina Beatrice Monti

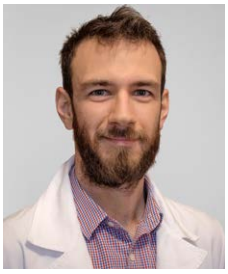
Davide Capra


Francesco Secchi

A Hybrid Cardio-Neuro MR Suite at the Geneva University Hospital in the Treatment of Cardiac Tachyarrhythmias

Pr. Jean-Paul Vallée[1]; Dr. Lindsey A Crowe[1]; Pr. Maria-Isabel Vargas[3]; Pr. Dipen Shah[2]

[1]Radiology division, Geneva University Hospital, Switzerland
[2]Cardiology division, Geneva University Hospital, Switzerland
[3]Neuroradiology division, Geneva University Hospital, Switzerland

Introduction

The GIBOR project of the Geneva University Hospitals comprises an interventional suite consisting of an operating room and an electrophysiology room coupled with an MRI room. The innovation and the technological challenge consisted in moving a standard 3T MRI on ceiling rails into a neurosurgical operating room as well as an MRI transfer table coupled with a fully operational cardiac electrophysiology and angiography suite in an adjacent room. This was realized with a 3T MAGNETOM Skyra MRI (Siemens Healthcare, Erlangen, Germany) integrated in the IMRIS Hybrid Operating Suite (IMRIS, Deerfield Imaging, Inc., Minnetonka, MN, USA), coupled with a Siemens Healthineers Artis CombiSuite for Cardiology/Electrophysiology. The operating room, the 3T enhanced MAGNETOM Skyra and the EP room are all CE certified. During a neurosurgical procedure, the MRI travels into the operating room on rails, thus avoiding the need to move the patient between operating and imaging rooms. In the case of a catheter ablation procedure or other cardiac intervention, the table-top on which the patient is located in the EP CombiSuite can be slid and inserted directly into the MRI via a transfer stretcher which also shortens and simplifies patient transport to MRI facilities. Finally, when used in a diagnostic mode, the MRI can be rotated from 90° to ease the patient placement and allow monitoring directly through the window of the control room.

Initiated in 2011, this project was made possible through reflection and close collaboration between the various medical clinics involved (Neurosurgery, Cardiology,

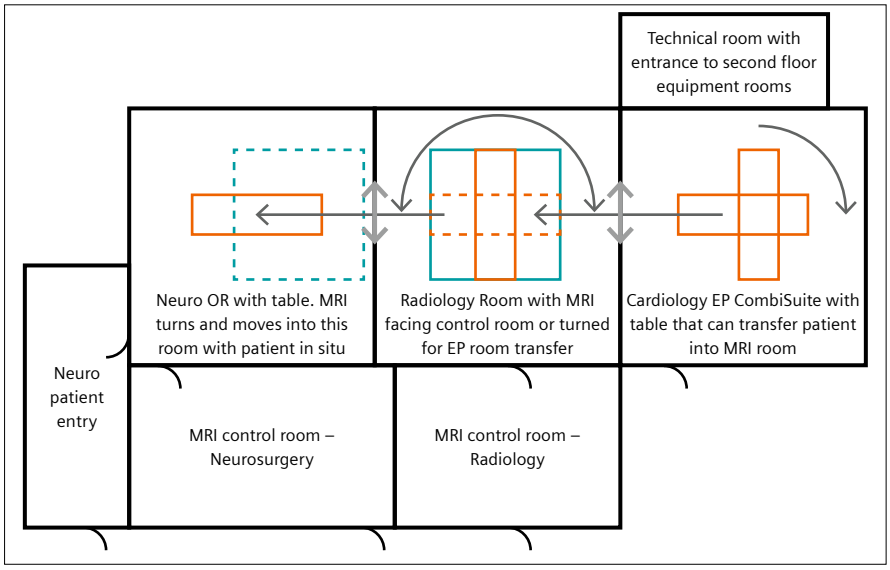

1 Floor plan showing the possible motion for the 3T MAGNETOM Skyra: shift into the neurosurgical operating room and 90° rotation from a diagnostic position to an interventional position with an easy transfer to the electrophysiology room.
Orange: Patient table position for MRI
Petrol square: Magnet positions
Grey arrows: Position of sliding doors
Dark grey arrows: Movement of patient or magnet

Radiology, Neuroradiology and Anesthesia), and the Biomedical Engineering Service. Currently, the MRI installation is used two days/week for neurosurgery patients, two days/week for atrial fibrillation (AF) patients and one day/week by the radiology clinic.

From its conception, the objectives of such a device have been focused on better patient care, with:

- the possibility of having an MRI examination in situ, on the operating table, during the course of a neurosurgical procedure in order to evaluate residual pathology – without having to move the patient. This helps avoid the risk of infection and reduce the duration of anesthesia.
  For electrophysiologic cardiac interventions this allows for the evaluation of the efficacy of tissue lesions both during and directly after the procedure by a rapid table-top transfer to the adjacent MRI followed by a return to the interventional electrophysiology suite to continue the procedure, if necessary,
- a decrease in the number of reoperations in the fields of neurosurgery and cardiac electrophysiology intervention.

GIBOR was officially inaugurated on 27 November 2019. The first neurosurgery operation, with MRI, was conducted on 7 October 2019 and the first cardiology patient with MRI was welcomed on 21 November 2019. However, since February 2020, the project has been suspended by the COVID-19 crisis due to internal reallocation of the resources. So far, 14 AF patients have been treated with this hybrid suite. When not coupled with MRI, both the operative room and the electrophysiological suite are fully used as standard standalone equipment. During the time without imaging of surgical and cardiac interventions, the MRI is used in a diagnostic mode for patients on the waiting list of the radiology clinic. This workflow allows an efficient use of all the devices.

2 MRI in diagnostic position 90° with conventional table. Neuro suite door can be seen to the left.

3 MRI with CombiTable in position 0° from the same perspective.

4 View towards MRI room doors showing position of table during EP procedure.

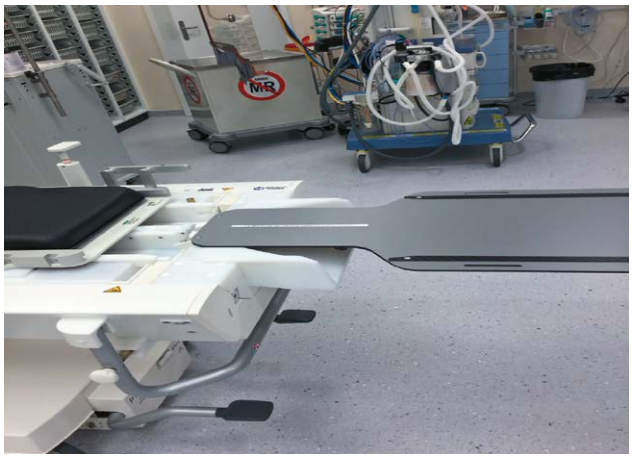

5 Connection of the two tables to transfer the patient on the table top.

6 CombiTable moving into the MRI room.

The cardiac project of the hybrid cardio-neuro MR suite

Aim

Atrial fibrillation (AF) is a serious health problem that is treated by medication as well as catheter ablation. Patients undergoing catheter ablation for AF have an improved quality of life. Recently evidence has shown reduced AF related morbidity-mortality in patients receiving ablation therapy, but also a 15–40% risk of arrhythmia recurrence. The factors associated with recurrence are not well known especially those related to the completion of the AF ablation procedure. Therefore, the aim of our project is to investigate if peroperative imaging can help to reduce AF recurrence. Multiple data including a multicentric study [1] suggested the utility of gadolinium delayed enhancement MRI (LGE-MRI) pre-operative MRI to evaluate patients being considered for AF ablation. The extent of left atrial uptake of contrast can identify patients that would not benefit from the RF procedure. However, LGE-MRI remains controversial in the electrophysiologic community mainly because of the technical difficulty in reproducing the results of delayed enhancement of the atria.

Our project will investigate the added advantage of an optimized pre-operative combined with a pre-operative MRI. We are currently evaluating the immediate effect of MR imaging in situ catheter ablation, so that catheter ablation can be performed and its efficacy evaluated while the patient is still in the operating room. It is not intended to serve as a post-operative follow-up, but to monitor the initial effect of the actual ablation procedure. This includes pre-intervention screening, intervention planning assistance images that will be completed immediately prior to the procedure, and use of the (up to one hour) surveillance time for conduction recovery after the procedure (catheter ablation) to evaluate the success of the procedure and to allow additional catheter ablation with the patient still in electrophysiologic room. Unlike the removal of a brain tumor, where the remaining contrast absorption indicates whether additional ablation is required, the area of RF-atrial ablation is less well defined. Significant enhancement on the LGE prior to the procedure may indicate that an intervention would not provide the desired improvement in arrhythmia outcomes. However, LGE-MRI uptake may also provide additional targets beyond isolation of the pulmonary veins. In addition, the distribution and extent of contrast uptake immediately after a standardized or routine catheter ablation procedure may provide useful prognostic information to indicate an incomplete procedure (see Fig. 7).

Extra-cardiac soft tissue effects may also provide early warning of collateral damage and potential complications. Native T1 and T2 imaging as well as atrial and ventricular function and flow can also be obtained, to bring complementary information to the fibrosis and scar assessment by LGE without repeated contrast injection. The correlation of the electrophysiological findings before and after ablation with the corresponding MR images in terms of contrast and signal intensity can be also performed allowing calibration of delivered ablation parameters in terms of tissue effects. The correlation of myocardial MR characteristics with electrophysiological findings before ablation may allow an improved understanding of the electropathology of atrial fibrillation and other arrhythmias such as ventricular tachycardia.

Similarly, anatomical as well as fibrosis and scar assessment of ventricular myocardium can be readily obtained, in order to allow detailed planning and targeting of the electrophysiology procedure. In-silico simulation based on MR scar models may allow the choice of the optimal ablation strategy from amongst multiple different options. Recently developed wide-band imaging sequences facilitate acquisition of useful information even from patients with intracardiac electrodes including defibrillator coils.

Advantage of the hybrid suite

There is no compromise on the MR system which is a standard fully operational MRI. Thanks to a strong and efficient support of both IMRIS and Siemens, all the available MR sequences for the MAGNETOM Skyra 3T MR systems, including prototypes and C2P, are available for an enhanced image quality.

An anatomical road map as well as complete functional and morphological assessment of the LA can be easily obtained just before the intervention in the same patient position to ease image registration. This could be especially relevant when esophagus modelling is integrated in the therapy planning. LAA thrombus can also be evaluated before the intervention.

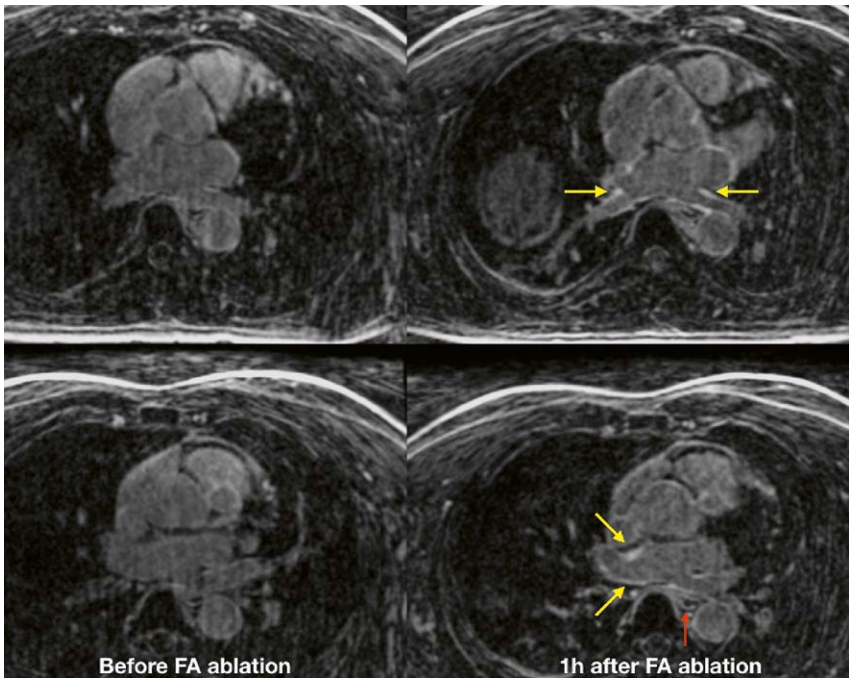

7 Comparison of late gadolinium delayed enhancement before and 1 hour after FA ablation with a 3D inversion recovery prepared GRE prototype sequence[1] featuring an incoherent Cartesian sampling pattern (VD CASPR) [2, 3], Dixon fat water separation and image based respiratory motion compensation with a non rigid iterative reconstruction [4]. Hyper signal around the ostia of the pulmonary veins is visible (yellow arrows) after the intervention. Small structures like the esophagus (red arrow) can be clearly identified with this sequence to attest the absence of iatrogenic complications. Acquired Resolution 1.25 x 1.25 x 1.3 mm.

Pre- and post-procedural MRI is easily acquired thanks to the CombiTable shift option. The close proximity of the two rooms and the fast transfer between them allows optimal comparison of physiological parameters measured by catheters and MRI like flow and pressure measured in the same patient state.

In comparison to an MRI-only guided AF ablation approach with MR compatible ablation catheters in a standard MRI room, the hybrid suite while providing similar information, does not require specific training to master catheter manipulation under MRI guidance. As a result, the learning curve is mainly focused on patient transfer between the electrophysiology and the MRI rooms with the main concerns related to security during transfer and MR imaging. All the clinical tools for the AF ablation in the electrophysiology room are available including high resolution 12 channels ECG monitoring system, TEE or intra-cardiac echocardiography, the CARTO® mapping system (Biosense Webster, Diamond Bar, CA, USA) or the Rythmia (Boston Scientific, MA, USA) or the EnSite™ NavX™ mapping systems (Abbott Laboratories, Chicago, IL, USA). In addition, faster transfer of the patient outside the magnet room can be achieved in case of resuscitation by comparison with conventional MR systems. This hybrid suite benefits from an increased SNR of a 3T magnet by comparison to MR systems for cardiac intervention that are mostly running at 1.5T. Finally, the cost effectiveness of such an approach – allowing scanning of additional patients during most of the AF procedure time – deserves further study.

Challenges

One of the main issues is related to the patient and team safety as most of the collaborators involved in the intervention are not familiar with the particularities of working in an MR environment. This can be solved by extensive and systematic training of the involved teams, with the establishment of detailed procedures.

The set-up, and team training, allows very fast (< 2 min) transfer from MRI to the CombiSuite, with the patient on a sliding transfer table.

Education and cooperation of a multidisciplinary team is needed to ensure MRI safety. The patient needs to be carefully prepared and the monitoring equipment and personnel screened before patient transfer (not as complex as the neuro side where the magnet comes in to the operating theatre). We have multiple safety check-lists in place and careful selection of material that is used in the cardio room.

Multi-lead wireless ECG monitoring allows continuous real-time rhythm monitoring of patients, which is particularly important for the cardiac electrophysiology interventions. In case of a need for defibrillation, a risk that is not negligible after an EP procedure, the patient can be transferred very rapidly back to the EP room to avoid damage to the MRI table. Intensive simulation drills for emergency transfer have been conducted along with periodic reinforcement and re-familiarization to ensure benchmark performance.

[1] *Work in progress: the product is currently under development and is not for sale in the U.S. and in other countries. Its future availability cannot be ensured.*

Sharing the infrastructure with neurosurgery improved the training of all the teams involved as well as the capability of ensuring optimal safety of the procedure.

The 3T field strength may induce severe susceptibility artifacts especially in patients with intracardiac electrodes, but advanced MR sequences facilitating a wide-band inversion for delayed enhancement sequences[1] [5–8] and motion correction [9] enabling free-breathing exams may reduce the artifact.

Another challenge is related to the whole procedure duration (AF ablation + pre- and postprocedural MRI) that may result in patient discomfort and prolonged sedation/anesthesia protocols. Faster MR sequences, using compressed sensing, and optimization of the protocols are therefore an important area of research.

Outlook

The hybrid EP-MR suite offers significant investigational opportunities with direct therapeutic implications. 3D time and respiratory resolved MR sequences for pulmonary vein anatomy are currently under development. When performed at the time of the AF ablation with the CombiSuite, such MR sequences may reduce the registration errors with the angio data related to variation of the LA filling pressure and size. Such a high-resolution mapping procedure can be used to significantly reduce radiation exposure for AF ablation and allow better individual anatomy tailored ablation solutions.

In the electrophysiology field, ventricular arrhythmias (ventricular premature beats, ventricular tachycardia and even ventricular fibrillation) ablation assessment is certainly the next step once our team have gained experience in patient monitoring inside the MR scanner.

In addition, when RF ablation catheters are available for a magnetic field strength of 3T, this hybrid suite will be set up to perform complex ablation, such as AF ablation, under MRI guidance with the safety backup of the angiographic suite; when needed the patients could be transferred very rapidly to an environment familiar to the electrophysiologist to deal with complications.

Other types of cardiac intervention that are beginning to be developed under MRI guidance will benefit from a safe and accessible backup of the CombiSuite. Combined coronary artery catheterization with MRI may be particularly relevant to assess coronary stenosis significance as well as myocardial viability during the intervention. For the diagnosis of pulmonary hypertension coupling invasive pressure measurement to MRI derived flow measurement is especially important to estimate pulmonary resistance.

References

1 Marrouche NF, Wilber D, Hindricks G, Jais P, Akoum N, Marchlinski F, et al. Association of atrial tissue fibrosis identified by delayed enhancement MRI and atrial fibrillation catheter ablation: the DECAAF study. JAMA. 2014;311(5):498-506. doi: 10.1001/jama.2014.3. PubMed PMID: 24496537.

2 Prieto C, Doneva M, Usman M, Henningsson M, Greil G, Schaeffter T, Botnar RM. Highly efficient respiratory motion compensated free-breathing coronary MRA using golden-step Cartesian acquisition. J. Magn. Reson. Imaging 2015;41:738–46.

3 Bustin A, Ginami G, Cruz G, Correia T, Ismail TF, Rashid I, Neji R, Botnar RM, Prieto C. Five-minute whole-heart coronary MRA with sub-millimeterisotropic resolution, 100% respiratory scan efficiency, and 3DPROSTreconstruction. Magn. Reso. Med. doi: 10.1002/mrm.27354. [Epub ahead of print].

4 Munoz C, Bustin A, Neji R, Kunze PK, Forman C, Schmidt M, Hajhosseiny R, Masci PG, Zeilinger M, Wuest W, Botnar RM, Prieto C. Motion-corrected 3D whole-heart water-fat high-resolution late gadolinium enhancement cardiovascular magnetic resonance imaging. J Cardiovasc Magn Reson. 2020 Jul 20;22(1):53. doi: 10.1186/s12968-020-00649-5.

5 Rashid S, Rapacchi S, Vaseghi M, Tung R, Shivkumar K, Finn JP, Hu P. Improved late gadolinium enhancement MR imaging for patients with implanted cardiac devices. Radiology. 2014; 270:269-74.

6 Stevens SM, Tung R, Rashid S, Gima J, Cote S, Pavez G, Khan S, Ennis DB, Finn JP, Boyle N, Shivkumar K, Hu P. Device artifact reduction for magnetic resonance imaging of patients with implantable cardioverter-defibrillators and ventricular tachycardia: late gadolinium enhancement correlation with electroanatomic mapping. Heart Rhythm. 2014;11:289-98.

7 Bhuva AN, Kellman P, Graham A, Ramlall M, Boubertakh R, Feuchter P, Hawkins A, Lowe M, Lambiase PD, Sekhri N, Schilling RJ, Moon JC, Manisty CH. Clinical impact of cardiovascular magnetic resonance with optimized myocardial scar detection in patients with cardiac implantable devices. Int J Cardiol. 2019;279:72-78.

8 Bhuva A, Ramlall M, Boubertakh R, Knott K, Feuchter P, Sekhri N, Schilling R, Kellman P, Moon J, Manisty CH. Wideband free breathing moco LGE changes patient care in patients with implantable cardiac defibrillators. Heart 2017; 103(Suppl 1):A1–A25.

9 Ledesma-Carbayo MJ, Kellman P, Hsu LY, Arai AE, McVeigh ER. Motion corrected free-breathing delayed-enhancement imaging of myocardial infarction using nonrigid registration. J Magn Reson Imaging. 2007; 26:184-90.

Contact

Professor Jean-Paul Vallée
Service de Radiologie
Département Diagnostique
Hôpitaux Universitaires de Genève
Rue Gabrielle-Perret-Gentil 4
CH-1211 Genève 14
Phone: +41 22 3727035
jean-paul.vallee@hcuge.ch

Extending the Reach of MRI with Remote Operations

Bac Nguyen[1]; Lukas Sevcik[2]

[1]ARISTRA, Rasta, Norway
[2]ARISTRA, Dübendorf, Switzerland

Introduction

In times of unexpected circumstances, one needs dedicated approaches and strategies to be able to perform as usual. Due to COVID-19, a lot of private institutes and hospitals are having to change their ways of thinking. One of the most important messages that we'd like to highlight and discuss in this article is that it is possible to provide high-quality examinations without local support.

The key to doing so is a well-connected digital network of specialists. At ARISTRA, our entire infrastructure is based on doctors and technicians in different locations. We have been operating in this way for almost two years now, and we have never had the feeling that we are missing something.

The MRI institutes, where we operate, are widely spread out. This means that, even before the coronavirus restrictions, we sometimes could not set our protocols onsite. We want to highlight some pitfalls and issues that users might run into, and show the solutions we find useful for our work processes.

Scanners at different sites may differ in many ways, even if they look alike.

Examples include:

- gradient strengths
- coils
- versions/releases
- magnetic field strength
- environmental circumstances
- licenses or software packages
- vendors and their specific sequences
- patients/study participants

As you can see, there are many aspects that can bring up plenty of challenges. To make sure our protocols provide the same quality on different scanners, we must keep all of them in mind.

Our approaches

Exporting protocols

When we finish our protocols, we have to export them from the scanner unit. The Dot Cockpit provides a simple solution: just click on the arrow in the 'Export' menu (Fig. 1).

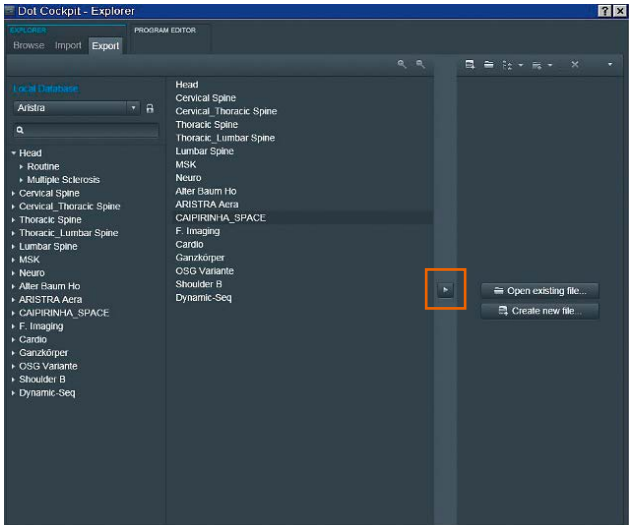

1 Prepare your protocol and use the arrow to export it to your favorite destination.

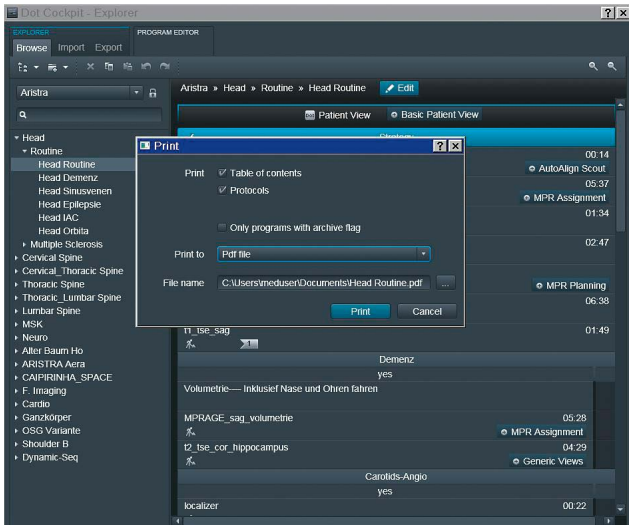

2 Choose your protocol and use the 'Print' option to export your data as a PDF or XML file.

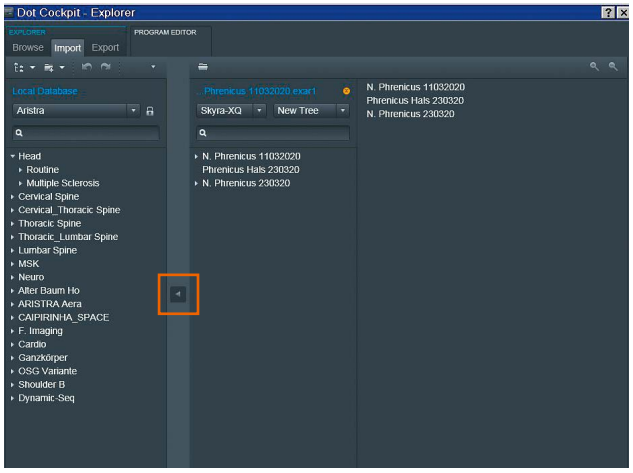

3 Choose your protocol from your source and click on the arrow to tell the Dot Cockpit to import it to your workstation.

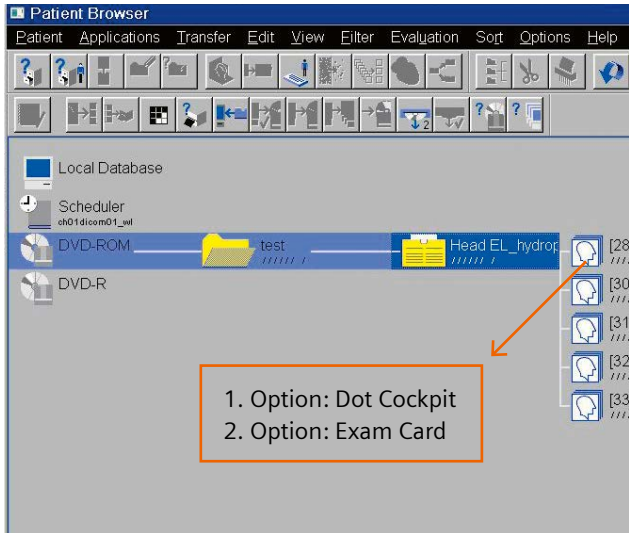

4 Choose your sequence and drag and drop it either to the Dot Cockpit or your exam card to scan immediately.

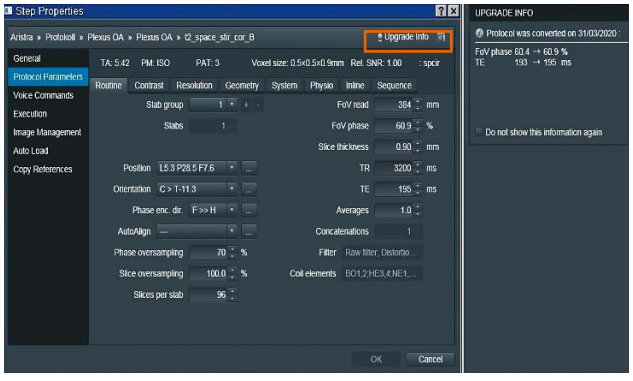

5 Choose 'Upgrade Info' to see the adaptation of relevant parameters.

It also gives you the opportunity to export the finished data as a PDF or XML file (Fig. 2). Our recommendation is to export it as all different file types to make sure that one of them will be suitable for the scanner on which you are about to implement the protocol.

Also, if you have images with your preferred protocol, *syngo*.via gives you the opportunity to export them to a CD or into your PACS. You'll see in the next step why this can be useful.

Importing protocols

Implementing protocols on a workstation can also be done in the Dot Cockpit. You'll find another arrow in the 'Import' menu (Fig. 3).

This can be done easily, but there can also be some difficulties with the scanner/release version. While trying to implement the .edx or .exar file, the Dot Cockpit will show you what the issue is caused by:

- Version/release incompatibility → take the information from the Dot Cockpit and set up the protocols on your scanner manually.
- Hardware incompatibility (e.g., differences in gradient system or local coils) → the system will show a popup window telling you that it is about to transform the sequences in your current system. After this process, you'll be able to see in the Dot Cockpit what parameters have changed (Fig. 5). We strongly recommend checking these parameter changes and adapting as necessary, probably with a sample patient.

If you only have images that you want to implement on your scanner, you can just drag and drop them into your Dot Cockpit or into the queue in the exam card.

Adapting protocols

Parameters can convert due to hardware differences, and these have to be adapted by technicians onsite. Check the mentioned list with changes before you start adapting. Protocols with parameter changes due to conversion are underlined, and can therefore be identified easily. Perform a sample examination to make sure the image quality is the same as before.

Remote approach

In certain situations it can be difficult to achieve the same quality as on the reference scanner. If no application specialist is available, we recommend using Expert-i. This software from Siemens Healthineers provides you with a fully remote workstation.

Another option from Siemens Healthineers is *syngo* Virtual Cockpit. This option allows technologists or radiologists to access the current examination from anywhere in the world. This can be very useful if the technologist needs assistance with difficult cases.

syngo Virtual Cockpit can also be a cost-effective way of teaching technologists remotely, or troubleshooting with application specialists. As Siemens Healthineers says, *syngo* Virtual Cockpit helps you move knowledge, not staff.

At ARISTRA, we do not currently have the *syngo* Virtual Cockpit available on any of our scanners, but this is something we looked into long before the pandemic hit. We hope the *syngo* Virtual Cockpit will be available on our scanners in the near future. This will enable us to maintain our protocols well, teach newer technologists, optimize processes together, and even manage difficult cases without being physically present.

Conclusion

Protocol maintenance can be a complicated process that has to be performed by highly skilled technicians. This is especially true when the hospital has different scanner types and different sites. However, there are ways to make it easier by using remote operating systems and staff. Our solutions show some of the basic approaches.

As institutes and hospitals spread their MRI scanners, there should be improvements in the entire infrastructure. We recommend considering and taking a look at the *syngo* Virtual Cockpit, which in our opinion is a holistic solution for remote maintenance and high-quality examinations.

Contact

Bac Nguyen, BSc, RT (R) (MR), App.Sc (MR)
Senior MR Radiographer
ARISTRA
MRI application Specialist
Rasta, Norway
Phone: +47 97702111
bac.nguyen@aristra.com

Lukas Sevcik
Senior MR Radiographer
ARISTRA – radiology network service
Applications Operations Manager
Dübendorf, Switzerland
Phone: +41764746332
lukas.sevcik@aristra.com

[1] *Törnqvist, E., Månsson, A., Larsson, E.-M., & Hallström, I. (2006). Impact of extended written information on patient anxiety and image motion artifacts during magnetic resonance imaging. Acta Radiologica, 47(5), 474–480. https://doi.org/10.1080/02841850600690355.*

Meet Siemens Healthineers

Siemens Healthineers: Our brand name embodies the pioneering spirit and engineering expertise that is unique in the healthcare industry. The people working for Siemens Healthineers are totally committed to the company they work for, and are passionate about their technology. In this section we introduce you to colleagues from all over the world – people who put their hearts into what they do.

Olga Dreger

Born in Kiev, Ukraine, Olga Dreger moved to Germany as a young teenager of 16 years together with her family. After studying medicine in Nuremberg, she had her first experience treating patients when working in the field of radiation oncology. Looking for new challenges, Olga moved into the field of MRI in 2013 to support MAGNETOM users and internal specialists from headquarters directly. For the past three years, her focus has been on developing training concepts, such as blended learning for MRI customer education, as part of product management within customer services. Olga works very closely with the MRI development team to support knowledge transfer to the Training Center, which is responsible for internal training of Education Specialists. She also collaborates with e-learning teams, such as PEPconnect and SmartSimulator, providing additional material and options for cloud-based virtual classroom training. Her aim is to make customer training "different and smarter".

Erlangen, Germany

How did you first come into contact with MRI?
Growing up in a family of doctors, it was always clear to me that I would work in the healthcare sector and this would be my focus in life.

When I moved from radiation oncology, I had to learn MRI from scratch. This took a while and, actually, it's an ongoing learning process. But this is exactly how I like it and I absolutely embrace it!

What do you find most fascinating about cardiovascular MRI?
Cardiovascular MRI is indeed a fascinating and challenging field. I'm always so impressed at how successfully the Cardiac Dot Engines work with their automation of different examination strategies based on patients' physiological conditions and diseases, for example the Ventricular Function workflow. Also, GOHeart – a new preconfigured cardiac examination program that allows patients to breathe freely during the scan with step-by-step user guidance.

What does your Training and Application Support work involve?
Improving the various training formats to include virtual customer training has played a major role over the past couple of years. This has become especially important during the COVID-19 pandemic. Key steps toward virtual delivery include providing you with individualized learning options through the PEPconnect e-learning platform and also offering guided virtual classroom training via the SmartSimulator solution. SmartSimulator is a virtual connection that enables a hands-on scanner experience using computing power in the cloud to simulate medical device interfaces from Siemens Healthineers. You will work together with our dedicated Education Specialists and are guided through the entire Cardiac Dot Engine workflows, including an in-depth look at the planned examination and postprocessing stages.

What would you do, if you could spend a month doing whatever you wanted?
This is a very interesting question and my list is so long that it's probably not manageable within a month. If I had to prioritize, I would travel to Norway and enjoy the peace of the fascinating landscapes. I love relaxing in nature; it helps me to refocus and reenergize. I would also like to share with my young son the value of this. This would give me a great opportunity to spend time with my family without any pressure, to come back to our roots and remind ourselves what is really important in life.

Michelle Steinkrug

After studying theater and media studies at Friedrich-Alexander-Universität Erlangen-Nürnberg, Michelle went on to study industrial engineering at the same institution. Michelle joined Siemens Healthineers in 2018 as an education consultant, which involves working closely with the application product managers, the marketing team, and the R&D team. Based on the blended learning strategy, Michelle develops customer learning material that is published on the e-learning platform PEPconnect. She uses different learning methods to serve different learner needs. She has helped to develop learning material for several modalities, such as CT, XP, and *syngo*.via. Michelle also began producing MR learning material in 2020, and has recently developed the XA30 cardiac training program.

Erlangen, Germany

How did you first come into contact with MRI?
My very first contact with MRI was when I was nine years old. The doctor showed me the images after my scan. This was the first time I had seen these kinds of images. I was so impressed by the idea that someone could see inside the human body.

Professionally, I had my first contact with MRI when I joined the Customer Services Education Team as a student. My job was to support my colleagues by creating customer education training material for our e-learning platform PEPconnect.

What do you find most fascinating about cardiovascular MRI?
With MRI in particular, there is plenty of potential to improve on established methods, develop new ones, and break with existing imaging limitations. We've seen this very recently with the development of GOHeart, which expands the patient population eligible for cardiac MRI. It makes it possible to examine patients who cannot hold their breath. GOHeart allows you to perform an automated and guided comprehensive cardiac examination, as it is one extension of the Cardiac Dot Engine.

Exam strategies can be selected based on the patient's physiological condition, and all protocols are adapted automatically. In summary, cardiac MRI is a fascinating field within MRI and has tremendous opportunities. I am really looking forward to participating in this development.

What does training and application support work involve?
With the current global health crisis, educational institutions have undergone radical changes in the past few months. Teachers and learners have had to adapt their learning methods using the associated technology within a very short time.

And this is where the blended learning strategy comes in, that was already well established long before the crisis, but now it is getting more and more important: a hybrid of in-person lessons and e-learning. Blended learning is a viable model for the future of education because the in-person and online components can be combined in any proportion. The model offers a lot of flexibility and promising opportunities and with the current situation its focus is turning more and more on the online part.

The learning material needs to be available online, allowing learners to access it at any time to refresh their memory, to check that they understand the course ontent, or to seek out additional, in-depth resources about a topic of interest. With our e-learning platform PEPconnect, you can access a large number of engaging in vivo and in vitro learning activities – including e-learnings, webinars, job aids, videos, virtual instructor-led events, and more.

If you haven't discovered it yet, take a look at PEPconnect here: **https://pep.siemens-info.com/en-us**

You will find a lot of material there, such as the basics for getting started with scanning, or ways to learn about MR View&GO and its functionalities in more detail. You can learn more about MRI application techniques such as SMS, Compressed Sensing, and – of course – the Cardiac Dot Engine: **https://pep.siemens-info.com/en-us/dot-cockpit-and-dot-engines**

This online training is a step-by-step guide to the Dot Engine concept and workflow. By creating your own account on PEPconnect, you can set up individual learning plans, track your progress, and view the learning objects you are interested in – any time and any place that suits you. I hope you enjoy your learning journey!

What would you do if you could spend a month doing whatever you wanted?
I love to travel and to be outside, to learn from different cultures and discover countries and cities on foot. That's why I usually avoid using public transport. I love to walk during my trips, because then I discover places I didn't know about.

Being outside to put things in perspective, and the time away from the normal day-to-day routine gives me the opportunity for personal reflection.

The entire editorial staff at the University of Sydney and at Siemens Healthineers extends their appreciation to all the radiologists, technologists, physicists, experts, and scholars who donate their time and energy – without payment – in order to share their expertise with the readers of MAGNETOM Flash.

MAGNETOM Flash – Imprint

Publisher:
Siemens Healthcare GmbH
Magnetic Resonance,
Karl-Schall-Str. 6, D-91052 Erlangen, Germany

Editor-in-chief:
Antje Hellwich
(antje.hellwich@siemens-healthineers.com)

Guest Editor:
Professor Gemma A Figtree, MB BS,
DPhil (Oxon), FRACP, FCSANZ, FAHA
University of Sydney and Royal North Shore Hospital,
Sydney, Australia

Editorial Board:
Rebecca Ramb, Ph.D.; Sunil Kumar S. L., M.D.;
Wellesley Were; Jane Kilkenny; Nadine Leclair, M.D.

Review Board:
Gaia Banks, Ph.D.; Xiaoming Bi, Ph.D.;
Xiaoying Cai, Ph.D.; Kelvin Chow, Ph.D.; Daniel Fischer;
Christian Geppert, Ph.D.; Michaela Schmidt

Copy Editing:
Sheila Regan, Jen Metcalf, UNIWORKS,
www.uni-works.org
(with special thanks to Kylie Martin)

Layout:
Agentur Baumgärtner,
Friedrichstr. 4, D-90762 Fürth, Germany

Production:
Norbert Moser,
Siemens Healthcare GmbH

Printer:
G. Peschke Druckerei GmbH,
Taxetstr. 4, D-85599 Parsdorf b. Munich, Germany

We welcome your questions and comments about the editorial content of MAGNETOM Flash. Please contact us at
magnetomworld.team@siemens-healthineers.com

Manuscripts as well as suggestions, proposals and information are always welcome; they are carefully examined and submitted to the editorial board for attention. MAGNETOM Flash is not responsible for loss, damage, or any other injury to unsolicited manuscripts or other materials. We reserve the right to edit for clarity, accuracy, and space. Include your name, address, and phone number and send to the editors, address above.

MAGNETOM Flash is also available online:

www.siemens-healthineers.com/magnetom-world

Not for distribution in the US

On account of certain regional limitations of sales rights and service availability, we cannot guarantee that all products included in this brochure are available through the Siemens sales organization worldwide. Availability and packaging may vary by country and is subject to change without prior notice. Some/All of the features and products described herein may not be available in the United States.

The information in this document contains general technical descriptions of specifications and options as well as standard and optional features which do not always have to be present in individual cases, and which may not be commercially available in all countries.

Due to regulatory reasons their future availability cannot be guaranteed. Please contact your local Siemens organization for further details.

Siemens reserves the right to modify the design, packaging, specifications, and options described herein without prior notice. Please contact your local Siemens sales representative for the most current information.

Note: Any technical data contained in this document may vary within defined tolerances. Original images always lose a certain amount of detail when reproduced.

Siemens Healthineers Headquarters
Siemens Healthcare GmbH
Henkestr. 127
91052 Erlangen, Germany
Phone: +49 9131 84-0
siemens-healthineers.com

Published by Siemens Healthcare GmbH · Order No. A91MR-1000-147C-7600 · Printed in Germany · 10187 0221 ·